Non-Monotonic Pricing Kernels, Conditional Physical Densities, and Risk-Neutral Bounds for Expected Returns

Stefanos Delikouras*

September 19, 2025

Abstract

This paper examines how non-monotonicities and VIX-dependence in the pricing kernel affect option-based physical densities and the accuracy of risk-neutral bounds for expected market returns. I show that monotonic and non-monotonic kernels generate broadly similar physical return distributions. In contrast, when non-monotonicities are combined with VIX-dependent parameters, the resulting physical densities differ markedly. Likewise, both monotonic and non-monotonic kernels with fixed parameters produce option-based expected returns that are well aligned with variance-based risk-neutral bounds, whereas VIX-dependent specifications yield expected returns that deviate from these bounds. Despite the shortcomings of risk-neutral bounds, they far outperform alternative measures of expected returns.

Keywords: options, risk-neutral density, physical density, expected returns, risk-neutral bounds, non-monotonic pricing kernels

JEL classification: G10, G12, G13

*Department of Finance, Miami Herbert Business School, University of Miami, email: *sdelikouras@bus.umiami.edu*

Non-Monotonic Pricing Kernels, Conditional Physical Densities, and Risk-Neutral Bounds for Expected Returns

Abstract

This paper examines how non-monotonicities and VIX-dependence in the pricing kernel affect option-based physical densities and the accuracy of risk-neutral bounds for expected market returns. I show that monotonic and non-monotonic kernels generate broadly similar physical return distributions. In contrast, when non-monotonicities are combined with VIX-dependent parameters, the resulting physical densities differ markedly. Likewise, both monotonic and non-monotonic kernels with fixed parameters produce option-based expected returns that are well aligned with variance-based risk-neutral bounds, whereas VIX-dependent specifications yield expected returns that deviate from these bounds. Despite the shortcomings of risk-neutral bounds, they far outperform alternative measures of expected returns.

Keywords: options, risk-neutral density, physical density, expected-returns, risk-neutral bounds, non-monotonic pricing kernels

JEL classification: G10, G12, G13

1 Introduction

Conditional densities of stock market returns under the physical measure, and, in particular, conditional expected market returns, are among the most important yet elusive objects in finance. Conditional expected returns are central because they form a core component of virtually all asset pricing models. Yet, these expectations are elusive because they cannot be observed directly.

Traditionally, aggregate market expected returns are inferred from time-series predictability regressions, while firm-level expected returns are obtained from cross-sectional factor regressions.[1] In either case, such derived conditional expected returns cannot be regarded as truly forward-looking, since they rely on contemporaneous or lagged historical data (e.g., asset pricing factors, the price-dividend ratio, dividend growth) and are obtained through backward-looking relations that rest on strong assumptions.

In recent years, one of the most prominent approaches to deriving conditional expected market returns under the physical measure has been the use of option prices and the option-implied risk-neutral density (e.g., Martin (2017)). Conditional expected market returns based on risk-neutral bounds are valuable because they rely on forward-looking option prices rather than traditional backward-looking regression approaches. Nonetheless, this methodology has faced criticism, as option-derived bounds for expected returns are constructed from risk-neutral moments and abstract from the physical measure.

One way to address the limitation of deriving expected returns from risk-neutral moments is to introduce a pricing kernel that captures investors' risk–return preferences. For instance, Bliss and Panigirtzoglou (2004) estimate a standard power-utility discount factor from option prices, while Linn et al. (2018) employ a nonparametric approach to recover the pricing kernel. Within this framework, the option-implied risk-neutral density can be adjusted by multiplying it with the inverse of the estimated discount factor, thereby yielding the option-based distribution of stock market returns under the physical measure. Forward-looking expected returns can then be computed directly from this physical density.

[1] Predictability tests: Campbell and Shiller (1988), Stambaugh (1999), Lettau and Ludvigson (2001a), Goyal and Welch (2003), Goyal and Welch (2008), Ang and Bekaert (2007), van Binsgergen and Koijen (2010), Lewellen (2015), Kostakis et al. (2015). Cross-sectional tests: Fama and French (1993), Fama and French (2015), Hou et al. (2019), Liu et al. (2009), Lettau and Ludvigson (2001b), Yogo (2006), Delikouras (2017), Delikouras and Kostakis (2019). These papers represent only a small sample of a vast literature.

However, even within this framework, several challenges remain regarding the properties of the true stochastic discount factor. First, discount factors are not directly observable. Second, the structural parameters of the discount factor (e.g., elasticity of intertemporal substitution, risk aversion, discount rate) may vary over time. Third, in contrast to the standard monotonicity assumptions for marginal utility in economics and finance, option-implied pricing kernels can exhibit non-monotonicities (e.g., Cuesdeanu and Jackwerth (2018)). Finally, because options are defined at different maturities, Driessen et al. (2022) emphasize the importance of analyzing option-based pricing kernels across horizons to assess the robustness of their properties.

Motivated by these observations, this paper is among the first to jointly examine how non-monotonicities, VIX-dependence, and investment horizon of the discount factor affect option-based physical moments and the validity of risk-neutral bounds for expected returns. I complement this empirical investigation with theoretical insights on the resulting physical densities that consider settings where the risk-neutral density is skewed and the pricing kernel is non-monotonic.

Specifically, I estimate four alternative specifications for the discount factor: standard power utility (fixed-parameter monotonic marginal utility), power utility with VIX-dependent risk aversion (monotonic marginal utility with time-varying parameters), power utility with a quadratic exponent (fixed-parameter non-monotonic marginal utility), and power utility with a VIX-dependent quadratic exponent (non-monotonic marginal utility with time-varying parameters). These kernels extend the standard power-utility specification by allowing for both non-monotonicities and time variation in risk preferences, providing a versatile framework to capture a rich set of investor behaviors. Importantly, I estimate each specification across four maturities (1-, 2-, 3-, and 6-month options) to construct a term structure of option-based physical densities.

To implement this analysis, I follow the standard methodology in Figlewski (2010), Linn et al. (2018), and Alexiou et al. (2025), which recovers the risk-neutral density from the second derivative of option prices with respect to the strike price (Huang and Litzenberger (1989)). I then estimate the parameters of the four discount factors using a GMM system exploiting the property that any cumulative distribution function follows a standard uniform distribution as in Linn et al. (2018). I further include a rational expectations restriction in the GMM, requiring that average option-based expected returns equal average realized returns over the sample period. Finally, I multiply the inverse of each of the four discount factors by the common risk-neutral density to derive alternative

option-based physical distributions across the four maturities.

To assess the role of non-monotonicities and VIX-dependence in the pricing kernel, I begin by examining, via standard GMM hypothesis testing, the statistical significance of the linear and quadratic parameters of the kernel, as well as the VIX-dependence parameters. The results provide little evidence in favor of non-monotonicities, as the quadratic terms are generally statistically insignificant. A similar pattern emerges for the VIX-dependence parameters, which are also insignificant in most cases. By contrast, the linear coefficients associated with risk aversion, and thus with monotonic marginal utility, are consistently statistically significant.

Beyond hypothesis testing, I also examine whether the physical distributions implied by the four discount factors differ meaningfully from one another. To do so, I employ Kolmogorov–Smirnov tests for the pairwise equality of distribution functions. The results show that the monotonic pricing kernels, whether based on fixed or VIX-dependent parameters, generate very similar physical distributions, which are also close to those generated by the non-monotonic kernel with fixed parameters. By contrast, the only specification that yields substantially different physical densities is the non-monotonic pricing kernel with VIX-dependent parameters.

To further identify the sources of differences across physical distributions, I examine the relation, both in levels and in comovement, among the first four option-based physical moments: expected value, variance, skewness, and kurtosis, derived from the alternative discount factor specifications across expirations. With respect to expected returns, all kernels generate values that exceed those implied by the risk-neutral density. This outcome arises because the GMM estimation incorporates moment conditions that enforce equality between average option-based expected returns and average realized returns over the sample period.

Although variances are not target moments in the GMM estimation of the discount factors, their levels are consistent across kernels and broadly similar to, though lower than, the corresponding risk-neutral variance. Among the specifications, the non-monotonic kernel with VIX-dependent parameters generates the lowest forward-looking variance. Similar patterns hold for skewness and kurtosis: the VIX-dependent non-monotonic kernel yields the smallest values of these higher-order moments, reflecting the effect of time-varying parameters.

Beyond analyzing the levels of option-based physical moments, I also study their comovement using coefficients of determination (R^2) from pairwise regressions of each moment (mean, variance,

skewness, kurtosis) across pricing kernels. The results show that variances are highly correlated, both across discount factors and with the risk-neutral moments. By contrast, the odd physical moments, expected returns and skewness, are much less correlated across kernels and also display weaker links to their risk-neutral counterparts. This paper is the first to document that the effects of non-monotonicities and VIX-dependence differ across moments. Even moments, especially variances, are strongly correlated across discount factors, whereas odd moments diverge substantially.

To complement these novel empirical findings, I provide theoretical insights that clarify the differential effects of non-monotonicities and VIX-dependence on option-based physical moments. Specifically, I draw on tools from actuarial science, namely, the linear and quadratic Esscher transforms (Esscher (1932), Monfort and Pegoraro (2012)), and apply them under normal or skew-normal assumptions for the risk-neutral density. This framework illustrates how each pricing kernel maps a common risk-neutral distribution, which need not be normal, into distinct physical moments, thereby explaining the empirical patterns observed across kernels.

Building on these results, the second major issue addressed in this paper concerns the accuracy of risk-neutral bounds for expected returns. Having derived option-based distributions under the physical measure for four alternative pricing kernels across different horizons, I test whether the risk-neutral bounds proposed in the literature, i.e., bounds based on risk-neutral variances, can reliably capture expected returns under the physical measure.

Expected returns are inherently unobservable, and deriving them from option prices requires assumptions about the pricing kernel. To circumvent this challenge, the existing literature (e.g., Martin (2017), Schneider and Trojani (2019)) proposes that forward-looking expected returns can be inferred from option-based risk-neutral moments, such as the risk-neutral variance, through an approach that is nearly assumption-free.Importantly, Martin (2017) and Chabi-Yo and Loudis (2020) provide empirical evidence that risk-neutral bounds serve as accurate proxies for expected returns by regressing realized returns on these bounds. More recently, however, Back et al. (2022), using a different methodology, cast doubt on whether risk-neutral bounds are sufficiently tight to capture expected returns.

I further extend these regression tests for the accuracy of risk-neutral bounds along two dimensions. First, in addition to regressing realized returns on risk-neutral variances, a methodology widely used in the existing literature to validate risk-neutral bounds, I also regress option-based

expected returns from the alternative pricing kernels on risk-neutral variances. For robustness, I supplement these tests with backward-looking fitted returns, obtained from predictive regressions of realized returns on the dividend yield, dividend growth, and the risk-free rate. Finally, unlike most previous studies, which typically focus on a single maturity (most often 1 month), my empirical analysis spans multiple maturities, allowing me to evaluate how the investment horizon influences the accuracy of risk-neutral bounds.

Second, I provide summary statistics and correlations for the risk-neutral bounds to assess whether these bounds, namely, the risk-neutral variances, are aligned with average realized returns or with average expected returns derived from the option-based physical densities. Thirdly, since the literature interprets risk-neutral bounds as lower bounds for expected returns, I specifically examine whether there are instances in which the risk-neutral bounds exceed realized returns or option-based expected returns.

The results of this analysis highlight four key findings. First, longer option expirations weaken the tightness of risk-neutral bounds. Second, realized returns and backward-looking fitted returns are unsuitable for testing the accuracy of these bounds through regressions. If the bounds were truly binding, regressions of expected returns on risk-neutral bounds would imply high R^2 values and strong explanatory power. Instead, regressions using realized or fitted returns yield near-zero fit, extremely large standard errors, and frequent violations of the strictly positive risk-neutral lower bounds, since realized returns can take negative values.

Third, for the baseline monotonic power utility pricing kernel with constant parameters, regressions of option-based expected returns on risk-neutral variances yield slope estimates close to one (approximately 1.2–1.3), intercepts near zero (around 0.01%), and very high explanatory power with R^2 values near 99%. These results suggest that, even though the slope coefficients are not exactly equal to one, risk-neutral variances serve as accurate proxies for expected returns implied by the standard monotonic power-utility kernel with constant parameters. This evidence stands in contrast to Back et al. (2022), who argue that risk-neutral bounds are not binding.

Fourth, for discount factors with VIX-dependent coefficients, regressions of option-based expected returns on risk-neutral bounds generate statistically significant intercepts and slope estimates that differ from one. This indicates that, in these cases, the risk-neutral bounds are not binding, regardless of whether the discount factor is monotonic or non-monotonic. Interestingly, non-

monotonicity does not affect the tightness of risk-neutral bounds as strongly as VIX-dependence. Expected returns derived from the fixed-parameter non-monotonic pricing kernel remain closely aligned with the risk-neutral variance bounds. The reason is that non-monotonicities occur only in regions of the return distribution that carry very low probabilities, typically in the extreme left or right tails, whereas VIX-dependence alters risk aversion across the entire distribution of returns.

Overall, this paper contributes to the growing literature that uses option markets to study investor preferences and evaluate the validity of competing macroeconomic asset pricing models. In particular, Ait-Sahalia and Lo (2000) and Rosenberg and Engle (2000) initiated a line of research on the monotonicity of discount factors implied by option prices, documenting that option-derived kernels can exhibit increasing regions over certain ranges of moneyness (i.e., U-shaped marginal utility). More recent studies, such as Linn et al. (2018) and Kim (2021), introduce conditional estimation of nonparametric discount factors across periods of high and low VIX, and, consistent with Barone-Adesi et al. (2020), find little evidence supporting non-monotonic marginal utility.

Beason and Schreindorfer (2022) use option prices to decompose risk premia and assess which macroeconomic asset pricing models, such as long-run risk, habit formation, or disappointment aversion, are most consistent with the data. Chabi-Yo et al. (2022) extend this framework to conditional risk premia. In closely related work, Heston et al. (2023) estimate option-based pricing kernels under restrictions such as monotonicity and path-independence (recovery theory), achieving both accurate option fits and reasonable estimates of equity and variance risk premia, while addressing long-standing pricing kernel anomalies.

The findings in this paper complement the above work by jointly examining the implied physical densities derived from four different pricing kernels across multiple option maturities. In particular, my empirical analysis isolates the distinct effects of non-monotonicity and VIX-dependence on the physical distributions by analyzing their impact on the first four moments—mean, variance, skewness, and kurtosis—under the physical measure. Importantly, this is among the first papers to provide a theoretical explanation for these effects, drawing on results from actuarial science through Esscher transforms (Esscher (1932), Monfort and Pegoraro (2012)) and incorporating skew-normal assumptions for the risk-neutral density.

Regarding risk-neutral bounds for expected returns, Martin (2017) establishes the link between risk-neutral variance and expected returns for the aggregate stock market. Chabi-Yo and Loudis

(2020) extend this framework by incorporating higher-order risk-neutral moments, while Martin and Wagner (2019) derive the relation between risk premia and risk-neutral moments at the individual stock level. More broadly, Schneider (2019) and Schneider and Trojani (2019) generalize the concept of risk-neutral bounds to encompass higher-order physical moments.

Back et al. (2022) conduct a comprehensive empirical investigation of risk-neutral bounds and conclude that, although the bounds are correctly signed, i.e., lower bounds, they are not binding. Gandhi et al. (2023) compare option-based expected returns with survey-based expectations (UBS/Gallup Investor Optimism Survey, Duke's CFO survey) and show that the two measures differ substantially. My analysis focuses on the option-based risk-neutral variance bounds of Martin (2017) for two reasons. First, subsequent extensions that incorporate higher-order moments (e.g., Chabi-Yo and Loudis (2020)) yield results that are nearly identical to Martin (2017). Second, the bounds in Martin (2017) remain widely used in the literature (e.g., Gandhi et al. (2023)).

In a related paper, Schreindorfer and Sischert (2025) derive physical densities to evaluate the validity of leading macroeconomic asset pricing models (e.g., habit formation, rare disasters, etc.). They also present results on the accuracy of risk-neutral bounds. Similar to Schreindorfer and Sischert (2025), I study the validity of risk-neutral bounds by examining their summary statistics, comparing them to those of realized and option-based expected returns, and analyzing the frequency with which expected returns violate the bounds. My contribution relative to Schreindorfer and Sischert (2025) is twofold. First, I formally regress expected returns on risk-neutral variances to directly assess the tightness of the lower bound and provide comparative results across alternative pricing kernel specifications. Second, I consider a cross-section of option expirations, which allows me to draw conclusions about the role of investment horizon in the accuracy of the bounds, an aspect absent from Schreindorfer and Sischert (2025), who focus only on a single maturity.

These methodological differences yield a richer set of conclusions regarding the accuracy of risk-neutral bounds. Specifically, I find that their accuracy depends on option maturity and the time variation of risk aversion, but not on the monotonicity of the pricing kernel. Although risk-neutral bounds are not perfect, particularly at longer maturities (e.g., 6-months) or under VIX-dependent specifications, my results show that they outperform alternative measures of expected returns, such as averages of realized returns or fitted values from predictive regressions (e.g., price–dividend ratio, dividend growth). This advantage stems from the forward-looking nature of option-based bounds.

2 Theoretical Background

To set the stage for the empirical analysis of how alternative stochastic discount factors affect moments under the physical measure and the accuracy of risk-neutral bounds for expected returns, I introduce the pricing kernels used to derive option-based moments. These discount factors are broadly classified into monotonic and non-monotonic specifications. For each class, I consider both constant-parameter and time-varying versions.

2.1 Monotonic Pricing Kernel

The baseline specification used in my tests is the power utility discount factor defined over stock market wealth W_t:

$$U(W_t) = \frac{W_t^{1-\gamma_1}}{1-\gamma_1}.$$

Based on the above functional form, the intertemporal marginal rate of substitution between dates t and $t+T$ is given by

$$M_{1,t,t+T}(R_{t,t+T}) = \beta \frac{U'(W_{t+T})}{U'(W_t)} \quad = \quad exp\{log\beta - \gamma_1 lnR_{t,t+T}\}. \tag{1}$$

The constant β is the rate of time preference, and $R_{t,t+T} = \frac{W_{t+T}}{W_t}$ is the return on total equity wealth. The parameter $\gamma_1 > 0$ describes (relative) risk aversion since

$$-\frac{R_{t,t+T}}{M_{1,t,t+T}} \frac{\partial M_{1,t,t+T}}{\partial R_{t,t+T}} = \gamma_1.$$

A natural extension to the standard power-utility pricing kernel of equation (1) is to assume that risk aversion is time-varying depending on observable variables that are known at time t. To this end, Linn et al. (2018) and Kim (2021) introduce conditional estimation of their non-parametric discount factor during periods of high and low VIX values. Given the importance of the VIX in option-pricing and the recent results in Schreindorfer and Sischert (2025), I assume an extension of the monotonic pricing kernel of equation (1) for which γ_1 is time-varying with an explicit dependence on the VIX:

$$M_{2,t,t+T}(R_{t,t+T}) = \beta \frac{U_2'(W_{t+T})}{U_2'(W_t)} = exp\{log\beta - \gamma_1 nvix_{t,t+T}^{\gamma_3} lnR_{t,t+T}\}. \tag{2}$$

Risk aversion in the above discount factor is given by $\gamma_1 nvix_{t,t+T}^{\gamma_3}$, where $nvix_{t,t+T}$ is the VIX ($VIX_{t,t+T}$) normalized by its unconditional average ($\overline{VIX_{t,t+T}}$) and scaled by $\sqrt{T}$, the number of days in 1-, 2-, 3-, and 6-month intervals ($T \approx 30, 60, 90, 180$), over $\sqrt{365}$:

$$nvix_{t,t+T} = \frac{VIX_{t,t+T}\sqrt{T}}{\overline{VIX_{t,t+T}}\sqrt{365}}. \tag{3}$$

The intuition behind this specification is that investing in the stock market entails a natural level of risk, captured by average VIX. When VIX deviates from its average, risk aversion is affected according to the coefficients γ_1 and γ_3. Since VIX is expressed in percentage terms, I use $nvix_{t,t+T}^{\gamma_3}$ in equation (2) rather than $VIX_{t,t+T}^{\gamma_3}$ to avoid extreme values of risk aversion when VIX is low (high) and γ_3 is negative (positive). To eliminate look-ahead bias, the average VIX, $\overline{VIX}$ in equation (3), is estimated over the 1986–1995 period, prior to the start of the sample.[2] Hence, at time t, investors observe both the VIX and the normalized VIX ($nvix$).

Given the positivity of the VIX and $nvix$, a well-defined risk-aversion coefficient requires a positive γ_1. The parameter γ_3 captures the procyclicality of risk aversion with respect to $nvix$. For $\gamma_1 > 0$, a positive (negative) γ_3 implies that risk aversion is procyclical (countercyclical) with respect to $nvix$. Intuitively, γ_3 is expected to be positive, implying that risk aversion rises with $nvix$. For $\gamma_3 = 0$, equation (2) reduces to the case of constant risk aversion.

2.2 Non-monotonic Pricing Kernel

One debated feature of the option-implied pricing kernel is its monotonicity. While Linn et al. (2018) find no evidence supporting non-monotonicities in option-based marginal utility, several studies advocate for U-shaped discount factors (e.g., Ait-Sahalia and Lo (2000), Rosenberg and Engle (2000)). Motivated by recent findings in Schreindorfer and Sischert (2025) and Driessen et al.

[2]The resulting VIX averages are 5.356%, 7.818%, 10.186%, and 13.119% for the 1-, 2-, 3-, and 6-month maturities. VIX values prior to 1990 are fitted by regressing the VIX on the old-methodology VIX at the daily frequency. The regression estimates are: intercept = 0.240% (t-stat = 1.04), slope = 0.987 (t-stat = 71.01), $R^2 = 96\%$. Standard errors for these regressions are computed using a 30-lag Newey–West correction for autocorrelation and heteroscedasticity.

(2022), I also allow for non-monotonicities in the pricing kernel. Specifically, the non-monotonic kernel is modeled using a power utility function with a quadratic exponent.

Specifically, I assume the following quadratic stochastic discount factor

$$M_{3,t,t+T}(R_{t,t+T}) = exp\{log\beta - \gamma_1 lnR_{t,t+T} - \gamma_2 ln^2 R_{t,t+T}\}. \tag{4}$$

The non-monotonicity of the pricing kernel is captured by the squared term $\ln^2 R_{t,t+T}$ and the parameter γ_2. As shown in Sichert (2023), quadratic functions provide a flexible and accurate way to capture non-monotonicities in option-based pricing kernels.

According to Bakshi and Madan (2007) and Bakshi et al. (2010), a prominent interpretation of the quadratic term is that it captures the risk aversion of investors who are shorting the market. In this setting, the aggregate risk aversion coefficient across investors, those holding the market long and those shorting it, becomes state-dependent, varying with stock market conditions:

$$-\frac{R_{t,t+T}}{M_{3,t,t+T}}\frac{\partial M_{3,t,t+T}}{\partial R_{t,t+T}} = \gamma_1 + 2\gamma_2 lnR_{t,t+T}. \tag{5}$$

Based on the above relation, the coefficient γ_2 governs the procyclicality of risk aversion with respect to stock market returns. A positive (negative) γ_2 implies that risk aversion is procyclical (countercyclical) with the stock market.

Similar to the VIX-dependent monotonic model in equation (2), I extend the non-monotonic specification by allowing the quadratic preference parameters to depend on the normalized VIX ($nvix$). This discount factor is defined as

$$M_{4,t,t+T}(R_{t,t+T}) = \exp\log\beta - \gamma_1 nvix_{t,t+T}^{\gamma_3} \ln R_{t,t+T} - \gamma_2 nvix_{t,t+T}^{\gamma_3} \ln^2 R_{t,t+T}. \tag{6}$$

The dependence of this kernel on $nvix$ is governed by the constant γ_3. In this case, risk aversion depends jointly on the VIX and the stock market:

$$-\frac{R_{t,t+T}}{M_{4,t,t+T}}\frac{\partial M_{4,t,t+T}}{\partial R_{t,t+T}} = \gamma_1 nvix_{t,t+T}^{\gamma_3} + 2\gamma_2 nvix_{t,t+T}^{\gamma_3} \ln R_{t,t+T}. \tag{7}$$

Because the VIX is positive, the coefficient γ_2 in equation (6) determines the procyclicality of

risk aversion with respect to the stock market. As in the fixed-parameter non-monotonic kernel of equation (4), a positive (negative) γ_2 implies that risk aversion is procyclical (countercyclical). However, the introduction of the quadratic term complicates the relation between risk aversion and *nvix* making it conditional on the state of the stock market.

The baseline monotonic power utility model in equation (1) is among the most widely used utility functions in macroeconomics and finance. The alternative pricing kernels are motivated by two empirical regularities observed in options markets. First, the dependence of option-implied pricing kernels on the VIX has received considerable attention in the literature (e.g., Linn et al. (2018), Kim (2021)). Second, the role of non-monotonic (quadratic) terms in the pricing kernel remains debated, with evidence both in support (e.g., Schreindorfer and Sischert (2025), Driessen et al. (2022)) and against (e.g., Linn et al. (2018), Barone-Adesi et al. (2020)). Consequently, the quadratic specifications in equations (4) and (6) are not ad hoc. Instead, consistent with the comprehensive analysis of potential sources of non-monotonicities in Cuesdeanu and Jackwerth (2018), these specifications are both theoretically justified and empirically micro-founded.

In my analysis, the pricing kernels are estimated at investment horizons of one, two, three, and six months. The cross-section of maturities serves two purposes. First, to verify the robustness of results across horizons; and second, to capture the term-structure implications of preference parameters, as in Driessen et al. (2022). I adopt parametric specifications of the pricing kernel rather than nonparametric ones (e.g., Linn et al. (2018)) for two main reasons. First, parametric discount factors facilitate the derivation of risk–return relations in terms of structural parameters, such as risk aversion. Second, and more importantly, they allow an analysis of how specific features, such as non-monotonicities or time variation in parameters, shape the option-implied physical distributions. In general, the parametric specifications employed here are sufficiently flexible to accommodate a wide range of risk attitudes.

2.3 Estimation of the Pricing Kernel and the Forward-looking Physical Measure

In estimating physical moments across different pricing kernels, I assume that $Q(R)$ denotes the cumulative distribution function of gross equity returns R under the risk-neutral measure. The risk-neutral density can be recovered from option prices. Let $P(R)$ denote the forward-looking continuous cumulative distribution function of equity returns under the physical measure, with

$dP(R)/dQ(R)$ as the Radon–Nikodym derivative linking the two measures. Since the forward-looking physical measure is unobservable, I follow Linn et al. (2018), who show that under suitable conditions the Radon–Nikodym derivative is unique and equals the inverse of the discount factor.

$$\frac{dP_{t,t+T}(R)}{dQ_{t,t+T}(R)} = M_{t,t+T}(R)^{-1}. \tag{8}$$

The forward-looking physical measure can therefore be calculated as the product of the risk-neutral measure with the inverse of the pricing kernel

$$dP_{t,t+T}(R) = M_{t,t+T}(R)^{-1} dQ_{t,t+T}(R). \tag{9}$$

In general, the pricing kernel is unobservable. However, I use equations (1), (2), (4), and (6) within a GMM system to estimate the unknown parameters of the discount factor. To this end, I employ two sets of GMM moment conditions. The first, introduced by Linn et al. (2018), relies on the property that any continuous distribution is a standard uniform random variable, such that $P_{t,t+T}(R) \sim U[0,1]$. Accordingly, based on uniform moments, the following holds:

$$\mathbb{E}\Big[\Big(\int_0^{R^*_{t,t+T}} M_{t,t+T}(R)^{-1} dQ_{t,t+T}(R)\Big)^n\Big] = \frac{1}{n+1},\ n = 1, 2, ..., \tag{10}$$

where the variable $R^*_{t,t+T}$ above is the realized gross equity return between dates t and $t+T$.

The second set of target GMM moments is a rational expectations restriction where the unconditional averages of option-based expected returns under the physical measure are equal to the sample averages of realized returns $\big(\frac{1}{N}\sum_{i=1}^{N} R^*_{it,it+T}\big)$:

$$\mathbb{E}\Big[\int_0^{+\infty} R\ M_{t,t+T}(R)^{-1} dQ_{t,t+T}(R)\Big] = \frac{1}{N}\sum_{i=1}^{N} R^*_{it,it+T}. \tag{11}$$

By equating average realized returns with average expected returns, we establish a direct link between realized and option-based expected returns. The rational expectations condition in equation (11) is a natural extension under the physical measure. The key innovation relative to Linn et al. (2018) is including equation (11) in the GMM estimation of option-based discount factors.

The physical density should integrate to one ($\int_0^{+\infty} dP_{t,t+T}(R) = 1$) and the inverse of the pricing

kernel should also satisfy

$$1 = \int_0^{+\infty} M_{t,t+T}(R)^{-1} dQ_{t,t+T}(R), \ \forall t. \tag{12}$$

Dividing equations (8) and (12) by parts, we estimate a normalized version of the pricing kernel

$$dP_{t,t+T}(R) = \frac{M_{t,t+T}(R)^{-1}}{\int_0^{+\infty} M_{t,t+T}(R)^{-1} dQ_{t,t+T}(R)} dQ_{t,t+T}(R), \tag{13}$$

which ensures that the estimated parameters imply well-behaved conditional physical density functions for every date in the sample. Thus, the GMM system from equations (10) and (11) becomes

$$\begin{bmatrix} \mathbb{E}\Big[\Big(\frac{\int_0^{R^*_{t,t+T}} M_{t,t+T}(R)^{-1} dQ_{t,t+T}(R)}{\int_0^{+\infty} M_{t,t+T}(R)^{-1} dQ_{t,t+T}(R)}\Big)^n\Big] - \frac{1}{n+1}, \ n = 1, 2, ..., \\ \mathbb{E}\Big[\frac{\int_0^{+\infty} R \ M_{t,t+T}(R)^{-1} dQ_{t,t+T}(R)}{\int_0^{+\infty} M_{t,t+T}(R)^{-1} dQ_{t,t+T}(R)}\Big] - \frac{1}{N}\sum_{i=1}^N R^*_{it,it+T} \end{bmatrix}. \tag{14}$$

As in Bliss and Panigirtzoglou (2004), due to normalization, the discount rate parameter β in equations (1), (2), (4), and (6) cannot be identified and will be dropped. The normalization in equation (14) is equivalent to imposing an additional parameter in the discount factor as in Schreindorfer and Sischert (2025) that forces the estimated physical densities to integrate to one. Further details about the GMM estimation (e.g., weighting matrix, standard errors) are reported in Section C of the Online Appendix.

After estimating the preference parameters via GMM, I obtain the option-based physical measure by multiplying the inverse of the estimated pricing kernel with the option-implied risk-neutral density. From the standard definition of moments, it then follows that the option-based physical density, the corresponding distribution function, and the associated physical moments are given by

$$\begin{aligned} dP_{t,t+T}(R)/dR &= \frac{M_{t,t+T}(R)^{-1} dQ_{t,t+T}(R)}{\int_0^{+\infty} M_{t,t+T}(R)^{-1} dQ_{t,t+T}(R)} / dR \\ P_{t,t+T}(R^*_{t,t+T}) &= \frac{\int_0^{R^*_{t,t+T}} M_{t,t+T}(R)^{-1} dQ_{t,t+T}(R)}{\int_0^{+\infty} M_{t,t+T}(R)^{-1} dQ_{t,t+T}(R)} \\ \mathbb{E}_t[R_{t,t+T}] &= \frac{\int_0^{+\infty} R \ M_{t,t+T}(R)^{-1} dQ_{t,t+T}(R)}{\int_0^{+\infty} M_{t,t+T}(R)^{-1} dQ_{t,t+T}(R)} \\ var_t(R_{t,t+T}) &= \frac{\int_0^{+\infty} (R - \mathbb{E}_t[R])^2 \ M_{t,t+T}(R)^{-1} dQ_{t,t+T}(R)}{\int_0^{+\infty} M_{t,t+T}(R)^{-1} dQ_{t,t+T}(R)} \end{aligned} \tag{15}$$

$$
\begin{aligned}
skew_t((R)_{t,t+T}) &= \frac{\int_0^{+\infty}(R-\mathbb{E}_t[R])^3\ M_{t,t+T}(R)^{-1}dQ_{t,t+T}(R)}{var_t(R_{t,t+T})^{3/2}\int_0^{+\infty}M_{t,t+T}(R)^{-1}dQ_{t,t+T}(R)} \\
kurt_t(R_{t,t+T}) &= \frac{\int_0^{+\infty}(R-\mathbb{E}_t[R])^4\ M_{t,t+T}(R)^{-1}dQ_{t,t+T}(R)}{var_t(R_{t,t+T})^{4/2}\int_0^{+\infty}M_{t,t+T}(R)^{-1}dQ_{t,t+T}(R)}.
\end{aligned}
$$

The same approach, but without the term $\frac{M_{t,t+T}(R)^{-1}}{\int_0^{+\infty}M_{t,t+T}(R)^{-1}dQ_{t,t+T}(R)}$, is used to compute the moments of the risk-neutral density. Finally, log-return moments are obtained by replacing $(R-\mathbb{E}t[R])^n$ with $(\ln R - \mathbb{E}t[\ln R])^n$, for both the physical and risk-neutral measures.

3 Option Data and the Risk-Neutral Density

In this section, I describe the options data employed in the empirical analysis, which investigates how alternative pricing kernels affect the moments of the physical distribution and the accuracy of risk-neutral bounds for expected returns.

3.1 Data

The sample of S&P500 option contracts for different expirations (1-, 2-, 3-, and 6-months) is from OptionMetrics and is summarized in Table OA.1 of the Online Appendix. High-frequency options (0DTEs) are excluded to ensure that the dataset spans a long time series covering major events such as the Great Recession and the COVID-19 pandemic. To construct the sample, I impose the following selection criteria: non-missing implied volatility, positive trading volume, and a bid price above \$3/8. Further, each date is included in the sample only if there are at least six option contracts outside the $\pm 2\%$ moneyness range, with a minimum of three puts and three calls.

At the beginning of the sample, two non-consecutive 2-month observations and eleven non-consecutive 3-month observations were dropped because the risk-neutral distributions could not be estimated given insufficient option contracts satisfying the selection criteria. Further, consecutive observations are required to compute autocorrelations for Newey–West standard errors in the GMM estimation, which led to the removal of additional early observations for the 2- and 3-month maturities. The final sample spans January 1996–December 2022 (1-month), May 1998–November 2022 (2-month), January 2002–October 2022 (3-month), and June 1996–June 2022 (6-month) options.

4 Estimation of the Alternative Pricing Kernels

Using the GMM estimation methodology in Section 2.3 and the RNDs from Section D of the Online Appendix, I estimate the parameters of the discount factors in equations (1), (2), (4), and (6). The estimated pricing kernels allow me to analyze how non-monotonicities and VIX dependence affect physical moments and the accuracy of risk-neutral bounds for expected returns.

4.1 Monotonic Pricing Kernels

Panel A of Table 1 reports estimates for the standard monotonic power utility model from equation (1). The risk-aversion parameter is positive across all expirations, ranging from 1.266 (2-month) to 1.524 (6-month). These estimates are consistent with Bliss and Panigirtzoglou (2004) and suggest that risk aversion is stable across maturities.

Panel B of Table 1 reports results for the monotonic pricing kernel with time-varying risk-aversion coefficients that depend on the normalized VIX ($nvix$) from equation (2). The γ_1 estimates are positive across all expirations, indicating positive risk aversion. For 1-month options, γ_1 is 0.518, while for the 2-, 3-, and 6-month options the estimates range from 1.295 to 1.661. The discrepancies in γ_1 across maturities can be attributed to the parameter governing the dependence of risk aversion on $nvix$, γ_3. This coefficient is positive for the 1-month horizon (1.936) but negative (between –0.817 and –0.558) for the longer expirations.

These estimates imply that risk aversion is procyclical with respect to the VIX for the 1-month expiration but countercyclical for the longer maturities. The increase in risk aversion with VIX at the 1-month horizon is intuitive, whereas the decline in risk aversion with VIX for 2-, 3- and 6-months expirations is puzzling. However, this result is consistent with the evidence in Schreindorfer and Sischert (2025), who document countercyclical risk aversion with respect to the VIX.

4.2 Non-Monotonic Pricing Kernels

Panel A of Table 1 reports GMM estimates for the non-monotonic discount factor in equation (4) with constant parameters. For the 1-month expiration, the linear coefficient γ_1 is positive (0.814) and the quadratic parameter γ_2 is negative (–7.412). This implies that risk aversion is countercyclical with respect to market returns (equation (5)) and that marginal utility is U-shaped.

By contrast, for the 2-, 3-, and 6-month expirations, both the linear coefficient γ_1 (1.386–1.672) and the quadratic coefficient γ_2 (0.334–0.779) are positive. According to equation (5), this implies procyclical risk aversion and an inverse U-shaped marginal utility. Although the procyclicality of risk aversion with respect to the stock market at these maturities may seem counterintuitive, it is consistent with the countercyclicality of risk aversion with respect to *nvix* in the VIX-dependent model of equation (2), as documented in Panel A of Table 1.

Finally, Panel B of Table 1 reports GMM estimates for the non-monotonic pricing kernel with VIX-dependent parameters from equation (6). Across all expirations, the linear coefficient γ_1 is positive (0.129–1.991) while the quadratic parameter γ_2 is negative (–47.470 to –2.143) . These estimates imply U-shaped marginal utility and countercyclical risk aversion with respect to the stock market. The parameter γ_3, which governs the dependence of the linear and quadratic coefficients on *nvix*, is also negative (γ_3 = –9.720 to –4.421). However, negative estimates of γ_3 do not necessarily imply that risk aversion decreases with *nvix*. As shown in equation (7), the cyclicality of risk aversion with respect to *nvix* in the VIX-dependent non-monotonic kernel depends jointly on both volatility and stock market returns.

Based on *t*-statistics in Table 1, the option-implied pricing kernel is most likely monotonic, as the quadratic terms are generally insignificant. The *t*-statistics for the linear coefficient γ_1 in the pricing kernels of equations (1), (2), and (6), range from 4.43 to 6.83 in Panel A, 0.31 to 5.12 in Panel B, and 0.23 to 4.08 in Panel D. These values are, on average, much larger in absolute magnitude than those for the quadratic coefficients γ_2 (–1.38 to 1.83 in Panels C and D). Regarding VIX dependence, the evidence generally supports VIX-independence, with the exception of two cases for the non-monotonic VIX-dependent kernel of equation (6), the 1- and 2-month maturities in Panel D. In this case, *t*-statistics for γ_3 are –2.21 and –2.29. For all other expirations in Panels B and D, the estimates of the VIX-dependence parameter γ_3 are statistically insignificant.

Figure 1 plots the pricing kernels implied by the GMM estimates in Table 1. For the VIX-dependent specifications in the graph, *nvix* is set equal to its sample average for each expiration. All discount factors are monotonically decreasing over most values of moneyness with the exception of the 2-, 3-, and 6-month expirations of the fixed-parameter non-monotonic kernel (equation (4)). In these expirations, the fixed-parameter non-monotonic kernel takes an inverse U-shape because both the linear coefficient γ_1 and the quadratic coefficient γ_2 are positive (Table 1, Panel A).

However, the upward-sloping region corresponds to extremely low returns (–100% to –50%) that receive negligible probability mass in practice. Across the range of realistic market returns (–50% to 30%), the non-monotonic kernel of equation (4) is decreasing.

The VIX-dependent non-monotonic specification in equation (6) is decreasing for most values of moneyness, with a small increasing region corresponding to large positive market returns. The U-shape of this kernel arises because the quadratic parameter γ_2 is negative (Table 1). As shown in equation (7), when γ_2 is negative and market returns are large enough, risk aversion becomes negative. In this case, the pricing kernel slopes upward, and the risk–return relation turns negative.

Overall, pricing kernel estimates are consistent across option expirations, with the notable exception of the fixed-parameter quadratic pricing kernel, whose shape shifts from U-shaped at the 1-month maturity to inverse U-shaped at longer maturities. Regardless of whether the non-monotonic pricing kernels are U-shaped or inverse U-shaped, these features arise only at extremely high or low returns, which lie in the far tails of the distribution and receive near-zero probability mass. This suggests that non-monotonicities may have limited influence on the moments of the physical density. We examine this conjecture in the empirical analysis below, where we compare physical densities and corresponding moments implied by the alternative pricing kernels, regardless of the statistical significance of their coefficients.

5 Physical Densities from Alternative Pricing Kernels

Using the estimated discount factors from the previous section, I derive option-based physical densities and moments for gross returns according to equation (15). These densities, obtained under alternative pricing kernels, allow me to assess how different functional forms of the kernel affect physical moments and the accuracy of risk-neutral bounds for expected returns. For comparison, I also construct the distribution and density of realized returns by fitting a kernel-density estimator to the realized return series and interpolating values over the full moneyness range with a piecewise cubic Hermite polynomial.

Figure 2 plots average option-based physical densities across pricing kernels and expirations to verify that these densities are well defined. Most of the physical distributions appear broadly similar, with the main exceptions being the density implied by the non-monotonic VIX-dependent

kernel of equation (6) and the density of realized returns. To this end, I conduct pairwise Kolmogorov–Smirnov test to examine equality of option-based physical distributions across discount factors.[3] I also compare option-based physical distributions with both the risk-neutral distribution and the distribution of realized returns.

5.1 Kolmogorov-Smirnov Tests

Results for the Kolmogorov–Smirnov are reported in Table 2, where option-based physical densities are identified by the exponents of the corresponding discount factors: $\gamma_1 r$ for equation (1), $\gamma_1 nvix^{\gamma_3} r$ for equation (2), $\gamma_1 r + \gamma_2 r^2$ for equation (4), and $\gamma_1 nvix^{\gamma_3} r + \gamma_2 nvix^{\gamma_4} r^2$ for equation (6). Based on the percentage of rejections over the sample period, the most similar densities are those from the two monotonic specifications (equations (1) and (2)), with rejection rates ranging from 3% (2-month) to 23% (6-month).

The option-based physical distributions from the non-monotonic model with fixed parameters (equation (4)) are somewhat similar to those from the monotonic specifications with rejections of the Kolmogorov-Smirnov tests ranging from 2% (2-month) to 77% (1-month). In contrast, the option-based distributions from the non-monotonic discount factor with VIX-dependent parameters (equation (6)) are substantially different from the rest of the distributions with very high rejection percentages (84% to 96%) across all expirations. In other words, either allowing for non-monotonicities with constant parameters or introducing VIX dependence in a monotonic kernel yields distributions close to the benchmark monotonic specification. On the contrary, combining non-monotonicities with VIX-dependent parameters results in distributions that differ markedly from all others.

According to the results in Table 2, all specifications yield physical distributions that differ from the risk-neutral measure, with Kolmogorov–Smirnov rejection rates ranging from 23% to 100%. Further, option-based physical distributions are quite different from the distribution of realized returns across all discount factors and maturities. To explore which moments drive the rejections of Kolmogorov–Smirnov test, I next compare the levels and comovement of the first four moments of the physical distributions across the various pricing kernels.

[3] In untabulated results, I also implement the Cramér–von Mises test, which yields similar conclusions.

5.2 Moments of the Physical Distribution

Table 3 reports summary statistics for the first four moments of option-based physical distributions across expirations and pricing kernels. Table 3 also reports summary statistics for the first four moments of the risk-neutral distribution, as well as the first four sample moments of the distribution for realized returns.

Panel A reports results for expected returns across distributions. All discount factors imply identical average expected returns, ranging from 0.61% (1-month) to 4.25% (6-month). These values match average realized returns, since this moment enters the GMM objective function (equation (2.3)). Expected returns under the physical measure are uniformly higher than those under the risk-neutral measure, which range from –0.06% (1-month) to 0.46% (6-month). While average expected returns are identical across kernels, volatility of expected returns differs substantially. In particular, the VIX-dependent non-monotonic model of equation (6) yields systematically lower volatility than the remaining specifications across maturities, with the exception of the 3-month horizon, where the lowest volatility of expected returns is generated by the VIX-dependent monotonic kernel.

Panel B of Table 3 reports results for variances from the option-based physical densities across discount factors and maturities. Although variance is not a target moment in the GMM estimation, the implied physical variances are broadly consistent across kernels—ranging from 0.34%–0.43% (1-month) to 1.33%–2.23% (6-month), and are uniformly lower than their risk-neutral counterparts. The option-based physical densities also imply average variances larger than the sample variance of realized returns (0.24% for 1-month to 1.13% for 6-month). Among the various discount factor specifications, the non-monotonic kernel with VIX-dependent parameters (equation (6)) generates the lowest physical variances.

Panel C of Table 3 reports results for physical skewness, which is negative across all expirations and discount factors (–1.45 to –0.59 for 1-month and –0.91 to –0.15 for 6-month). Option-based physical skewness is uniformly smaller in absolute value than its risk-neutral counterpart. Consistent with the variance results, the non-monotonic VIX-dependent model (equation (6)) generates the lowest absolute skewness (–0.59 for 1-month to –0.15 for 6-month). By contrast, the remaining kernels imply physical skewness values that are broadly similar in magnitude, though smaller, to the risk-neutral skewness. Results for physical kurtosis in Panel D of Table 3 reveal a similar pat-

tern. The lowest values for physical kurtosis (3.24 for 6-month to 4.37 for 1-month) are generated by the non-monotonic VIX-dependent discount factor.

In general, risk-neutral densities exhibit negative skewness (–1.51 for 1-month to –0.98 for 6-month) and positive excess kurtosis (7.67 for 1-month to 4.99 for 6-month). These features carry over to the physical densities. Notably, the non-monotonic specification with VIX-dependent parameters implies the least negative skewness and the lowest excess kurtosis under the physical measure. Finally, Table OA.3 in the Online Appendix reports moments for the physical and risk-neutral distributions of log-returns ($\ln R_{t,t+T}$). The results are qualitatively similar to those in Table 3, with the key difference that skewness and kurtosis for log-returns are larger (in absolute value) than for gross returns.

The different discount factors generate plausible and consistent higher-order moments. In particular, risk-neutral variance and skewness exceed their physical counterparts in all cases, while risk-neutral kurtosis is broadly similar to the physical one. The VIX-dependent non-monotonic kernel of equation (6) stands out by generating the lowest higher-order moments across specifications and by generating moments with the least time variation.

This arises because combining non-monotonicity with VIX-dependence yields a discount factor whose time-series variability is substantially greater than that of specifications featuring only non-monotonicities or only VIX-dependence. The pronounced variation of the non-monotonic VIX-dependent pricing kernel soaks up most of the time variation of the risk-neutral density, and the result is a fairly stable physical distribution. This might be an important argument regarding the plausibility of this kernel.

5.3 Coefficients of Determination for Physical Moments

To complement the analysis on the magnitude of the first four moments of the option-based physical densities, Table 4 reports adjusted coefficients of determination (R^2) from regressions of physical moments across pricing kernels and the risk-neutral measure:

$$moment_{j,t} = a + b \cdot moment_{k,t} + \eta_{j,k,t}. \tag{16}$$

Above, $moment_{j,t}$ denotes the physical moment (mean, variance, skewness, kurtosis) of pricing kernel j at time t, and $moment_{k,t}$ is the corresponding moment from pricing kernel k at time t. These regressions assess the comovement of option-based physical moments implied by alternative discount factors.

The most striking result in Table 4 is that physical variance is nearly perfectly correlated across all four discount factors and the risk-neutral density, with R^2s ranging from 82% to 99%. By contrast, the greatest divergence occurs for expected returns, where average R^2 values fall between 33% and 43% across expirations (42%–50% when excluding regressions against risk-neutral expected returns). Skewness and kurtosis also exhibit considerable divergence across discount factors, but this divergence is mainly driven by the VIX-dependent non-monotonic kernel.

More specifically, the results from Table 4 suggest that expected returns, skewness, and kurtosis are strongly correlated (R^2 values from 62% to 99%) across the monotonic pricing kernels of equations (1) and (2), and remain highly correlated (R^2 values from 54% to 99%) with the moments of the fixed-parameter non-monotonic kernel of equation (4). In contrast, the corresponding moments from the VIX-dependent non-monotonic kernel (equation (6)) are largely orthogonal to those of the other kernels, with R^2 values ranging only from 0% to 23%.

This is one of the first papers to demonstrate that the effects of monotonic and non-monotonic pricing kernels vary considerably across moments. Option-implied variances are strongly correlated across discount factors, whereas other moments, particularly odd moments such as expected returns and skewness, differ markedly. The contrast between odd and even moments is illustrated in Table 5, which reports the coefficients of determination across pricing kernels for the third and fourth central moments (skewness and kurtosis, excluding variance scaling).

The average R^2 for third moments ranges from 46% (1-month) to 86% (3-month), while the average R^2 for fourth moments ranges from 87% (1-month) to 93% (3-month). Across all expirations, comovement in fourth moments is much stronger than in third moments. Thus, Table 4 and Table 5 underscore the differential effects of the various pricing kernels across odd and even moments. Even moments, especially variances, are highly correlated across specifications, whereas odd moments exhibit a weaker relationship.[4]

[4]Table OA.4 and Table OA.5 report adjusted R^2 values from regressions of option-based physical moments for log-returns across pricing kernels. The results are qualitatively similar to those presented here for gross returns.

The results in Table 3 and Table 4 suggest that the fixed-parameter monotonic kernel (equation (1)), the VIX-dependent monotonic kernel (equation (2)), and the fixed-parameter non-monotonic kernel (equation (4)) generate broadly similar moments, which are strongly correlated. By contrast, the non-monotonic kernel with VIX-dependent parameters generates physical moments that are almost orthogonal to those implied by the other specifications. The only exception is physical variance, which is strongly correlated across all discount factors, including the VIX-dependent non-monotonic model.

Overall, Table 3 and Table 4 show that non-monotonicity (equation (4)) or VIX-dependence (equation (2)) alone yields physical moments that are similar to those generated by the standard fixed-parameter monotonic kernel (equation (1)). It is only when non-monotonicity is combined with VIX-dependence that the resulting physical distribution becomes distinctly different from those implied by the other discount factors.

5.4 Pricing Kernels and Moments of the Physical Distribution: Theoretical Explanation

The empirical findings for the effects of non-monotonicities and VIX-dependence on physical moments can be interpreted using standard results from the normal distribution. The theoretical results in this section focus on log-return moments derived from log-normal and skew log-normal distributions. These results can be extended to gross returns by the approximation $\ln R \approx R - 1$ or by applying the exact formulas of the log-normal distribution.[5]

In actuarial science, the monotonic utilities in equations (1) and (2), together with the normalization in equation (13), correspond to the linear Esscher transform (Esscher (1932)). More recently, Monfort and Pegoraro (2012) introduced the second-order Esscher transform, which relates to the quadratic pricing kernels of equations (4) and (6). Within this framework, if the risk-neutral density for log-returns is normal with mean $\widetilde{r}^{f}_{t,t+T}$ and variance $\sigma^2_{RND,t,t+T}$, then the monotonic discount factors in equations (1) and (2) preserve normality and generate physical densities with mean and variance given by

[5]For consistency with the theoretical discussion of log-returns, I replicate the empirical analysis for log-returns in the Online Appendix.

$$\mathbb{E}_t[\ln R_{t,t+T}] = \widetilde{r}^f_{t,t+T} + \gamma_{1,t}\sigma^2_{RND,t,t+T}, \tag{17}$$

$$var\big(\ln R_{t,t+T}\big) = \sigma^2_{RND,t,t+T}. \tag{18}$$

Above, $\gamma_{1,t}$ captures risk aversion, either as a fixed parameter ($\gamma_{1,t} = \gamma_1$, equation (1)) or as a time-varying coefficient ($\gamma_{1,t} = \gamma_1 nvix^{\gamma_3}_{t,t+T}$, equation (2)). Thus, under normality of the risk-neutral density, linear discount factors, whether constant or VIX-dependent, shift expected returns by $\gamma_{1,t}\sigma^2_{RND,t,t+T}$ and leave the variance unchanged (Section E.1 of the Online Appendix). This explains why option-based expected returns and variances are nearly identical, both in levels (Table 3) and in comovement (Table 4), across the two monotonic pricing kernels.

On the other hand, when the risk-neutral density is normal, the quadratic pricing kernels of equations (4) and (6) preserve normality but modify both the mean and variance of log-returns. As shown in Section E.1 of the Online Appendix, if the risk-neutral density for log-returns is normal, then quadratic discount factors, with either constant or time-varying coefficients, yield physical densities with mean and variance given by

$$\mathbb{E}_t[\ln R_{t,t+T}] = \frac{\widetilde{r}^f_{t,t+T} + \gamma_{1,t}\sigma^2_{RND,t,t+T}}{1 - 2\gamma_{2,t}\sigma^2_{RND,t,t+T}}, \tag{19}$$

$$var_t\big(\ln R_{t,t+T}\big) = \frac{\sigma^2_{RND,t,t+T}}{1 - 2\gamma_{2,t}\sigma^2_{RND,t,t+T}}. \tag{20}$$

In this setting, the physical variance is lower than the risk-neutral variance only when the quadratic coefficient $\gamma_{2,t}$ is negative.

The fixed-parameter non-monotonic kernel in equation (4) for 1-month options and the VIX-dependent non-monotonic kernel in equation (6) across all maturities are characterized by negative $\gamma_{2,t}$ parameters (Table 1). According to equations (5) and (20), these specifications imply risk aversion that is countercyclical to market returns and generate physical variances below the risk-neutral counterparts (Table 3). By contrast, the fixed-parameter non-monotonic kernel of equation (4) with positive $\gamma_{2,t}$ coefficients at the 2-, 3-, and 6-month maturities (Table 1, Panel A) implies procyclical risk aversion (equation (5)) and relatively large physical variances (e.g., Table 3 and Table OA.3 in the Online Appendix).

Further, the denominator in equation (20), $1-\gamma_{2,t}\sigma^2_{RND,t,t+T}$, is close to one for both the fixed and VIX-dependent specifications because $\sigma^2_{RND,t,t+T}$ takes relatively small values (Table 3). This helps explain the results in Table 3 and Table 4 for gross returns (Table OA.3 and Table OA.4 in the Online Appendix for log-returns), which show that physical variances are very similar across pricing kernels and highly correlated with each other as well as with the risk-neutral variance.

Average expected returns are identical across pricing kernels (Table 3), since they are imposed in the GMM estimation (equation (14)). Nevrtheless, conditional expected returns differ across kernels and from the risk-neutral density (Table 4) because of the $\gamma_{1,t}\sigma^2_{RND,t,t+T}$ term in equation (17) and in the numerator of equation (19). In particular, for the non-monotonic VIX-dependent kernel of equation (6), the non-linear structure of equation (19) is amplified by VIX dependence. As a result, expected returns implied by this specification are almost orthogonal to those of the other discount factors (Table 4), even though their average levels are identical across pricing kernels and coincide with realized returns (Table 3).

As shown in Table 3 (and Table OA.3 in the Online Appendix), risk-neutral densities for gross and log-returns are negatively skewed and exhibit excess kurtosis across all maturities. Thus, while the assumption of normality is useful for deriving intuition, it is also restrictive. To address this, I re-examine the results in Table 3 and Table 4 for gross returns under the assumption that the risk-neutral density follows a skewed log-normal distribution, with location, scale, and shape parameters ω_t, σ_t, λ_t, and θ_t, respectively. Under the log skew-normal specification of Henze (1986), the density function, up to a normalization constant, is given by

$$dQ_t(R) = \frac{1}{R} Exp\Big[\frac{lnR-\omega_t}{2\sigma_t^2}\Big]\Phi\Big(\lambda_t\frac{lnR-\omega_t}{\sigma_t}+\xi_t\Big).$$

The sign of λ_t determines the sign of skewness, while the parameter $\xi_t(>0)$ amplifies skewness and kurtosis. In this case, the risk-neutral expected log-return is

$$\mathbb{E}_t^{RND}[lnR_{t,t+T}] = \omega_t + \frac{\lambda_t}{\sqrt{1+\lambda_t^2}}\frac{\phi\big(-\frac{\xi_t}{\sqrt{1+\lambda_t^2}}\big)}{1-\Phi\big(-\frac{\xi_t}{\sqrt{1+\lambda_t^2}}\big)}\sigma_t, \tag{21}$$

where $\phi(x)/(1-\Phi(x))$ is the inverse Mills ratio. Based on the risk-neutral moments of gross returns in Table 3 and log-returns in Table OA.3 of the Online Appendix, λ_t should be negative and ξ_t

should be positive for the option-based RND's across all expirations.

As shown in Section E.6 of the Online Appendix, applying a linear pricing kernel with positive risk-aversion parameter $\gamma_{1,t}$ to the above skew log-normal RND implies that the mean under the physical density becomes

$$\mathbb{E}_t[lnR_{t,t+T}] = \omega_t + \gamma_{1,t}\sigma_t^2 + \frac{\lambda_t}{\sqrt{1+\lambda_t^2}} \frac{\phi\big(-\frac{\xi_t+\lambda_t\gamma_{1,t}\sigma_t^2}{\sqrt{1+\lambda_t^2}}\big)}{1-\Phi\big(-\frac{\xi_t+\lambda_t\gamma_{1,t}\sigma_t^2}{\sqrt{1+\lambda_t^2}}\big)}\sigma_t. \tag{22}$$

Hence, under non-normality, the linear pricing kernel increases the risk-neutral expected return by the term $\gamma_{1,t}\sigma_t^2$, as in the case of a normal RND (equation (17)), and by increasing the negative skewness term in equation (21)

$$\frac{\lambda_t}{\sqrt{1+\lambda_t^2}} \frac{\phi\big(-\frac{\xi_t}{\sqrt{1+\lambda_t^2}}\big)}{1-\Phi\big(-\frac{\xi_t}{\sqrt{1+\lambda_t^2}}\big)}\sigma_t < \frac{\lambda_t}{\sqrt{1+\lambda_t^2}} \frac{\phi\big(-\frac{\xi_t+\lambda_t\gamma_{1,t}\sigma_t^2}{\sqrt{1+\lambda_t^2}}\big)}{1-\Phi\big(-\frac{\xi_t+\lambda_t\gamma_{1,t}\sigma_t^2}{\sqrt{1+\lambda_t^2}}\big)}\sigma_t. \tag{23}$$

Since the parameter λ_t is negative for a negatively skewed RND, and the inverse Mills ratio is positive and monotonically increasing (Section E.5 in the Online Appendix), the terms in equation (23) are negative. A positive risk aversion coefficient $\gamma_{1,t}$, combined with a negative λ_t, reduces the argument in the inverse Mills ratio from $\frac{\xi_t}{\sqrt{1+\lambda_t^2}}$ to $\frac{\xi_t+\lambda_t\gamma_{1,t}\sigma_t^2}{\sqrt{1+\lambda_t^2}}$. Given the monotonicity of the inverse Mills ratio, decreasing its argument diminishes the absolute value of the negative term in equation (23), thereby increasing the expected value under the physical measure (equation (22)) relative to the risk-neutral expected value (equation (21)).

Section E.6 in the Online Appendix (equation (OA.4)) derives the physical variance for skew log-normal RNDs with linear discount factors. These results confirm that when the RND is non-normal, the linear pricing kernel affects both the mean and the variance of the RND. This helps explain why the physical variances of the monotonic pricing kernels differ from those of the risk-neutral densities (Table 3). In contrast, when the RND is normal, linear pricing kernels alter the mean of the risk-neutral distribution but leave its variance unchanged (equations (17) and (18)).

With respect to the non-monotonic pricing kernels, the findings in Section E.6 of the Online Appendix underscore the importance of negative values for the quadratic parameter $\gamma_{2,t}$ in equations (4) and (6) to generate plausible physical variances, skewness, and kurtosis that are smaller in

absolute magnitude than the risk-neutral ones. Negative $\gamma_{2,t}$ parameters in quadratic pricing kernels are also crucial for generating option-based physical means that exceed RND means, especially when the RND is either normal or negatively skewed. These theoretical results cast doubt on the plausibility of the fixed-parameter non-monotonic pricing kernel with positive quadratic γ_2 parameters (as seen in the 2-, 3-, and 6-month expirations in Table 1, Panel A).

6 Option-based Expected Returns and Risk-Neutral Lower Bounds

Expected returns under the physical measure are unobservable. Extracting them from option prices requires assumptions about the pricing kernel. However, recent works (Martin (2017), Schneider (2019), Schneider and Trojani (2019), Chabi-Yo and Loudis (2020)) argue that forward-looking expected returns can be approximated by risk-neutral moments through an assumption-free approach. The accuracy of these risk-neutral bounds for expected returns can be evaluated using the option-based expected returns under the physical measure derived from the alternative pricing kernels in the previous section.

Martin (2017) derives lower bounds for risk premia based on risk-neutral variances

$$\mathbb{E}_t[R_{t,t+T}] - R^f_{t,t+T} \geq var^{RND}(R_{t,t+T})/R^f_{t,t+T}. \tag{24}$$

Chabi-Yo and Loudis (2020) derive a similar lower bound for expected returns that also depends on high-order risk-neutral moments. Schneider and Trojani (2019) propose a risk-neutral lower bound for expected returns which is given by

$$\mathbb{E}_t[R_{t,t+T}] \geq \frac{\mathbb{E}^{RND}_t[R^{p+1}_{t,t+T}]}{\mathbb{E}^{RND}_t[R^{p}_{t,t+T}]}, \tag{25}$$

where $p \in [0, 1]$. With the exception of Schneider and Trojani (2019), the above risk-neutral bounds are not completely assumption-free. Martin (2017) assumes that $cov_t(M_{t,t+T}R_{t,t+T}, R_{t,t+T})$ is non-positive, while Chabi-Yo and Loudis (2020) impose restrictions on preferences.

The lower bound in equation (24) introduced by Martin (2017) becomes a strict equality for log-preferences, i.e., for $\gamma_1 = 1$ in equation (1). However, this is only a sufficient condition, and there can be alternative specifications under which the bound is binding. To empirically assess

whether risk-neutral bounds are binding in a general setting, the existing literature, e.g., Martin (2017), Chabi-Yo and Loudis (2020), regresses realized excess returns on these bounds:

$$R_{t,t+T} - R^f_{t,t+T} = a + b \cdot var^{RND}(R_{t,t+T})/R^f_{t,t+T} + \epsilon_t. \tag{26}$$

If a is statistically insignificant and b is statistically equal to one, inequality (24) holds as an equality, and the lower bound is binding. I expand these tests along the following dimensions.

First, in addition to the regression results, I provide summary statistics and correlations for the risk-neutral variances to verify whether these bounds are aligned with average realized returns or average expected returns from the option-based physical densities. Secondly, although Martin (2017) derives the lower-bound condition in terms of the risk-neutral variance (equation (24)), in his empirical tests he uses the SVIX, which is defined as $var^{RND}(\frac{R_{t,t+T}}{R^f_{t,t+T}})$.[6] For consistency with the rest of my tests, I measure the risk-neutral lower bound for expected returns using the risk-neutral variance from equation (15), which is consistent with Martin's original framework (equation (4) in his paper and equation (24) here).

Thirdly, in addition to using realized returns as the dependent variable in equation (26), I test whether the risk-neutral bounds are binding by regressing option-based risk premia from the different pricing kernels on these variance-based bounds, i.e.,

$$\mathbb{E}_t[R_{t,t+T}] - R^f_{t,t+T} = a + b \cdot var^{RND}(R_{t,t+T})/R^f_{t,t+T} + \epsilon_t. \tag{27}$$

I also consider a specification where the dependent variable in equation (27) is fitted returns from predictive regressions of realized returns on the dividend yield, dividend growth, and the risk-free rate. Additionally, I test whether the realized returns and option-based risk premia from the different pricing kernels violate the risk-neutral lower bounds. Specifically, I examine whether there are instances where the inequality in equation (24) is reversed. Finally, unlike the existing literature, which typically focuses on a single option expiration (usually 1-month), my empirical analysis spans multiple maturities to examine whether investment horizons affect the accuracy of risk-neutral bounds.

[6]The SVIX is equal to $\frac{2R^f{}_{t,t+T}}{T \cdot F_{t,t+T}}\Big(\int_0^{F_{t,t+T}} Put_{t,t+T}dK + \int_{F_{t,t+T}}^{\infty} Call_{t,t+T}dK\Big)$, where $F_{t,t+T}$ is the forward price of the underlying asset, with $F_{t,t+T} = \mathbb{E}_t[S_{t+T}]$.

I only report results for the risk-neutral variance bound of Martin (2017) in equation (24) for the following reasons. First, my analysis shows that the risk-neutral bounds in Chabi-Yo and Loudis (2020) are mainlyinfluenced by the second moment term and are nearly identical to those in Martin (2017). Second, Schneider and Trojani (2019) demonstrates that when $p = 1$ in equation (25), the tightest lower bound for expected returns is obtained, which aligns with the risk-neutral variance bound in Martin (2017).

6.1 Summary Statistics for Risk-Neutral Lower Bounds

Table 6 reports summary statistics and correlations for the risk-neutral bound in Martin (2017), as defined by equation (24). The risk-free rate, $R^f_{t,t+T}$, is measured by the mean of the risk-neutral distribution. These statistics should be compared with the statistics in Panel A of Table 3 for expected returns across different pricing kernels and expirations, as well as with statistics for realized returns in Panel B of Table OA.2 in the Online Appendix. According to these statistics, the levels of the risk-neutral bounds from equation (24) (0.45% for 1-month, 1.05% for 2-month, 1.37% for 3-month, and 3.23% for 6-month) diverge from average expected and realized returns (0.63% for 1-month, 1.28% for 2-months, 1.66% for 3-month, and 4.25% for 6-month) reported in Table 3. Importantly, as option expiration increases, this divergence becomes more pronounced.

Nevertheless, the correlations between the risk-neutral variance bounds and expected returns are notably high across all pricing kernels and expirations, with values ranging from 0.8 to 1. The key exception is the VIX-dependent non-monotonic pricing kernel, where expected returns exhibit a negative correlation with the risk-neutral variance bounds. These findings suggest that, for short maturities, risk-neutral variance bounds serve as a valid proxy for expected returns across all pricing kernels, except for the VIX-dependent non-monotonic specification. Importantly, regardless of the stochastic discount factor, as the expiration period increases, risk-neutral bounds tend to diverge from expected returns.

This paper is among the first to highlight that the validity of risk-neutral bounds as a measure of expected returns under the physical measure is contingent on both option expiration and the VIX-dependence of preference parameters. These findings are significant because they provide a nuanced perspective that complements the existing literature, which either unconditionally accepts the tightness of these bounds (e.g., Martin (2017)) or unconditionally rejects them (e.g., Back et al.

(2022)). Schreindorfer and Sischert (2025) also document the effects of conditional volatility on the accuracy of risk-neutal bounds. However, their analysis is limited to a single option maturity (1-month) and does not include formal regression tests across different maturities and pricing kernels to disentangle the effects of monotonicity, VIX-dependence, and investment horizon on the tightness of risk-neutral bounds.

6.2 Regressions of Expected Returns on Risk-Neutral Lower Bounds

Table 7 reports results from regressions of realized and option-based expected returns on the risk-neutral bound of equation (24). Consistent with the findings in Martin (2017) and Chabi-Yo and Loudis (2020), when regressing realized returns on the risk-neutral bound (Panel A in Table 7), I cannot reject the hypothesis that the intercept in equation (27) is zero (t-stats: -0.47 to 1.06) or that the slope is one (t-stats: -0.66 to 0.89).

However, the results of these regressions, which assess the accuracy of risk-neutral bounds using realized returns, should be interpreted with caution for several reasons. First, as indicated by the low R^2 values, ranging from 0.13% to 4.63%, the fit of these regressions is poor, suggesting that realized returns are significantly more volatile than risk-neutral bounds. This empirical finding contradicts the strict theoretical lower-bound relationship from equation (24), which suggests that the coefficients of determination between returns and risk-neutral variances should be large. Second, the slope estimates for these regressions are only marginally statistically significant (t-stats: 0.25 to 2.06), indicating that these parameters provide limited insight into the relationship between realized returns and risk-neutral bounds.

Results become more reliable in Panel B of Table 7, where realized returns are replaced by fitted returns from regressions of realized returns on the dividend yield, dividend growth, and the risk-free rate. Estimation of fitted returns is outlined in Table OA.2 of the Online Appendix. Compared to realized returns, fitted returns yield more accurate slope estimates (t-stats: 2.87 to 4.73) in regressions with risk-neutral bounds. In this case, the null hypothesis that risk-neutral bounds for expected returns are binding (i.e., slope equals one and intercept equals zero) is rejected for short expirations (1- and 2-month options), with t-statistics of -4.15 and -4.16 for slopes, and 2.65 and 2.83 for intercepts. In contrast, the null hypothesis cannot be rejected for 3- and 6-month expirations (t-stats: -1.90 and 0.03 for slopes, 1.40 and 0.57 for intercepts). Consistent with these

statistics, the slope estimates for short expirations are 0.532 and 0.409, while the slope estimates for long expirations are closer to one, with values of 0.602 and 1.011.

The precision of the fitted return regressions in Panel B of Table 7 is considerably better than that of the realized return regressions in panel A, with values of R^2 ranging from 8. 76% to 14. 68%. However, the relatively low coefficient of determination still raises concerns about the overall explanatory power of these regressions. A tight risk-neutral bound, as specified in equation (24), should be able to explain a substantial portion of the variation in physical expected returns.

The accuracy of regressions with risk-neutral bounds increases substantially when option-based expected returns from the different pricing kernels are used as dependent variables. In particular, the R^2 values rise sharply for all expirations and pricing kernels, ranging from 70% to 99%. The only exception is the VIX-dependent non-monotonic discount factor, for which the explanatory power remains limited, with R^2 values between 1% and 25%.

As shown in Panel C of Table 7, regressing physical expected returns on risk-neutral variances achieves the best fit under the baseline power utility model with constant coefficients frpm equation (1). For this discount factor, the intercepts in equation (27) remain economically negligible across all expirations (0.01% to 0.15%), despite their strong statistical significance (t-statistics between 4.78 and 7.23). Moreover, although the null hypothesis that the slope equals one is strongly rejected (t-statistics between 23.19 and 67.13), the estimated slopes are economically close to unity, ranging from 1.195 to 1.371. Panel E of Table 7 presents similar results for the non-monotonic pricing kernel with constant coefficients from equation (4). In this case, however, the intercepts (0.1% to 0.5%) are economically more meaningful than those obtained for the monotonic model in Panel C (0.01% to 0.15%).

For both the monotonic and non-monotonic VIX-dependent pricing kernels from equations (2) and (6), the null hypothesis in equation (27) that the risk-neutral bounds are binding is rejected (Panels D and F). This rejection is driven by regression intercepts that are both statistically significant (t-statistics ranging from 4.80 to 13.44) and economically meaningful (0.51% to 4%). Additionally, slope estimates deviate markedly from unity. They range from 0.623 to 4 for the VIX-dependent monotonic kernel of equation (2), and from -0.276 to -0.081 for the VIX-dependent non-monotonic kernel of equation (6).

For most regressions in Table 7, the economic magnitude and statistical significance of the

intercept in equation (27) increase with option expiration, though not always monotonically. This pattern indicates that longer expirations affect the accuracy of risk-neutral bounds in capturing expected returns, and is consistent with the summary statistics of risk-neutral bounds in Table 6

6.3 Violations of Risk-Neutral Lower Bounds

The unsuitability of realized or fitted returns for testing risk-neutral lower bounds is further confirmed in Table 8, which reports the percentage of cases in which realized and expected returns violate the risk-neutral lower bound of equation (24).

The percentage of violations of the risk-neutral lower bound by realized and fitted returns is roughly 40% and remains stable across expirations. By contrast, expected returns from the fixed-parameter monotonic (equation (1)) and non-monotonic (equation (4)) discount factors almost never violate the lower bound in equation (24), regardless of maturity. Although the frequency of violations remains constant for the fixed-parameter pricing kernels across expiration, the magnitude of these violations increases with maturity, underscoring the effect of option expiration on the tightness of risk-neutral bounds.

Contrary to the fixed-parameter discount factors, expected returns from the VIX-dependent pricing kernels (equations (2) and (6)) violate risk-neutral bounds, with the effect being particularly pronounced for the VIX-dependent quadratic kernel of equation (6). In this case, violations occur about 40% of the time across expirations, while the magnitude of these violations increases with option expiration. Overall, the evidence in Table 8 indicates that realized and fitted returns are unreliable for testing risk-neutral lower bounds, as they exhibit violations in 40% of cases. Option-based expected returns, by comparison, rarely violate the bounds, except in the case of the VIX-dependent non-monotonic kernel of equation (6).

The results in this section underscore four key findings. First, longer option maturities weaken the tightness of risk-neutral bounds. Second, realized (or fitted) returns are unsuitable for evaluating the accuracy of risk-neutral bounds through the OLS regression of equation (27). Regressions using realized returns exhibit near-zero explanatory power, large standard errors, and frequent violations of the strictly positive risk-neutral lower bounds due to negative realized returns. Third, for pricing kernels with constant parameters (equations (1) and (4)), regressions of expected returns on risk-neutral bounds yield slope estimates close to one, intercepts near zero, and high R^2

values. Contrary to Back et al. (2022), who argue that risk-neutral bounds are not binding, the results indicate that risk-neutral variances provide an accurate proxy for expected returns implied by fixed-parameter pricing kernels.

Finally, non-monotonicity of the pricing kernel does not materially affect the tightness of the risk-neutral bounds. Both the monotonic and non-monotonic discount factors with fixed parameters (equations (1) and (4)) generate expected returns that remain well aligned with the risk-neutral variance bounds, as shown in Panels C and E of Table 7. In contrast, VIX-dependent risk aversion disrupts this alignment, regardless of the monotonicity of the discount factor. The distinction arises because non-monotonicities occur only in states with very low probabilities, typically in the far left or right tails of the distribution (Figure 1), whereas VIX dependence alters risk aversion across the entire distribution of returns.

Despite the limitations of risk-neutral lower bounds, the evidence from Table 6 and Panels C and E of Table 7 shows that if preference parameters are assumed to be constant over time, risk-neutral bounds are closely align with expected returns, regardless of monotonicity. In this setting, risk-neutral variances outperform fitted returns from backward-looking predictive regressions (e.g., Table OA.2 in the Online Appendix) in capturing expected returns.

6.4 Risk-neutral Bounds and Pricing Kernels: Theoretical Explanation

The close alignment between risk-neutral bounds and expected returns for the fixed-parameter linear pricing kernel of equation (1), documented in Table 7, can be traced back to the fundamental result in Martin (2017) underlying the derivation of the risk-neutral bound in equation (24). Specifically, Martin (2017) show that expected returns equal risk-neutral moments minus a covariance term, which is assumed to be negative.

$$\mathbb{E}_t[R_{t,t+T}] - R^f_{t,t+T} = var^{RND}(R_{t,t+T})/R^f_{t,t+T} - cov_t\big(M_{t,t+T}R_{t,t+T}, R_{t,t+T}\big). \tag{28}$$

According to the estimates in Table 1, Panel A, for the linear pricing kernel, γ_1 values across expirations are close to one, which corresponds to log utility. Under this specification, the covariance term in equation (28) is zero, implying that expected returns align tightly with risk-neutral bounds, even when the regression coefficients are statistically different from one.

Similarly, as shown by the interepts in Table 7 or the frequency of risk-neutral bound violations in Table 8, the covariance term in equation (28) is nontrivial for longer option maturities (e.g., 3 or 6 months) or for pricing kernels with VIX-dependent parameters. For kernels where the covariance in equation (28) is non-zero, or potentially positive, the evidence in Table 8 indicates that the risk-neutral bound is not binding and may even be reversed. This explains why the regressions in Table 7 for longer maturities or for VIX-dependent pricing kernels (equations (2) and (6)) imply economically and statistically significant intercepts, along with slope coefficients that differ substantially from one.

7 Conclusion

The goal of this paper is twofold. The first part of the analysis examines how different pricing kernels interact with the option-implied risk-neutral density across maturities (1-, 2-, 3-, and 6-month options) to generate distinct forward-looking distributions of stock market returns under the physical measure. The theoretical framework builds on four power-utility pricing kernels, characterized by either linear (monotonic) or quadratic (non-monotonic) exponents, with risk aversion parameters that are either fixed or VIX-dependent. The second part of the analysis uses the option-based physical distributions derived from these kernels to evaluate the accuracy of the risk-neutral variance bounds for expected market returns proposed in the literature.—

Results from Kolmogorov–Smirnov tests show that option-based physical distributions derived from the fixed-parameter monotonic, VIX-dependent monotonic, and fixed-parameter non-monotonic discount factors are broadly similar. By contrast, the distribution generated by the non-monotonic pricing kernel with VIX-dependent parameters differs significantly from the others. These findings suggest that non-monotonicities must be combined with time-varying parameters in order to generate physical densities that deviate meaningfully from the standard fixed-parameter monotonic (power-utility) specification. Additional tests of the first four physical moments across pricing kernels reveal that the variances of the option-based distributions are highly correlated, whereas odd moment, expected returns and skewness, are least correlated. This analysis provides one of the first systematic attempts to illustrate how alternative discount factors shape the moments of the option-based physical distribution.

With respect to risk-neutral bounds for expected returns, I find that alignment between option-based expected returns and risk-neutral variances holds only for fixed-parameter pricing kernels, regardless of whether they are monotonic or non-monotonic. By contrast, for discount factors with VIX-dependent parameters, the evidence does not support the hypothesis that risk-neutral bounds are binding or consistent with option-based expected returns. Importantly, my results also show that risk-neutral bounds diverge from option-based expected returns across all kernels as option maturity increases.

These results highlight that the accuracy of risk-neutral bounds for forward-looking expected returns is primarily affected by VIX-dependence of the pricing kernel and option maturity. By contrast, non-monotonicities appear to have little effect on the tightness of these bounds. Despite the shortcomings of risk-neutral bounds, my evidence suggests that they far outperform alternative measures of expected returns, such as rolling averages of realized returns or fitted values from predictive regressions, because the forward-looking nature of option-based moments.

References

Ait-Sahalia, Y. and A. W. Lo (2000). Non-parametric risk management and implied risk aversion. *Journal of Econometrics 94*, 9–51.

Alexiou, L., A. Goyal, A. Kostakis, and L. Rompolis (2025). Pricing event risk: Evidence from concave implied volatility curves. *Review of Finance Forthcoming*.

Ang, A. and G. Bekaert (2007). Stock return predictability: Is it there? *Review of Financial Studies 20*, 651–707.

Back, K., K. Crotty, and S. M. Kazempour (2022). Validity, tightness, and forecasting power of risk premium bounds. *Journal of Financial Economics 144*, 732–760.

Bakshi, G. and D. B. Madan (2007). Investor heterogeneity, aggregation, and the non-monotonicity of the aggregate marginal rate of substitution in the price of market-equity. *Working paper*.

Bakshi, G., D. B. Madan, and G. Panayotov (2010). Returns of claims on the upside and the viability of u-shaped pricing kernels. *Journal of Financial Economics 97*, 130–154.

Barone-Adesi, G., N. Fusari, A. Mira, and C. Sala (2020). Option market trading activity and the estimation of the pricing kernel: A bayesian approach. *Journal of Econometrics 216*, 430–449.

Beason, T. and D. Schreindorfer (2022). Dissecting the equity premium. *Journal of Polictical Economy 130*, 2203–2222.

Birru, J. and S. Figlewski (2012). Anatomy of a meltdown: The risk neutral density for the S&P 500 in the fall of 2008. *Journal of Financial Markets 15*(2), 151–180.

Black, F. and M. Scholes (1973). The pricing of options and corporate liabilities. *Journal of Political Economy 81*(3), 637–654.

Bliss, R. R. and N. Panigirtzoglou (2004). Option-implied risk aversion estimates. *Journal of Finance 59*(1), 407–444.

Breeden, D. and R. Litzenberger (1978). Prices of state-contigent claims implicit in option prices. *Journal of Business 51*(4), 621–51.

Campbell, J. Y. and R. J. Shiller (1988). Stock prices, earnings, and expected dividends. *Journal of Finance 43*(3), 661–76.

Chabi-Yo, F., C. Dim, and G. Vilkov (2022). Generalized bounds on the conditional expected excess return on individual stocks. *Management Science 69*(2), 922–939.

Chabi-Yo, F. and J. Loudis (2020). The conditional expected market return. *Journal of Financial Economics 137*(3), 752–786.

Cochrane, J. H. (2005). *Asset pricing*. Princeton, NJ: Princeton University Press.

Cuesdeanu, H. and J. C. Jackwerth (2018). The pricing kernel puzzle: Survey and outlook. *Annals Finance 14*, 289–329.

Delikouras, S. (2017). Where's the kink? disappointment events in consumption growth and equilibrium asset prices. *Review of Financial Studies 30*(8), 2851–2889.

Delikouras, S. and A. Kostakis (2019). A single factor consumption-based asset pricing model. *Journal of Financial and Quantitative Analysis 54*(2), 789–827.

Driessen, J., J. Koëter, and O. Wilms (2022). Horizon effects in the pricing kernel: How investors price short-term versus long-term risks. *Jounral of Financial and Quantitative Analysis Forthcoming*.

Esscher, F. (1932). Onn the probability function in the collective theory of risk. *Skandinavisk Aktuarietidskrift 15*(3), 175–195.

Fama, E. F. and K. R. French (1993). Common risk factors in the returns on stocks and bonds. *Journal of Financial Economics 33*(1), 3–56.

Fama, E. F. and K. R. French (2015). A five-factor asset pricing model. *Journal of Financial Economics 116*(1), 1–22.

Figlewski, S. (2010). Estimating the implied risk-neutral density for the us market portfolio. *Volatility and Time Series Econometrics: Essay in Honor of Robert F. Engle*, 323–353.

Gandhi, M., N. J. Gormsen, and E. Lazarus (2023). Forward return expectations. *Working Paper*.

Goyal, A. and I. Welch (2003). Predicting the equity premium with dividend ratios. *Management Science 49*, 639–654.

Goyal, A. and I. Welch (2008). A comprehensive look at the empirical performance of the equity premium prediction. *Review of FInancial Studies 21*, 1455–1508.

Henze, N. (1986). A probabilistic representation of the 'skew-normal' distribution. *Scandinavian Journal of Statistics 13*(4), 271–275.

Heston, S., K. Jacobs, and H. J. Kim (2023). The pricing kernel in options. *Working Paper*.

Hou, K., C. Xue, and L. Zhang (2019). Which factors? *Review of Finance 23*(1), 1–35.

Huang, C.-F. and R. H. Litzenberger (1989). *Foundations for Financial Economics*. New York, NY: North-Holland.

Kim, H. J. (2021). Characterizing the conditional pricing kernel: A new approach. *Working Paper*.

Kostakis, A., T. Magdalinos, and M. P. Stamatogiannis (2015). Robust econometric inference for stock return predictability. *Review of Financial Studies 28*, 1506–1553.

Lettau, M. L. and S. C. Ludvigson (2001a). Consumption, aggregate wealth, and expected stock returns. *Journal of Finance 56*(3), 815–49.

Lettau, M. L. and S. C. Ludvigson (2001b). Resurrecting the (c)capm: A cross-sectional test when risk premia are time-varying. *Journal of Political Economy 109*(6), 1238–1287.

Lewellen, J. (2015). The cross-section of expected stock returns. *Critical Finance Review 4*, 1–44.

Linn, M., S. Shive, and T. Shumway (2018). Pricing kernel monotonicity and conditional infromation. *Review of Financial Studies 31*(2), 493–531.

Liu, L. X., T. M. Whited, and L. Zhang (2009). Investment-based expected stock returns. *Journal of Political Economy 117*, 1105–39.

Martin, I. (2017). What is the expected return on the market. *Quarterly Journal of Economics 132*(2), 367–433.

Martin, I. and C. Wagner (2019). What is the expected return on a stock. *Journal of Finance 74*(4), 1887–1929.

Monfort, A. and F. Pegoraro (2012). Asset pricing with second-order esscher transforms. *Journal of Banking & Finance 36*(6), 1678–1687.

Newey, W. K. and K. D. West (1987). A simple, positive semi-definite, heteroskedasticity and autocorrelation consistent covariance matrix. *Econometrica 55*, 703–8.

Rosenberg, J. V. and R. F. Engle (2000). Empirical pricing kernels. *Journal of Financial Economics 64*, 341–72.

Schneider, P. (2019). An anatomy of the market return. *Journal of Financial Economics 132*(2), 325–350.

Schneider, P. and F. Trojani (2019). (almost) model-free recovery. *Journal of Finance 74*(1), 323–370.

Schreindorfer, D. and T. Sischert (2025). Conditional risk and the pricing kernel. *Journal of Financial Economics 171*, 104106.

Sichert, T. (2023). The pricing kernel is u-shaped. *Working Paper*.

Stambaugh, R. F. (1999). Predictive regressions. *Journal of Financial Economics 54*, 375–421.

van Binsgergen, J. H. and R. S. J. Koijen (2010). Predictive ergressions: A present-value approach. *Journal of Finance 65*, 1439–1471.

Yogo, M. (2006). A consumption-based explanation of expected stock returns. *Journal of Finance 61*(2), 539–80.

Figures

Figure 1 Pricing Kernels

This figure depicts the monotonic and non-monotonic pricing kernels implied by equations (1), (2), (4), and (6) for option maturities of 1 month (Panel A), 2 months (Panel B), 3 months (Panel C), and 6 months (Panel D). The corresponding parameter estimates are reported in Table 1. For pricing kernels with VIX-dependent parameters (Panels B and D), the normalized VIX ($nvix$) is fixed at its sample average. Estimation samples cover January 1996–December 2022 for 1-month options, May 1998–November 2022 for 2-month options, January 2002–October 2022 for 3-month options, and June 1996–June 2022 for 6-month options.

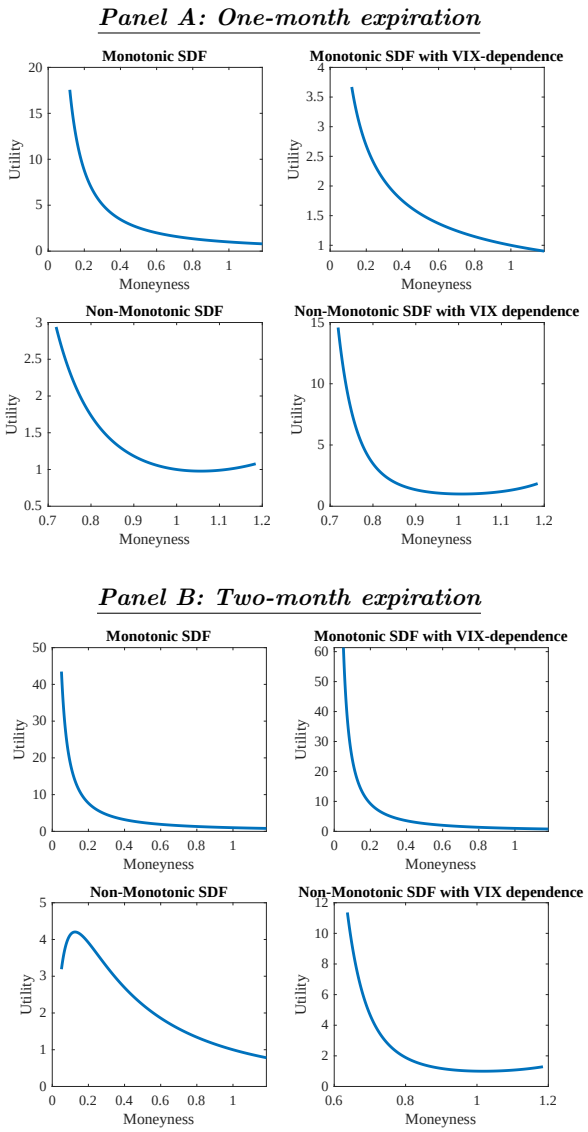

Panel C: Three-month expiration

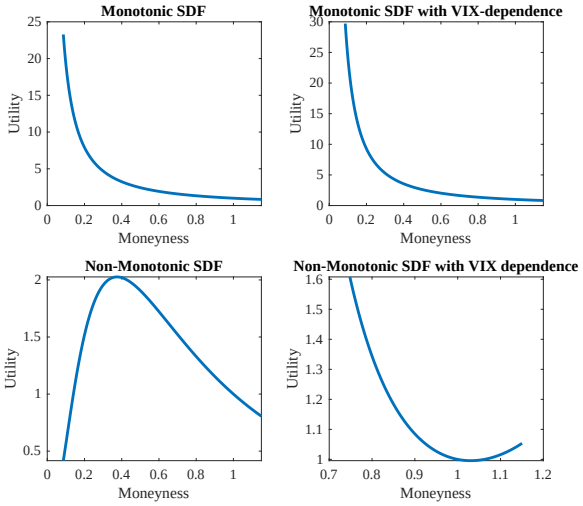

Panel D: Six-month expiration

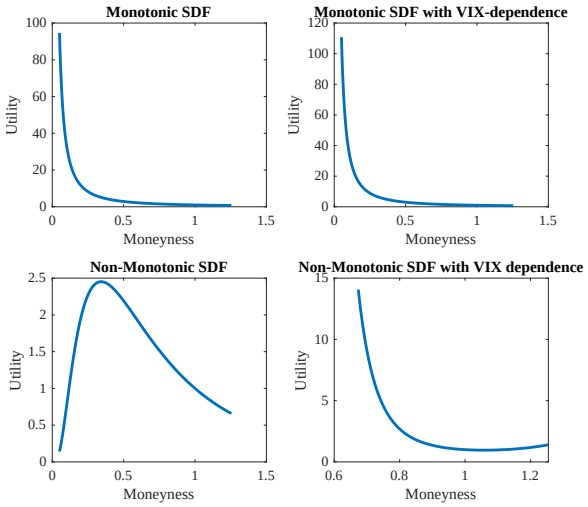

Figure 2 Option-based Physical Distribution and Density Functions

This figure presents the average distribution and density functions under the physical measure implied by the monotonic and non-monotonic pricing kernels of equations (1), (2), (4), and (6) for option maturities of 1 month (Panel A), 2 months (Panel B), 3 months (Panel C), and 6 months (Panel D). Each graph is labeled by the exponent of the corresponding pricing kernel: $\gamma_1 r$ (equation 1), $\gamma_1 nvix^{\gamma_3} r$ (equation 2), $\gamma_1 r + \gamma_2 r^2$ (equation 4), and $\gamma_1 nvix^{\gamma_3} r + \gamma_2 nvix^{\gamma_3} r^2$ (equation 6). Here, r denotes log returns and $nvix$ the normalized VIX, defined as the VIX divided by its 1986–1995 average (to avoid look-ahead bias) and scaled by option maturity. *risk-neutral* is the risk-neutral density. Parameter estimates for the pricing kernels are reported in Table 1, while the physical distributions and densities are estimated following equation (15). For each maturity, the graphs display time-averaged distribution and density functions. The realized distribution (realized) is obtained from kernel-density estimates of historical returns, interpolated over the full moneyness range using a piecewise cubic Hermite polynomial. The sample periods are January 1996–December 2022 (1 month), May 1998–November 2022 (2 months), January 2002–October 2022 (3 months), and June 1996–June 2022 (6 months).

Panel A: One-month expiration

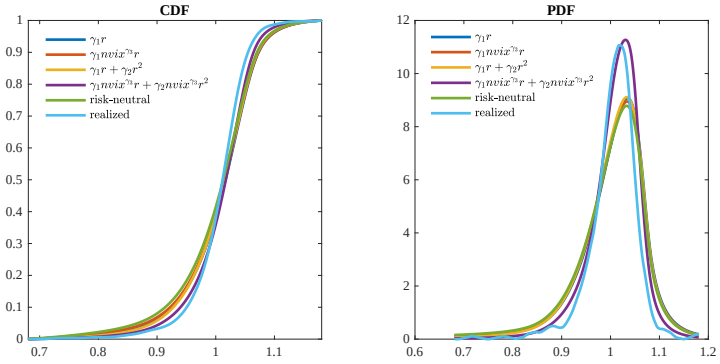

Panel B: Two-month expiration

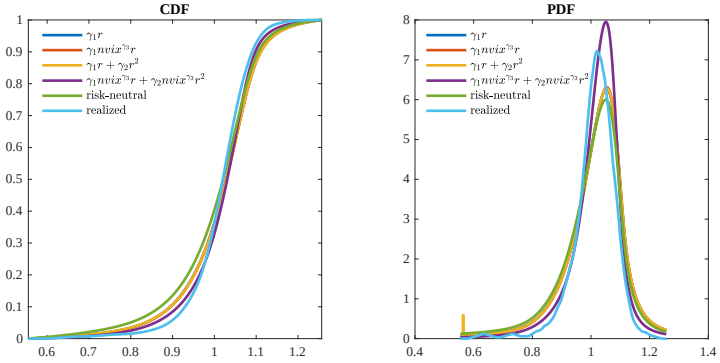

Panel C: Three-month expiration

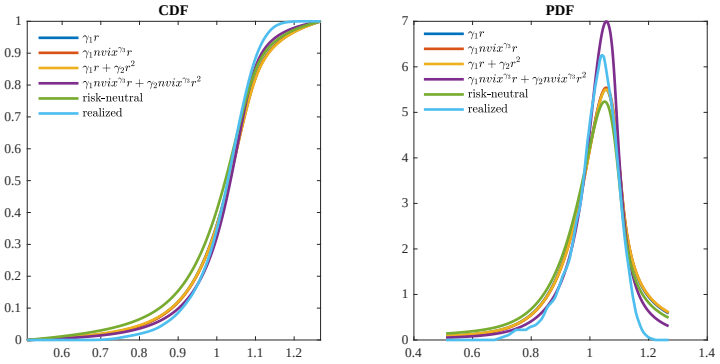

Panel D: Six-month expiration

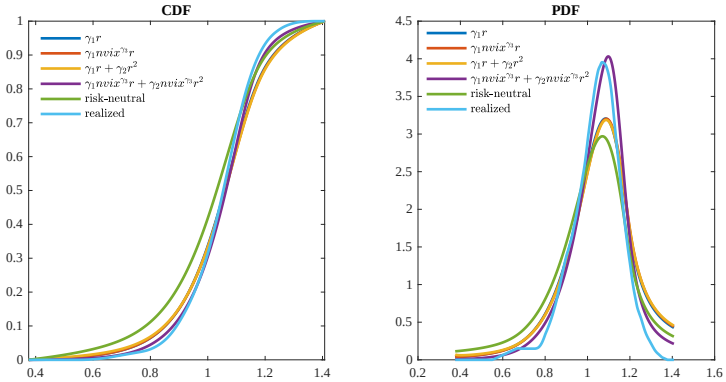

Tables

Table 1 GMM Estimation of the Option-based Non-monotonic Pricing Kernel

This table reports GMM estimates for the option-based pricing kernels. Panels A and B present results for the monotonic kernels of equations (1) and (2), while Panels C and D report results for the non-monotonic kernels of equations (4) and (6). γ_1 denotes the the coefficient on the linear term, γ_2 is the coefficient on the quadratic term (Panels C and D), and γ_3 is the VIX-dependence coefficient. VIX-dependence is modeled using the normalized VIX ($nvix$), defined as the VIX divided by its 1986–1995 average (to avoid look-ahead bias) and scaled to each option maturity. The GMM moment conditions follow equation (14). Reported t-statistics (in parentheses) are corrected for heteroscedasticity and autocorrelation using Newey–West standard errors with 12, 6, 4, and 2 lags for the 1-, 2-, 3-, and 6-month maturities, respectively. χ^2, dof, and p denote the χ^2 test, degrees of freedom, and p-value for the joint null that all target moments equal zero. GMM is the minimized value of the GMM objective function. The sample covers January 1996–December 2022 (1-month), May 1998–November 2022 (2-month), January 2002–October 2022 (3-month), and June 1996–June 2022 (6-month) expirations.

Panel A: Fixed-parameter monotonic discount factor

	1-month	2-month	3-month	6-month
γ_1	1.349	1.266	1.284	1.524
	(4.77)	(4.65)	(4.43)	(6.83)
χ^2	0.21	0.01	0.01	0.01
dof	1	1	1	1
p	0.64	0.90	0.91	0.89
GMM	$3.99e^{-05}$	$6.01e^{-06}$	$9.08e^{-06}$	$2.49e^{-05}$

Panel B: VIX-dependent monotonic discount factor

	1-month	2-month	3-month	6-month
γ_1	0.518	1.439	1.295	1.661
	(0.31)	(1.03)	(5.12)	(2.13)
γ_3	1.936	-0.558	-0.817	-0.813
	(0.47)	(-0.12)	(-0.11)	(-0.15)
χ^2	-	-	-	-
dof	0	0	0	0
p	-	-	-	-
GMM	$1.45e^{-13}$	$2.64e^{-13}$	$3.42e^{-17}$	$1.73e^{-15}$

Panel C: Fixed-parameter non-monotonic discount factor

	1-month	2-month	3-month	6-month
γ_1	0.814	1.386	1.439	1.672
	(0.57)	(1.27)	(0.92)	(1.35)
γ_2	-7.412	0.334	0.732	0.779
	(-0.32)	(1.83)	(0.16)	(0.29)
χ^2	-	-	-	-
dof	0	0	0	0
p	-	-	-	-
GMM	$9.70e^{-14}$	$1.11e^{-15}$	$1.86e^{-14}$	$5.32e^{-17}$

Panel D: VIX-dependent non-monotonic discount factor

	1-month	2-month	3-month	6-month
γ_1	0.700	0.660	0.129	1.991
	(2.78)	(2.61)	(0.23)	(4.08)
γ_2	-47.470	-19.068	-2.143	-17.422
	(-1.26)	(-1.06)	(-0.30)	(-1.38)
γ_3	-8.153	-7.415	-9.720	-4.421
	(-2.21)	(-2.29)	(-0.43)	(-1.09)
χ^2	-	-	-	-
dof	0	0	0	0
p	-	-	-	-
GMM	$6.85e^{-13}$	$4.68e^{-14}$	$1.73e^{-14}$	$7.81e^{-14}$

Table 2 Kolmogorov-Smirnov Tests for the Option-based Physical Distribution Functions Across Pricing Kernels

This table reports the frequency of rejections of the null hypothesis that any two option-based physical distribution functions are equal, using the two-sample Kolmogorov–Smirnov test at the 5% significance level. Panel A reports results for the 1-month expiration, Panel B for the 2-month expiration, Panel C for the 3-month expiration, and Panel D for the 6-month expiration. The option-based physical distributions are derived from alternative pricing kernels, labeled by the exponents of the corresponding discount factors: $\gamma_1 r$ (equation (1)), $\gamma_1 nvix^{\gamma_3} r$ (equation (2)), $\gamma_1 r + \gamma_2 r^2$ (equation (4)), and $\gamma_1 nvix^{\gamma_3} r + \gamma_2 nvix^{\gamma_3} r^2$ (equation (6)). Here, r denotes log-returns and $nvix$ the normalized VIX, defined as the VIX divided by its 1986–1995 average (to avoid look-ahead bias) and scaled by option maturity. Parameter estimates for the pricing kernels are obtained from the GMM system of equation (14), with results reported in Table and Table 1. *risk-neutral* denotes the risk-neutral distribution, while *realized* refers to the empirical distribution of returns. Option-based physical and risk-neutral distributions are constructed using equation (15), while the realized distribution is obtained by fitting a kernel-density estimator to historical returns and interpolating values across moneyness with a piecewise cubic Hermite polynomial. For realized distributions, the Kolmogorov–Smirnov tests compare the density of realized returns to the averages of the option-implied densities. Reported numbers in brackets are the average values of the Kolmogorov–Smirnov statistic. N is the number of observations. The sample covers January 1996–December 2022 (1-month), May 1998–November 2022 (2-month), January 2002–October 2022 (3-month), and June 1996–June 2022 (6-month) expirations.

Panel A: Rejections of the Kolmogorov-Smirnov tests, 1-month expiration (N=323)

N=323	$\gamma_1 r$	$\gamma_1 nvix^{\gamma_3} r$	$\gamma_1 r + \gamma_2 r^2$	$\gamma_1 nvix^{\gamma_3} r + \gamma_2 nvix^{\gamma_3} r^2$	risk-neutral
$\gamma_1 nvix^{\gamma_3} r$	22% [4%]				
$\gamma_1 r + \gamma_2 r^2$	50% [7%]	77% [9%]			
$\gamma_1 nvix^{\gamma_3} r + \gamma_2 nvix^{\gamma_3} r^2$	84% [26%]	87% [27%]	85% [25%]		
risk-neutral	65% [7%]	23% [4%]	88% [12%]	86% [27%]	
realized (N=1)	100% [14%]	100% [16%]	100% [10%]	100% [6%]	100% [19%]

Panel B: Rejections of the Kolmogorov-Smirnov tests, 2-month expiration (N=147)

N=147	$\gamma_1 r$	$\gamma_1 nvix^{\gamma_3} r$	$\gamma_1 r + \gamma_2 r^2$	$\gamma_1 nvix^{\gamma_3} r + \gamma_2 nvix^{\gamma_3} r^2$	risk-neutral
$\gamma_1 nvix^{\gamma_3} r$	3% [2%]				
$\gamma_1 r + \gamma_2 r^2$	2% [1%]	5% [2%]			
$\gamma_1 nvix^{\gamma_3} r + \gamma_2 nvix^{\gamma_3} r^2$	87% [26%]	85% [26%]	89% [27%]		
risk-neutral	87% [9%]	95% [10%]	90% [9%]	84% [29%]	
realized (N=1)	100% [11%]	100% [11%]	100% [12%]	100% [7%]	100% [18%]

Panel C: Rejections of the Kolmogorov-Smirnov tests, 3-month expiration (N=83)

N=83	$\gamma_1 r$	$\gamma_1 nvix^{\gamma_3} r$	$\gamma_1 r + \gamma_2 r^2$	$\gamma_1 nvix^{\gamma_3} r + \gamma_2 nvix^{\gamma_3} r^2$	risk-neutral
$\gamma_1 nvix^{\gamma_3} r$	15% [3%]				
$\gamma_1 r + \gamma_2 r^2$	20% [3%]	33% [5%]			
$\gamma_1 nvix^{\gamma_3} r + \gamma_2 nvix^{\gamma_3} r^2$	87% [26%]	84% [25%]	88% [27%]		
risk-neutral	86% [10%]	92% [11%]	87% [8%]	78% [27%]	
realized (N=1)	100% [23%]	100% [23%]	100% [24%]	100% [23%]	100% [25%]

Panel D: Rejections of the Kolmogorov-Smirnov tests, 6-month expiration (N=52)

N=52	$\gamma_1 r$	$\gamma_1 nvix^{\gamma_3} r$	$\gamma_1 r + \gamma_2 r^2$	$\gamma_1 nvix^{\gamma_3} r + \gamma_2 nvix^{\gamma_3} r^2$	risk-neutral
$\gamma_1 nvix^{\gamma_3} r$	23% [3%]				
$\gamma_1 r + \gamma_2 r^2$	40% [6%]	52% [7%]			
$\gamma_1 nvix^{\gamma_3} r + \gamma_2 nvix^{\gamma_3} r^2$	94% [27%]	90% [27%]	96% [30%]		
risk-neutral	100% [14%]	100% [15%]	100% [11%]	100% [32%]	
realized (N=1)	100% [18%]	100% [18%]	100% [19%]	100% [17%]	100% [21%]

Table 3 Summary Statistics of Option-based Moments under the Physical Measure Across Pricing Kernels

This table reports summary statistics for the option-based moments of returns under the physical measure, computed from the pricing kernels in equations (1), (2), (4), and (6). Panel A presents option-based expected returns, Panel B variances, Panel C skewness, and Panel D kurtosis. The pricing kernels are labeled by the exponents of their discount factors: $\gamma_1 r$ (equation (1)), $\gamma_1 nvix^{\gamma_3} r$ (equation (2)), $\gamma_1 r + \gamma_2 r^2$ (equation (4)), and $\gamma_1 nvix^{\gamma_3} r + \gamma_2 nvix^{\gamma_3} r^2$ (equation (6)). Here, r denotes log-returns and $nvix$ the normalized VIX, defined as the VIX divided by its 1986–1995 average (to avoid look-ahead bias) and scaled by option maturity. Estimation of the pricing kernels is based on the GMM system in equation (14), with results reported in Table 1. *risk-neutral* denotes moments of the risk-neutral density, while *realized* refers to unconditional sample moments of realized returns. Both option-based physical and risk-neutral moments are derived using equation (15). The sample covers January 1996–December 2022 (1-month), May 1998–November 2022 (2-month), January 2002–October 2022 (3-month), and June 1996–June 2022 (6-month) expirations.

Panel A: Option-based expected returns across pricing kernels

i) $\gamma_1 r$	1-month	2-month	3-month	6-month
mean	0.61%	1.29%	1.67%	4.26%
st. deviation	0.77%	1.46%	1.41%	2.20%
N	323	147	83	52
ii) $\gamma_1 nvix^{\gamma_3} r$	1-month	2-month	3-month	6-month
mean	0.63%	1.28%	1.66%	4.25%
st. deviation	2.56%	1.04%	0.94%	1.46%
N	323	147	83	52
iii) $\gamma_1 r + \gamma_2 r^2$	1-month	2-month	3-month	6-month
mean	0.63%	1.28%	1.66%	4.25%
st. deviation	0.69%	1.29%	1.42%	2.18%
N	323	147	83	52
iv) $\gamma_1 nvix^{\gamma_3} r + \gamma_2 nvix^{\gamma_3} r^2$	1-month	2-month	3-month	6-month
mean	0.63%	1.28%	1.66%	4.25%
st. deviation	0.40%	0.74%	1.12%	1.16%
N	323	147	83	52
v) risk-neutral	1-month	2-month	3-month	6-month
mean	-0.06%	0.01%	0.11%	0.46%
st. deviation	0.44%	0.87%	0.97%	1.39%
N	323	147	83	52
vi) realized mean	1-month	2-month	3-month	6-month
	0.63%	1.28%	1.66%	4.25%

Panel B: Option-based physical variances across pricing kernels

i) $\gamma_1 r$	1-month	2-month	3-month	6-month
mean	0.42%	0.82%	0.97%	1.98%
st. deviation	0.44%	0.76%	0.70%	1.02%
N	323	147	83	52

ii) $\gamma_1 nvix^{\gamma_3} r$	1-month	2-month	3-month	6-month
mean	0.43%	0.82%	0.98%	2.00%
st. deviation	0.36%	0.88%	0.81%	1.19%
N	323	147	83	52

iii) $\gamma_1 r + \gamma_2 r^2$	1-month	2-month	3-month	6-month
mean	0.34%	0.89%	1.05%	2.23%
st. deviation	0.28%	1.37%	0.83%	1.39%
N	323	147	83	52

iv) $\gamma_1 nvix^{\gamma_3} r + \gamma_2 nvix^{\gamma_3} r^2$	1-month	2-month	3-month	6-month
mean	0.36%	0.70%	0.87%	1.33%
st. deviation	0.62%	1.17%	1.10%	1.31%
N	323	147	83	52

v) risk-neutral	1-month	2-month	3-month	6-month
mean	0.51%	1.04%	1.26%	2.67%
st. deviation	0.60%	1.12%	0.99%	1.52%
N	323	147	83	52

vi) realized variance	1-month	2-month	3-month	6-month
	0.24%	0.49%	0.54%	1.13%

Panel C: Option-based physical skewness across pricing kernels

i) $\gamma_1 r$	1-month	2-month	3-month	6-month
mean	-1.43	-1.34	-1.26	-0.72
st. deviation	0.77	0.71	0.62	0.29
N	323	147	83	52

ii) $\gamma_1 nvix^{\gamma_3} r$	1-month	2-month	3-month	6-month
mean	-1.45	-1.32	-1.23	-0.68
st. deviation	0.79	0.68	0.57	0.21
N	323	147	83	52

iii) $\gamma_1 r + \gamma_2 r^2$	1-month	2-month	3-month	6-month
mean	-1.17	-1.37	-1.39	-0.91
st. deviation	0.64	0.72	0.71	0.38
N	323	147	83	52

iv) $\gamma_1 nvix^{\gamma_3} r + \gamma_2 nvix^{\gamma_3} r^2$	1-month	2-month	3-month	6-month
mean	-0.59	-0.50	-0.56	-0.15
st. deviation	0.45	0.37	0.47	0.18
N	323	147	83	52

v) risk-neutral	1-month	2-month	3-month	6-month
mean	-1.51	-1.47	-1.41	-0.98
st. deviation	0.76	0.75	0.71	0.42
N	323	147	83	52

vi) realized skewness	1-month	2-month	3-month	6-month
	-1.24	-1.67	-1.15	-0.87

Panel D: Option-based physical kurtosis across pricing kernels

i) $\gamma_1 r$	1-month	2-month	3-month	6-month
mean	7.96	7.55	6.97	4.75
st. deviation	4.43	3.91	3.49	1.33
N	323	147	83	52

ii) $\gamma_1 nvix^{\gamma_3} r$	1-month	2-month	3-month	6-month
mean	7.78	7.54	6.92	4.61
st. deviation	4.16	3.91	3.37	1.06
N	323	147	83	52

iii) $\gamma_1 r + \gamma_2 r^2$	1-month	2-month	3-month	6-month
mean	6.84	7.73	7.58	5.45
st. deviation	3.36	4.10	4.16	2.00
N	323	147	83	52

iv) $\gamma_1 nvix^{\gamma_3} r + \gamma_2 nvix^{\gamma_3} r^2$	1-month	2-month	3-month	6-month
mean	4.37	4.01	4.12	3.24
st. deviation	1.51	1.14	1.55	0.23
N	323	147	83	52

v) risk-neutral	1-month	2-month	3-month	6-month
mean	7.67	7.39	6.92	4.99
st. deviation	3.94	3.69	3.44	1.75
N	323	147	83	52

vi) realized kurtosis	1-month	2-month	3-month	6-month
	9.10	9.36	4.71	4.55

Table 4 Coefficient of Determination for Option-based Moments under the Physical Measure across Pricing Kernels

This table reports coefficients of determination (R^2) from regressions of option-based moments of market returns (mean, variance, skewness, kurtosis) across pricing kernels from equations (1), (2), (4), and (6). Panel A presents R^2 values for the 1-month expiration, Panel B for the 2-month expiration, Panel C for the 3-month expiration, and Panel D for the 6-month expiration. Option-based physical moments are derived using equation (15). The pricing kernels are labeled by the exponents of their discount factors: $\gamma_1 r$ (equation (1)), $\gamma_1 nvix^{\gamma_3} r$ (equation (2)), $\gamma_1 r + \gamma_2 r^2$ (equation (4)), and $\gamma_1 nvix^{\gamma_3} r + \gamma_2 nvix^{\gamma_3} r^2$ (equation (6)). Here, r denotes log-returns and $nvix$ the normalized VIX, defined as the VIX divided by its 1986–1995 average (to avoid look-ahead bias) and scaled by option maturity. Estimation of the pricing kernels is based on the GMM system in equation (14), with results reported in Table 1. *risk-neutral* denotes the moments of the risk-neutral density. N is the number of observations. The sample covers January 1996–December 2022 (1-month), May 1998–November 2022 (2-month), January 2002–October 2022 (3-month), and June 1996–June 2022 (6-month) expirations.

Panel A: Coefficients of determination for 1-month expiration

R^2's of option-based expected returns regressions (average R^2 = 33.72%; excl. risk-neutral: 49.51%)

	$\gamma_1 r$	$\gamma_1 nvix^{\gamma_3} r$	$\gamma_1 r + \gamma_2 r^2$	$\gamma_1 nvix^{\gamma_3} r + \gamma_2 nvix^{\gamma_3} r^2$
$\gamma_1 nvix^{\gamma_3} r$	74.28%			
$\gamma_1 r + \gamma_2 r^2$	95.80%	63.66%		
$\gamma_1 nvix^{\gamma_3} r + \gamma_2 nvix^{\gamma_3} r^2$	18.84%	21.39%	23.07%	
risk-neutral	8.43%	0.19%	4.97%	26.58%

R^2's of option-based variances regressions (average R^2 = 95.39%; excl. risk-neutral: 95.46%)

	$\gamma_1 r$	$\gamma_1 nvix^{\gamma_3} r$	$\gamma_1 r + \gamma_2 r^2$	$\gamma_1 nvix^{\gamma_3} r + \gamma_2 nvix^{\gamma_3} r^2$
$\gamma_1 nvix^{\gamma_3} r$	96.21%			
$\gamma_1 r + \gamma_2 r^2$	96.94%	94.82%		
$\gamma_1 nvix^{\gamma_3} r + \gamma_2 nvix^{\gamma_3} r^2$	98.14%	90.57%	96.06%	
risk-neutral	98.24%	92.60%	92.88%	97.43%

R^2's of option-based skewness regressions (average R^2 = 55.47%; excl. risk-neutral: 46.18%)

	$\gamma_1 r$	$\gamma_1 nvix^{\gamma_3} r$	$\gamma_1 r + \gamma_2 r^2$	$\gamma_1 nvix^{\gamma_3} r + \gamma_2 nvix^{\gamma_3} r^2$
$\gamma_1 nvix^{\gamma_3} r$	98.80%			
$\gamma_1 r + \gamma_2 r^2$	86.09%	86.23%		
$\gamma_1 nvix^{\gamma_3} r + \gamma_2 nvix^{\gamma_3} r^2$	0.66%	0.39%	4.93%	
risk-neutral	98.78%	97.17%	79.33%	2.34%

R^2's of option-based kurtosis regressions (average R^2 =55.87%; excl. risk-neutral: 45.63%)

	$\gamma_1 r$	$\gamma_1 nvix^{\gamma_3} r$	$\gamma_1 r + \gamma_2 r^2$	$\gamma_1 nvix^{\gamma_3} r + \gamma_2 nvix^{\gamma_3} r^2$
$\gamma_1 nvix^{\gamma_3} r$	99.66%			
$\gamma_1 r + \gamma_2 r^2$	84.24%	82.54%		
$\gamma_1 nvix^{\gamma_3} r + \gamma_2 nvix^{\gamma_3} r^2$	1.66%	2.27%	3.44%	
risk-neutral	99.44%	99.55%	83.64%	2.30%

Panel B: Coefficients of determination for 2-month expiration

R^2's of option-based expected returns regressions (average R^2 = 38.60%; excl. risk-neutral: 42.98%)

	$\gamma_1 r$	$\gamma_1 nvix^{\gamma_3} r$	$\gamma_1 r + \gamma_2 r^2$	$\gamma_1 nvix^{\gamma_3} r + \gamma_2 nvix^{\gamma_3} r^2$
$\gamma_1 nvix^{\gamma_3} r$	91.44%			
$\gamma_1 r + \gamma_2 r^2$	74.54%	84.39%		
$\gamma_1 nvix^{\gamma_3} r + \gamma_2 nvix^{\gamma_3} r^2$	6.33%	0.25%	0.93%	
risk-neutral	16.64%	39.46%	33.79%	38.24%

R^2's of option-based variances regressions (average R^2 = 93.30%; excl. risk-neutral: 92.26%)

	$\gamma_1 r$	$\gamma_1 nvix^{\gamma_3} r$	$\gamma_1 r + \gamma_2 r^2$	$\gamma_1 nvix^{\gamma_3} r + \gamma_2 nvix^{\gamma_3} r^2$
$\gamma_1 nvix^{\gamma_3} r$	99.61%			
$\gamma_1 r + \gamma_2 r^2$	82.47%	86.20%		
$\gamma_1 nvix^{\gamma_3} r + \gamma_2 nvix^{\gamma_3} r^2$	98.57%	99.41%	87.28%	
risk-neutral	97.33%	98.01%	87.49%	96.62%

R^2's of option-based skewness regressions (average R^2 = 59.14%; excl. risk-neutral: 49.73%)

	$\gamma_1 r$	$\gamma_1 nvix^{\gamma_3} r$	$\gamma_1 r + \gamma_2 r^2$	$\gamma_1 nvix^{\gamma_3} r + \gamma_2 nvix^{\gamma_3} r^2$
$\gamma_1 nvix^{\gamma_3} r$	99.84%			
$\gamma_1 r + \gamma_2 r^2$	98.79%	99.13%		
$\gamma_1 nvix^{\gamma_3} r + \gamma_2 nvix^{\gamma_3} r^2$	0.02%	0.21%	0.39%	
risk-neutral	96.52%	97.20%	97.77%	1.49%

R^2's of option-based kurtosis regressions (average R^2 = 60.41%; excl. risk-neutral: 50.73%)

	$\gamma_1 r$	$\gamma_1 nvix^{\gamma_3} r$	$\gamma_1 r + \gamma_2 r^2$	$\gamma_1 nvix^{\gamma_3} r + \gamma_2 nvix^{\gamma_3} r^2$
$\gamma_1 nvix^{\gamma_3} r$	99.95%			
$\gamma_1 r + \gamma_2 r^2$	99.33%	99.23%		
$\gamma_1 nvix^{\gamma_3} r + \gamma_2 nvix^{\gamma_3} r^2$	1.44%	1.45%	2.94%	
risk-neutral	98.36%	98.26%	99.34%	3.79%

Panel C: Coefficients of determination for 3-month expiration

R^2's of option-based expected returns regressions (average R^2 = 43.15%; excl. risk-neutral: 48.45%)

	$\gamma_1 r$	$\gamma_1 nvix^{\gamma_3} r$	$\gamma_1 r + \gamma_2 r^2$	$\gamma_1 nvix^{\gamma_3} r + \gamma_2 nvix^{\gamma_3} r^2$
$\gamma_1 nvix^{\gamma_3} r$	87.50%			
$\gamma_1 r + \gamma_2 r^2$	98.81%	89.70%		
$\gamma_1 nvix^{\gamma_3} r + \gamma_2 nvix^{\gamma_3} r^2$	8.30%	0.35%	6.06%	
risk-neutral	29.45%	59.03%	35.83%	16.53%

R^2's of option-based variances regressions (average R^2 = 97.33%; excl. risk-neutral: 97.95%)

	$\gamma_1 r$	$\gamma_1 nvix^{\gamma_3} r$	$\gamma_1 r + \gamma_2 r^2$	$\gamma_1 nvix^{\gamma_3} r + \gamma_2 nvix^{\gamma_3} r^2$
$\gamma_1 nvix^{\gamma_3} r$	99.65%			
$\gamma_1 r + \gamma_2 r^2$	98.40%	98.55%		
$\gamma_1 nvix^{\gamma_3} r + \gamma_2 nvix^{\gamma_3} r^2$	96.85%	97.72%	96.51%	
risk-neutral	96.25%	96.22%	99.08%	94.08%

R^2's of option-based skewness regressions (average R^2 = 58.31%; excl. risk-neutral: 48.50%)

	$\gamma_1 r$	$\gamma_1 nvix^{\gamma_3} r$	$\gamma_1 r + \gamma_2 r^2$	$\gamma_1 nvix^{\gamma_3} r + \gamma_2 nvix^{\gamma_3} r^2$
$\gamma_1 nvix^{\gamma_3} r$	99.09%			
$\gamma_1 r + \gamma_2 r^2$	93.10%	95.12%		
$\gamma_1 nvix^{\gamma_3} r + \gamma_2 nvix^{\gamma_3} r^2$	0.00%	0.73%	2.97%	
risk-neutral	94.59%	96.44%	98.51%	2.56%

R^2's of option-based kurtosis regressions (average R^2 = 54.91%; excl. risk-neutral: 55.11%)

	$\gamma_1 r$	$\gamma_1 nvix^{\gamma_3} r$	$\gamma_1 r + \gamma_2 r^2$	$\gamma_1 nvix^{\gamma_3} r + \gamma_2 nvix^{\gamma_3} r^2$
$\gamma_1 nvix^{\gamma_3} r$	62.33%			
$\gamma_1 r + \gamma_2 r^2$	54.35%	55.55%		
$\gamma_1 nvix^{\gamma_3} r + \gamma_2 nvix^{\gamma_3} r^2$	1.55%	0.90%	0.12%	
risk-neutral	62.03%	63.14%	79.68%	34.70%

Panel D: Coefficients of determination for 6-month expiration

R^2's of option-based expected returns regressions (average R^2 = 39.67%; excl. risk-neutral: 46.68%)

	$\gamma_1 r$	$\gamma_1 nvix^{\gamma_3} r$	$\gamma_1 r + \gamma_2 r^2$	$\gamma_1 nvix^{\gamma_3} r + \gamma_2 nvix^{\gamma_3} r^2$
$\gamma_1 nvix^{\gamma_3} r$	82.06%			
$\gamma_1 r + \gamma_2 r^2$	98.07%	86.74%		
$\gamma_1 nvix^{\gamma_3} r + \gamma_2 nvix^{\gamma_3} r^2$	0.17%	0.12%	0.05%	
risk-neutral	13.86%	41.75%	21.63%	39.36%

R^2's of option-based variances regressions (average R^2 = 95.89%; excl. risk-neutral: 96.37%)

	$\gamma_1 r$	$\gamma_1 nvix^{\gamma_3} r$	$\gamma_1 r + \gamma_2 r^2$	$\gamma_1 nvix^{\gamma_3} r + \gamma_2 nvix^{\gamma_3} r^2$
$\gamma_1 nvix^{\gamma_3} r$	99.66%			
$\gamma_1 r + \gamma_2 r^2$	96.77%	97.32%		
$\gamma_1 nvix^{\gamma_3} r + \gamma_2 nvix^{\gamma_3} r^2$	94.60%	96.64%	93.20%	
risk-neutral	96.20%	96.18%	98.42%	89.91%

R^2's of option-based skewness regressions (average R^2 = 44.37%; excl. risk-neutral: 35.91%)

	$\gamma_1 r$	$\gamma_1 nvix^{\gamma_3} r$	$\gamma_1 r + \gamma_2 r^2$	$\gamma_1 nvix^{\gamma_3} r + \gamma_2 nvix^{\gamma_3} r^2$
$\gamma_1 nvix^{\gamma_3} r$	86.59%			
$\gamma_1 r + \gamma_2 r^2$	62.86%	62.75%		
$\gamma_1 nvix^{\gamma_3} r + \gamma_2 nvix^{\gamma_3} r^2$	1.11%	2.04%	0.14%	
risk-neutral	71.35%	61.75%	90.33%	4.75%

R^2's of option-based kurtosis regressions (average R^2 = 56.49%; excl. risk-neutral: 46.63%)

	$\gamma_1 r$	$\gamma_1 nvix^{\gamma_3} r$	$\gamma_1 r + \gamma_2 r^2$	$\gamma_1 nvix^{\gamma_3} r + \gamma_2 nvix^{\gamma_3} r^2$
$\gamma_1 nvix^{\gamma_3} r$	95.20%			
$\gamma_1 r + \gamma_2 r^2$	79.27%	83.71%		
$\gamma_1 nvix^{\gamma_3} r + \gamma_2 nvix^{\gamma_3} r^2$	2.85%	9.34%	9.42%	
risk-neutral	93.70%	92.96%	92.91%	5.50%

Table 5 Coefficient of Determination for Third and Fourth Central Moments under the Physical Measure across Pricing Kernels

This table reports coefficients of determination (R^2) from regressions of option-based third and fourth central moments across pricing kernels from equations (1), (2), (4), and (6). Panel A presents R^2 values for the 1-month expiration, Panel B for the 2-month expiration, Panel C for the 3-month expiration, and Panel D for the 6-month expiration. N is the number of observations. Option-based physical moments are computed using equation (15). The pricing kernels are labeled by the exponents of their discount factors: $\gamma_1 r$ (equation (1)), $\gamma_1 nvix^{\gamma_3} r$ (equation (2)), $\gamma_1 r + \gamma_2 r^2$ (equation (4)), and $\gamma_1 nvix^{\gamma_3} r + \gamma_2 nvix^{\gamma_3} r^2$ (equation (6)). Here, r denotes log-returns and $nvix$ the normalized VIX, defined as the VIX divided by its 1986–1995 average (to avoid look-ahead bias) and scaled by option maturity. Estimation of the pricing kernels is based on the GMM system in equation (14), with results reported in Table 1. *risk-neutral* refers to the moments of the risk-neutral density. The sample spans January 1996–December 2022 (1-month), May 1998–November 2022 (2-month), January 2002–October 2022 (3-month), and June 1996–June 2022 (6-month) expirations.

Panel A: Coefficients of determination for 1-month expiration

R^2's of option-based third central moment regressions (average R^2 = 46.87%; excl. risk-neutral: 38.79%)

	$\gamma_1 r$	$\gamma_1 nvix^{\gamma_3} r$	$\gamma_1 r + \gamma_2 r^2$	$\gamma_1 nvix^{\gamma_3} r + \gamma_2 nvix^{\gamma_3} r^2$
$\gamma_1 nvix^{\gamma_3} r$	31.36%			
$\gamma_1 r + \gamma_2 r^2$	49.08%	45.05%		
$\gamma_1 nvix^{\gamma_3} r + \gamma_2 nvix^{\gamma_3} r^2$	81.39%	3.19%	22.70%	
risk-neutral	95.89%	20.85%	31.96%	87.29%

R^2's of option-based fourth central moment regressions (average R^2 =87.47%; excl. risk-neutral: 86.02%)

	$\gamma_1 r$	$\gamma_1 nvix^{\gamma_3} r$	$\gamma_1 r + \gamma_2 r^2$	$\gamma_1 nvix^{\gamma_3} r + \gamma_2 nvix^{\gamma_3} r^2$
$\gamma_1 nvix^{\gamma_3} r$	85.44%			
$\gamma_1 r + \gamma_2 r^2$	96.26%	82.88%		
$\gamma_1 nvix^{\gamma_3} r + \gamma_2 nvix^{\gamma_3} r^2$	93.86%	67.92%	89.78%	
risk-neutral	95.22%	77.93%	88.31%	97.07%

Panel B: Coefficients of determination for 2-month expiration

R^2's of option-based third central moment regressions (average R^2 = 79.58%; excl. risk-neutral: 78.70%)

	$\gamma_1 r$	$\gamma_1 nvix^{\gamma_3} r$	$\gamma_1 r + \gamma_2 r^2$	$\gamma_1 nvix^{\gamma_3} r + \gamma_2 nvix^{\gamma_3} r^2$
$\gamma_1 nvix^{\gamma_3} r$	96.59%			
$\gamma_1 r + \gamma_2 r^2$	60.71%	69.90%		
$\gamma_1 nvix^{\gamma_3} r + \gamma_2 nvix^{\gamma_3} r^2$	81.39%	92.75%	70.85%	
risk-neutral	95.77%	93.19%	57.81%	76.83%

R^2's of option-based fourth central moment regressions (average R^2 = 88.55%; excl. risk-neutral: 86.75%)

	$\gamma_1 r$	$\gamma_1 nvix^{\gamma_3} r$	$\gamma_1 r + \gamma_2 r^2$	$\gamma_1 nvix^{\gamma_3} r + \gamma_2 nvix^{\gamma_3} r^2$
$\gamma_1 nvix^{\gamma_3} r$	99.44%			
$\gamma_1 r + \gamma_2 r^2$	70.50%	75.67%		
$\gamma_1 nvix^{\gamma_3} r + \gamma_2 nvix^{\gamma_3} r^2$	96.69%	98.69%	79.53%	
risk-neutral	97.61%	97.47%	75.94%	93.93%

Panel C: Coefficients of determination for 3-month expiration

R^2's of option-based third central moment regressions (average R^2 = 86.45%; excl. risk-neutral: 86.57%)

	$\gamma_1 r$	$\gamma_1 nvix^{\gamma_3} r$	$\gamma_1 r + \gamma_2 r^2$	$\gamma_1 nvix^{\gamma_3} r + \gamma_2 nvix^{\gamma_3} r^2$
$\gamma_1 nvix^{\gamma_3} r$	93.89%			
$\gamma_1 r + \gamma_2 r^2$	89.38%	90.26%		
$\gamma_1 nvix^{\gamma_3} r + \gamma_2 nvix^{\gamma_3} r^2$	75.14%	90.17%	80.60%	
risk-neutral	89.23%	85.32%	97.07%	73.50%

R^2's of option-based fourth central moment regressions (average R^2 = 92.92%; excl. risk-neutral: 93.51%)

	$\gamma_1 r$	$\gamma_1 nvix^{\gamma_3} r$	$\gamma_1 r + \gamma_2 r^2$	$\gamma_1 nvix^{\gamma_3} r + \gamma_2 nvix^{\gamma_3} r^2$
$\gamma_1 nvix^{\gamma_3} r$	98.82%			
$\gamma_1 r + \gamma_2 r^2$	91.23%	91.47%		
$\gamma_1 nvix^{\gamma_3} r + \gamma_2 nvix^{\gamma_3} r^2$	92.58%	96.09%	90.85%	
risk-neutral	91.79%	90.15%	98.62%	87.57%

Panel D: Coefficients of determination for 6-month expiration

R^2's of option-based third central moment regressions (average R^2 = 65.66%; excl. risk-neutral: 66.73%)

	$\gamma_1 r$	$\gamma_1 nvix^{\gamma_3} r$	$\gamma_1 r + \gamma_2 r^2$	$\gamma_1 nvix^{\gamma_3} r + \gamma_2 nvix^{\gamma_3} r^2$
$\gamma_1 nvix^{\gamma_3} r$	87.39%			
$\gamma_1 r + \gamma_2 r^2$	58.46%	76.48%		
$\gamma_1 nvix^{\gamma_3} r + \gamma_2 nvix^{\gamma_3} r^2$	44.83%	72.75%	60.47%	
risk-neutral	68.28%	69.88%	82.89%	35.09%

R^2's of option-based fourth central moment regressions (average R^2 = 91.74%; excl. risk-neutral: 92.26%)

	$\gamma_1 r$	$\gamma_1 nvix^{\gamma_3} r$	$\gamma_1 r + \gamma_2 r^2$	$\gamma_1 nvix^{\gamma_3} r + \gamma_2 nvix^{\gamma_3} r^2$
$\gamma_1 nvix^{\gamma_3} r$	99.40%			
$\gamma_1 r + \gamma_2 r^2$	91.09%	91.75%		
$\gamma_1 nvix^{\gamma_3} r + \gamma_2 nvix^{\gamma_3} r^2$	91.76%	94.98%	84.58%	
risk-neutral	93.70%	92.64%	96.15%	81.38%

Table 6 Summary Statistics of the Risk-neutral Variance Bounds for Expected Returns

Panel A of this table reports summary statistics for the Martin (2017) bound of expected returns, which is based on the risk-neutral variance according to equation (24), bound=$R^f_{t,t+T} + var^{RND}(R_{t,t+T})/R^f_{t,t+T}$. The risk-free rate is the expected return to the stock market according to the risk-neutral density, $R^f_{t,t+T} = \mathbb{E}^{RND}_t[R_{t,t+T}]$. Panel B reports correlations between the risk-neutral variance bound for expected returns and the option-based expected returns from the different pricing kernels. The pricing kernels are labeled according to their exponents: $\gamma_1 r$ (equation (1)), $\gamma_1 nvix^{\gamma_3} r$ (equation (2)), $\gamma_1 r + \gamma_2 r^2$ (equation (4)), and $\gamma_1 nvix^{\gamma_3} r + \gamma_2 nvix^{\gamma_3} r^2$ (equation (6)). r denotes log-returns, and *nvix* is the normalized VIX, which is the VIX divided by its 1986-1995 average (to avoid look-ahead bias) and appropriately scaled for each expiration. The estimation of the various pricing kernels is based on the GMM system of equation (14), and the results are reported in Table 1. *risk-neutral* denotes the moments of the risk-neutral density. Option-based physical and risk-neutral moments are derived according to equation (15). The sample is from January 1996 to December 2022 for 1-month expiration options, May 1998 to November 2022 for 2-month expiration, January 2002 to October 2022 for 3-month expiration, and June 1996 to June 2022 for 6-month expiration options.

Panel A: Risk-neutral bound for expected returns

$R^f_{t,t+T} + \frac{var^{RND}(R_{t,t+T})}{R^f_{t,t+T}} - 1$	1-month	2-month	3-month	6-month
mean	0.45%	1.05%	1.37%	3.12%
st. deviation	0.64%	1.28%	1.26%	1.77%
N	323	147	83	52

Panel B: Correlations of risk-neutral bound for expected returns with option-based expected returns

1-month expiration

	$\gamma_1 r$	$\gamma_1 nvix^{\gamma_3} r$	$\gamma_1 r + \gamma_2 r^2$	$\gamma_1 nvix^{\gamma_3} r + \gamma_2 nvix^{\gamma_3} r^2$	risk-neutral
$R^f_{t,t+T} + \frac{var^{RND}(R_{t,t+T})}{R^f_{t,t+T}}$	0.99	0.81	0.96	-0.33	0.42

2-month expiration

	$\gamma_1 r$	$\gamma_1 nvix^{\gamma_3} r$	$\gamma_1 r + \gamma_2 r^2$	$\gamma_1 nvix^{\gamma_3} r + \gamma_2 nvix^{\gamma_3} r^2$	risk-neutral
$R^f_{t,t+T} + \frac{var^{RND}(R_{t,t+T})}{R^f_{t,t+T}}$	0.99	0.97	0.87	-0.17	0.49

3-month expiration

	$\gamma_1 r$	$\gamma_1 nvix^{\gamma_3} r$	$\gamma_1 r + \gamma_2 r^2$	$\gamma_1 nvix^{\gamma_3} r + \gamma_2 nvix^{\gamma_3} r^2$	risk-neutral
$R^f_{t,t+T} + \frac{var^{RND}(R_{t,t+T})}{R^f_{t,t+T}}$	0.99	0.96	0.99	-0.20	0.63

6-month expiration

	$\gamma_1 r$	$\gamma_1 nvix^{\gamma_3} r$	$\gamma_1 r + \gamma_2 r^2$	$\gamma_1 nvix^{\gamma_3} r + \gamma_2 nvix^{\gamma_3} r^2$	risk-neutral
$R^f_{t,t+T} + \frac{var^{RND}(R_{t,t+T})}{R^f_{t,t+T}}$	0.98	0.95	0.99	0.09	0.53

Table 7 Regressions of Risk-Neutral Variances as a Binding Lower Bound for Option-based Expected Returns Across Pricing Kernels

This table reports regression results for equation (27), which tests whether the variance-based risk-neutral lower bound for risk premia from equation (24) is binding across the different pricing kernels. $var_t^{RND}(R_{t,t+T})$ denotes the risk-neutral variance and $R^f_{t,t+T}$ the risk-free rate, measured as the mean stock market return under the risk-neutral distribution, $R^f_{t,t+T} = \mathbb{E}_t^{RND}[R_{t,t+T}]$. Panel A reports regressions with realized excess returns, $R^e_{t,t+T} = R_{t,t+T} - R^f_{t,t+T}$, as the dependent variable. Panel B uses backward-looking fitted excess returns, $\widehat{R}^e_{t,t+T} = \widehat{R}_{t,t+T} - R^f_{t,t+T}$, where $\widehat{R}_{t,t+T}$ are fitted values from regressions of realized returns on the price–dividend ratio, dividend growth, and the risk-free rate (see Table OA.2 in the Online Appendix). Panels C and D examine the risk-neutral bounds with the forward-looking option-based risk premium, $\mathbb{E}_t[R^e_{t,t+T}] = \mathbb{E}_t[R_{t,t+T}] - R^f_{t,t+T}$, implied by the monotonic pricing kernels in equations (1) and (2). Panels E and F report analogous results for the non-monotonic kernels in equations (4) and (6). Option-based expected returns, $\mathbb{E}_t[R_{t,t+T}]$, are computed using equation (15). The pricing kernels are labeled by the exponents of their discount factors: $\gamma_1 r$ (equation (1)), $\gamma_1 nvix^{\gamma_3} r$ (equation (2)), $\gamma_1 r + \gamma_2 r^2$ (equation (4)), and $\gamma_1 nvix^{\gamma_3} r + \gamma_2 nvix^{\gamma_3} r^2$ (equation (6)). Here, r denotes log-returns and $nvix$ the normalized VIX, defined as the VIX divided by its 1986–1995 average (to avoid look-ahead bias) and scaled to each option maturity. *risk-neutral* refers to the moments of the risk-neutral density. Estimation of the pricing kernels is based on the GMM system in equation (14), with results reported in Table 1. All variables are contemporaneous, and regressions are estimated over non-overlapping intervals. Reported t-statistics (in parentheses) are corrected for heteroscedasticity and autocorrelation using Newey–West standard errors with 12, 6, 4, and 2 lags for the 1-, 2-, 3-, and 6-month expirations, respectively. N denotes the number of observations. The sample spans January 1996–December 2022 (1-month), May 1998–November 2022 (2-month), January 2002–October 2022 (3-month), and June 1996–June 2022 (6-month) expirations.

Panel A: Realized returns

$R^e_{t,t+T}$	1-month	2-month	3-month	6-month
$var_t^{RND}(R_{t,t+T})/R^f_{t,t+T}$	1.763	1.106	0.280	1.196
	(2.06)	(1.39)	(0.25)	(1.82)
	{0.89}	{0.13}	{-0.66}	{0.30}
constant	-0.207%	0.120%	1.202%	0.604%
	(-0.47)	(0.14)	(1.06)	(0.28)
R^2	4.63%	3.18%	0.13%	2.88%
N	323	147	83	52

Panel B: Backward-looking fitted returns

$\widehat{R}^e_{t,t+T}$	1-month	2-month	3-month	6-month
$var_t^{RND}(R_{t,t+T})/R^f_{t,t+T}$	0.532	0.409	0.602	1.011
	(4.73)	(2.89)	(2.89)	(2.87)
	{-4.15}	{-4.16}	{-1.90}	{0.03}
constant	0.410%	0.823%	0.821%	0.653%
	(2.65)	(2.83)	(1.40)	(0.57)
R^2	12.38%	10.33%	8.76%	14.68%
N	321	146	82	50

Panel C: Option-based risk premia from pricing kernel in equation (1) ***($\gamma_1 r$)***

$\mathbb{E}_t[R^e_{t,t+T}]$	1-month	2-month	3-month	6-month
$var_t^{RND}(R_{t,t+T})/R^f_{t,t+T}$	1.282	1.195	1.219	1.371
	(172.37)	(141.76)	(204.61)	(247.90)
	{37.98}	{23.19}	{36.83}	{67.13}
constant	0.014%	0.033%	0.026%	0.148%
	(4.96)	(4.78)	(5.36)	(7.23)
R^2	99.96%	99.96%	99.94%	99.85%
N	323	147	83	52

Panel D: Option-based risk premia from pricing kernel in equation (2) ***($\gamma_1 nvix^{\gamma_3} r$)***

$\mathbb{E}_t[R^e_{t,t+T}]$	1-month	2-month	3-month	6-month
$var_t^{RND}(R_{t,t+T})/R^f_{t,t+T}$	3.993	0.725	0.623	0.735
	(7.34)	(23.09)	(10.94)	(16.41)
	{5.50}	{-8.75}	{-6.61}	{-5.91}
constant	-1.348%	0.517%	0.769%	1.834%
	(-4.80)	(12.33)	(10.59)	(13.44)
R^2	84.26%	96.84%	89.61%	89.11%
N	323	147	83	52

Panel E: Option-based risk premia from pricing kernel in equation (4) ***($\gamma_1 r + \gamma_2 r^2$)***

$\mathbb{E}_t[R^e_{t,t+T}]$	1-month	2-month	3-month	6-month
$var_t^{RND}(R_{t,t+T})/R^f_{t,t+T}$	1.192	0.773	1.146	1.257
	(16.20)	(2.66)	(26.41)	(43.10)
	{2.61}	{-0.78}	{3.38}	{8.81}
constant	0.084%	0.467%	0.110%	0.442%
	(2.30)	(1.83)	(3.04)	(6.62)
R^2	95.41%	69.95%	97.93%	97.26%
N	323	147	83	52

Panel F: Option-based risk premia from pricing kernel in equation (6) ***($\gamma_1 nvix^{\gamma_3} r + \gamma_2 nvix^{\gamma_3} r^2$)***

$\mathbb{E}_t[R^e_{t,t+T}]$	1-month	2-month	3-month	6-month
$var_t^{RND}(R_{t,t+T})/R^f_{t,t+T}$	-0.276	-0.271	-0.582	-0.081
	(-4.53)	(-3.66)	(-4.17)	(-1.08)
	{-20.92}	{-17.16}	{-11.34}	{-14.45}
constant	0.835%	1.557%	2.289%	4.009%
	(11.47)	(11.23)	(7.39)	(11.15)
R^2	16.20%	18.76%	25.08%	1.25%
N	323	147	83	52

Table 8 Violations of Risk-Neutral Lower Bounds for Option-based Expected Returns Across Pricing Kernels

This table reports the frequency with which realized returns and option-based risk premia fall below the variance-based risk-neutral lower bound from equation (24). Panel A reports violations for the 1-month expiration, Panel B for the 2-month expiration, Panel C for the 3-month expiration, and Panel D for the 6-month expiration. Violations are calculated for alternative measures of realized and expected excess returns. Realized excess returns are $R^e_{t,t+T} = R_{t,t+T} - R^f_{t,t+T}$. Backward-looking fitted excess returns are $\widehat{R}^e_{t,t+T} = \widehat{R}_{t,t+T} - R^f_{t,t+T}$, where $\widehat{R}_{t,t+T}$ are fitted values from regressions of realized returns on the price–dividend ratio, dividend growth, and the risk-free rate (see Table OA.2 in the Online Appendix). Option-based risk premia, $\mathbb{E}_t[R^e_{t,t+T}] = \mathbb{E}_t[R_{t,t+T}] - R^f_{t,t+T}$, are computed from the pricing kernels in equations (1), (2), (4), and (6). The pricing kernels are labeled by the exponents of their discount factors: $\gamma 1r$ (equation (1)), $\gamma_1 nvix^{\gamma_3} r$ (equation (2)), $\gamma_1 r + \gamma_2 r^2$ (equation (4)), and $\gamma_1 nvix^{\gamma_3} r + \gamma_2 nvix^{\gamma_3} r^2$ (equation (6)). Here, r denotes log-returns and $nvix$ the normalized VIX, defined as the VIX divided by its 1986–1995 average (to avoid look-ahead bias) and scaled by maturity. Estimation of the pricing kernels is based on the GMM system in equation (14), with results reported in Table 1. Option-based expected returns are computed from equation (15). N denotes the number of observations. In all tests, the risk-free rate is measured as the expected return under the risk-neutral distribution, $R^f_{t,t+T} = \mathbb{E}^{RND}_t[R_{t,t+T}]$. Numbers in brackets report the average absolute differences between the excess return measures and the variance-based risk-neutral bound. The sample covers January 1996–December 2022 (1-month), May 1998–November 2022 (2-month), January 2002–October 2022 (3-month), and June 1996–June 2022 (6-month) expirations.

Panel A: Violations of risk-neutral lower bounds for expected returns, 1-month expiration

$R^e_{t,T+T}$	$\widehat{R}^e_{t,T+T}$	$\mathbb{E}_t[R^e_{t,t+T}]$ $\gamma_1 r$	$\mathbb{E}_t[R^e_{t,t+T}]$ $\gamma_1 nvix^{\gamma_3} r$	$\mathbb{E}_t[R^e_{t,t+T}]$ $\gamma_1 r + \gamma_2 r^2$	$\mathbb{E}_t[R^e_{t,t+T}]$ $\gamma_1 nvix^{\gamma_3} r + \gamma_2 nvix^{\gamma_3} r^2$	N
41% [3.41%]	36% [0.76%]	0% [0.15%]	83% [0.41%]	5% [0.18%]	45% [0.54%]	323

Panel B: Violations of risk-neutral lower bounds for expected returns, 2-month expiration

$R^e_{t,T+T}$	$\widehat{R}^e_{t,T+T}$	$\mathbb{E}_t[R^e_{t,t+T}]$ $\gamma_1 r$	$\mathbb{E}_t[R^e_{t,t+T}]$ $\gamma_1 nvix^{\gamma_3} r$	$\mathbb{E}_t[R^e_{t,t+T}]$ $\gamma_1 r + \gamma_2 r^2$	$\mathbb{E}_t[R^e_{t,t+T}]$ $\gamma_1 nvix^{\gamma_3} r + \gamma_2 nvix^{\gamma_3} r^2$	N
40% [4.93%]	36% [1.26%]	0% [0.23%]	5% [0.31%]	1% [0.32%]	41% [0.96%]	147

Panel C: Violations of risk-neutral lower bounds for expected returns, 3-month expiration

$R^e_{t,T+T}$	$\widehat{R}^e_{t,T+T}$	$\mathbb{E}_t[R^e_{t,t+T}]$ $\gamma_1 r$	$\mathbb{E}_t[R^e_{t,t+T}]$ $\gamma_1 nvix^{\gamma_3} r$	$\mathbb{E}_t[R^e_{t,t+T}]$ $\gamma_1 r + \gamma_2 r^2$	$\mathbb{E}_t[R^e_{t,t+T}]$ $\gamma_1 nvix^{\gamma_3} r + \gamma_2 nvix^{\gamma_3} r^2$	N
40% [5.83%]	40% [1.64%]	0% [0.30%]	8% [0.43%]	1% [0.29%]	53% [1.44%]	83

Panel D: Violations of risk-neutral lower bounds for expected returns, 6-month expiration

$R^e_{t,T+T}$	$\widehat{R}^e_{t,T+T}$	$\mathbb{E}_t[R^e_{t,t+T}]$ $\gamma_1 r$	$\mathbb{E}_t[R^e_{t,t+T}]$ $\gamma_1 nvix^{\gamma_3} r$	$\mathbb{E}_t[R^e_{t,t+T}]$ $\gamma_1 r + \gamma_2 r^2$	$\mathbb{E}_t[R^e_{t,t+T}]$ $\gamma_1 nvix^{\gamma_3} r + \gamma_2 nvix^{\gamma_3} r^2$	N
36% [8.42%]	36% [3.15%]	0% [1.13%]	4% [1.19%]	0% [1.13%]	42% [2.10%]	52

Online Appendix: Non-Monotonic Pricing Kernels, Conditional Physical Densities, and Risk-Neutral Bounds for Expected Returns

Online Appendix A Supplemental Figures

Figure OA.1 Risk-neutral Density Functions

This figure shows the average risk-neutral density functions across expirations, with and without tail adjustment. The tail adjustment is implemented by appending a type-I (two-parameter) Pareto distribution to the tails of the risk-neutral density (equation (OA.1)). The parameters of the left-tail (right-tail) Pareto distribution are identified by matching the fitted Pareto distribution to the empirical risk-neutral densities at the 2% (98%) and 5% (95%) quantiles. Details on the construction of the risk-neutral distribution are provided in Section Online Appendix D. For each expiration, the figure plots time-averaged risk-neutral density functions, both adjusted and unadjusted. The sample spans January 1996–December 2022 (1-month), May 1998–November 2022 (2-month), January 2002–October 2022 (3-month), and June 1996–June 2022 (6-month) expirations.

Panel A: One-month expiration

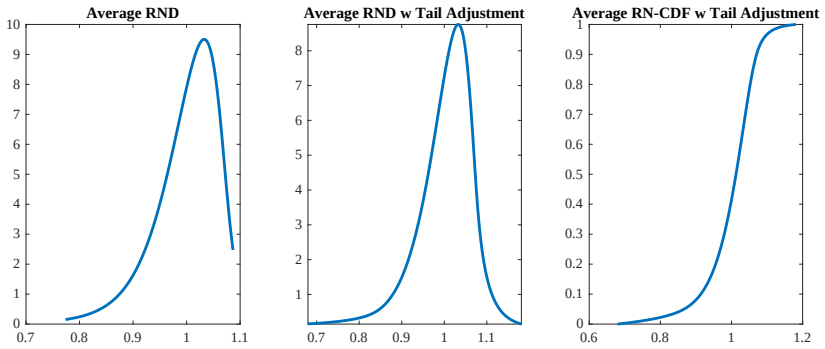

Panel B: Two-month expiration

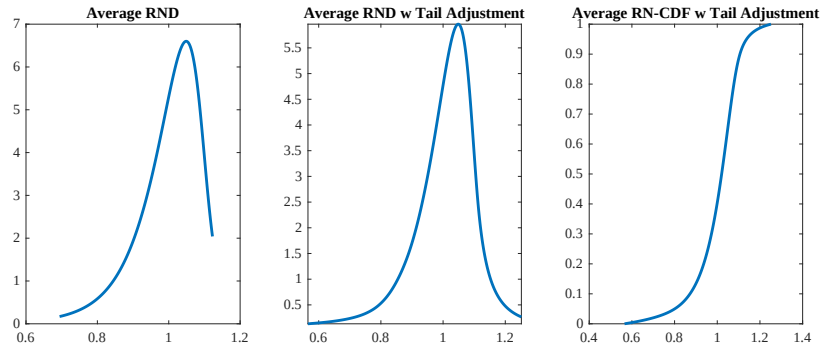

Panel C: Three-month expiration

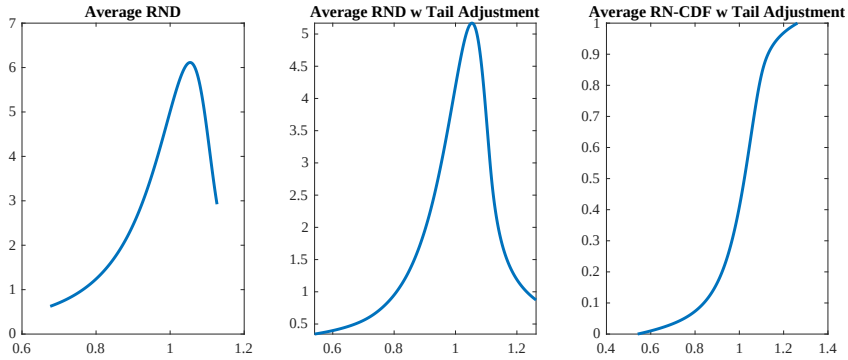

Panel D: Six-month expiration

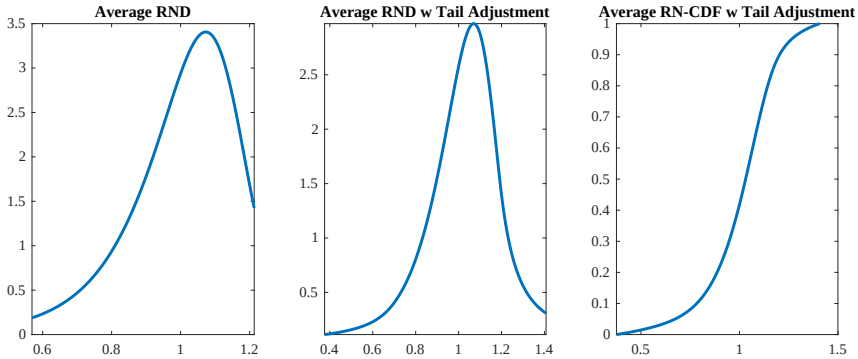

Online Appendix B Supplemental Tables

Table OA.1 Sample of Option Contracts

This table summarizes the S&P 500 option contracts from OptionMetrics used to construct option-implied densities under the physical measure. The following selection criteria are imposed: non-missing implied volatility, positive trading volume, and a bid price above \$3/8. In addition, each date must contain at least six eligible contracts, with a minimum of three puts and three calls outside the ±2% moneyness band. At the beginning of the sample, two non-consecutive 2-month observations and eleven non-consecutive 3-month observations were excluded because the risk-neutral density could not be estimated given insufficient contracts. Moreover, since a consecutive series of observations is required to compute autocorrelations for Newey–West standard errors in the GMM estimation, additional early observations for the 2- and 3-month maturities were dropped. The final sample spans January 1996–December 2022 for 1-month options, May 1998–November 2022 for 2-month options, January 2002–October 2022 for 3-month options, and June 1996–June 2022 for 6-month options.

	1-month	2-month	3-month	6-month
Num. of Calls	38,577	14,329	6,141	3,368
Num. of Puts	46,420	18,980	8,432	3,574
Total	84,997	33,309	14,573	6,942
Num. of Expiration Dates (without filters)	323	161	107	52
Num. of Expiration Dates (with filters)	323	159	96	52
Num. of Expiration Dates (with filters and consecutive non-missing observations)	323	147	83	52

Table OA.2 Backward-looking Fitted Returns

anel A of this table reports four sets of regression results for the backward-looking fitted returns of the S&P500. Fitted returns, $\widehat{R}_{t,t+T}-1$, are obtained by regressing realized returns, $R_{t,t+T}-1$, on the dividend yield $divp_t$, lagged dividend growth $\Delta div_{t-T,t}$, and the risk-free rate $R^f_{t,t+T}$. Realized returns, dividends, and dividend yields are from the CRSP S&P Index files. The risk-free rate is the mean of the option-based RND, $\mathbb{E}_t^{RND}[R_{t,t+T}-1]$. Reported t-statistics (in parentheses) are corrected for heteroscedasticity and autocorrelation using Newey–West standard errors with 12, 6, 4, and 2 lags for the 1-, 2-, 3-, and 6-month expirations, respectively. All regressions are estimated on non-overlapping intervals. Panel B reports summary statistics for realized and backward-looking fitted returns. Panel C presents correlations of realized and backward-looking returns with option-based expected returns derived from the pricing kernels in equations (1), (2), (4), and (6). Option-based expected returns are labeled according to the exponent of the corresponding discount factor: $\gamma_1 r$ (equation (1)), $\gamma_1 nvix^{\gamma_3} r$ (equation (2)), $\gamma_1 r+\gamma_2 r^2$ (equation (4)), and $\gamma_1 nvix^{\gamma_3} r+\gamma_2 nvix^{\gamma_3} r^2$ (equation (6)). Here, r denotes log-returns, and $nvix$ is the normalized VIX, defined as the VIX divided by its 1986–1995 average (to avoid look-ahead bias) and appropriately scaled for each expiration. Estimation of the pricing kernels is based on the GMM system in equation (14), with results reported in Table 1. *risk-neutral* denotes the moments of the risk-neutral density, and option-based physical and risk-neutral moments are derived according to equation (15). *risk-neutral bound* is the expected return according to the variance-based lower bound in equation (24) from Martin (2017). ρ^* is the correlation between realized and backward-looking fitted returns. The sample spans January 1996–December 2022 (1-month expiration), May 1998–November 2022 (2-month), January 2002–October 2022 (3-month), and December 1996–June 2022 (6-month).

Panel A: Regressions for backward-looking fitted returns

$R_{t,t+T}$	1-month	2-month	3-month	6-month
$divp_t$	12.954	16.092	10.930	14.037
	(1.56)	(1.24)	(0.84)	(1.22)
$\Delta div_{t-T,t}$	-0.011	-0.018	0.029	-0.028
	(-1.15)	(-0.57)	(0.28)	(-0.25)
$R^f_{t,t+T}$	-0.520	0.314	-0.719	-0.359
	(-0.66)	(0.35)	(-0.82)	(-0.21)
constant	-1.376%	-3.797%	-3.755%	-9.082%
	(-1.13)	(-0.97)	(-0.59)	(-0.84)
R^2	1.45%	2.25%	3.20%	8.59%
N	321	146	82	50

Panel B: Summary statistics for realized and backward-looking fitted returns

i) $R_{t,t+T}$	1-month	2-month	3-month	6-month
mean	0.63%	1.28%	1.66%	4.25%
st. deviation	4.88%	7.01%	7.41%	10.62%
N	323	147	83	52

ii) $\widehat{R}_{t,t+T}$	1-month	2-month	3-month	6-month
mean	0.62%	1.24%	1.67%	3.78%
st. deviation	0.59%	1.05%	1.33%	3.10%
N	321	146	82	50

Panel C: Correlations of realized and backward-looking fitted returns with option-based expected returns

1-month expiration

	$\gamma_1 r$ $\mathbb{E}_t[R_{t,t+T}]$	$\gamma_1 nvix^{\gamma_3} r$ $\mathbb{E}_t[R_{t,t+T}]$	$\gamma_1 r + \gamma_2 r^2$ $\mathbb{E}_t[R_{t,t+T}]$	$\gamma_1 nvix^{\gamma_3} r + \gamma_2 nvix^{\gamma_3} r^2$ $\mathbb{E}_t[R_{t,t+T}]$	risk-neutral $\mathbb{E}_t^{RND}[R_{t,t+T}]$	risk-neutral bound $R^f_{t,t+T} + \frac{var_t^{RND}(R_{t,t+T})}{R^f_{t,t+T}}$	ρ^*
$R_{t,t+T}$	0.15	0.20	0.14	-0.17	-0.06	0.14	
$\widehat{R}_{t,t+T}$	0.01	0.27	0.01	-0.41	-0.56	-0.07	0.12

2-month expiration

	$\gamma_1 r$ $\mathbb{E}_t[R_{t,t+T}]$	$\gamma_1 nvix^{\gamma_3} r$ $\mathbb{E}_t[R_{t,t+T}]$	$\gamma_1 r + \gamma_2 r^2$ $\mathbb{E}_t[R_{t,t+T}]$	$\gamma_1 nvix^{\gamma_3} r + \gamma_2 nvix^{\gamma_3} r^2$ $\mathbb{E}_t[R_{t,t+T}]$	risk-neutral $\mathbb{E}_t^{RND}[R_{t,t+T}]$	risk-neutral bound $R^f_{t,t+T} + \frac{var_t^{RND}(R_{t,t+T})}{R^f_{t,t+T}}$	ρ^*
$R_{t,t+T}$	0.14	0.10	0.04	-0.10	-0.01	0.13	
$\widehat{R}_{t,t+T}$	0.17	0.04	0.10	-0.24	-0.15	0.14	0.15

3-month expiration

	$\gamma_1 r$ $\mathbb{E}_t[R_{t,t+T}]$	$\gamma_1 nvix^{\gamma_3} r$ $\mathbb{E}_t[R_{t,t+T}]$	$\gamma_1 r + \gamma_2 r^2$ $\mathbb{E}_t[R_{t,t+T}]$	$\gamma_1 nvix^{\gamma_3} r + \gamma_2 nvix^{\gamma_3} r^2$ $\mathbb{E}_t[R_{t,t+T}]$	risk-neutral $\mathbb{E}_t^{RND}[R_{t,t+T}]$	risk-neutral bound $R^f_{t,t+T} + \frac{var_t^{RND}(R_{t,t+T})}{R^f_{t,t+T}}$	ρ^*
$R_{t,t+T}$	-0.05	-0.09	-0.05	-0.13	-0.10	-0.06	
$\widehat{R}_{t,t+T}$	-0.09	-0.31	-0.10	-0.26	-0.53	-0.15	0.18

6-month expiration

	$\gamma_1 r$ $\mathbb{E}_t[R_{t,t+T}]$	$\gamma_1 nvix^{\gamma_3} r$ $\mathbb{E}_t[R_{t,t+T}]$	$\gamma_1 r + \gamma_2 r^2$ $\mathbb{E}_t[R_{t,t+T}]$	$\gamma_1 nvix^{\gamma_3} r + \gamma_2 nvix^{\gamma_3} r^2$ $\mathbb{E}_t[R_{t,t+T}]$	risk-neutral $\mathbb{E}_t^{RND}[R_{t,t+T}]$	risk-neutral bound $R^f_{t,t+T} + \frac{var_t^{RND}(R_{t,t+T})}{R^f_{t,t+T}}$	ρ^*
$R_{t,t+T}$	0.05	-0.05	0.02	-0.17	-0.11	0.02	
$\widehat{R}_{t,t+T}$	-0.02	-0.26	-0.08	-0.40	-0.62	-0.14	0.29

Table OA.3 Summary Statistics of Option-based Log-return Moments for the Physical Measure Across Pricing Kernels

This table reports summary statistics for option-based moments of log-returns under the physical measure, derived from the pricing kernels in equations (1), (2), (4), and (6). The kernels are labeled by their discount factor exponents: $\gamma_1 r$, $\gamma_1 nvix^{\gamma_3} r$, $\gamma_1 r + \gamma_2 r^2$, and $\gamma_1 nvix^{\gamma_3} r + \gamma_2 nvix^{\gamma_3} r^2$, where r denotes log-returns and $nvix$ the normalized VIX. Estimation follows the GMM system in equation (14) (see Table 1). *risk-neutral* indicates moments of the risk-neutral density, and *realized* refers to sample moments of realized returns. Option-based physical and risk-neutral moments are computed using equation (15). Panel A reports expected returns, Panel B variances, Panel C skewness, and Panel D kurtosis. The sample spans January 1996–December 2022 (1-month), May 1998–November 2022 (2-month), January 2002–October 2022 (3-month), and June 1996–June 2022 (6-month).

Panel A: Option-based expected log-returns across pricing kernels

i) $\gamma_1 r$	1-month	2-month	3-month	6-month
mean	0.38%	0.83%	1.13%	3.14%
st. deviation	0.58%	1.11%	1.12%	1.71%
N	323	147	83	52
ii) $\gamma_1 nvix^{\gamma_3} r$	1-month	2-month	3-month	6-month
mean	0.38%	0.82%	1.11%	3.12%
st. deviation	2.19%	0.80%	0.78%	1.19%
N	323	147	83	52
iii) $\gamma_1 r + \gamma_2 r^2$	1-month	2-month	3-month	6-month
mean	0.45%	0.49%	1.04%	2.88%
st. deviation	0.57%	4.26%	1.13%	1.70%
N	323	147	83	52
iv) $\gamma_1 nvix^{\gamma_3} r + \gamma_2 nvix^{\gamma_3} r^2$	1-month	2-month	3-month	6-month
mean	0.43%	0.86%	1.13%	3.49%
st. deviation	0.74%	1.49%	1.69%	1.65%
N	323	147	83	52
v) risk-neutral	1-month	2-month	3-month	6-month
mean	-0.36%	-0.64%	-0.68%	-1.24%
st. deviation	0.67%	1.42%	1.32%	2.13%
N	323	147	83	52
vi) realized mean	1-month	2-month	3-month	6-month
	0.51%	1.01%	1.37%	3.60%

Panel B: Option-based physical variances of log-returns across pricing kernels

i) $\gamma_1 r$	1-month	2-month	3-month	6-month
mean	0.47%	0.94%	1.13%	2.19%
st. deviation	0.51%	0.90%	0.82%	1.08%
N	323	147	83	52

ii) $\gamma_1 nvix^{\gamma_3} r$	1-month	2-month	3-month	6-month
mean	0.47%	0.98%	1.17%	2.25%
st. deviation	0.32%	1.27%	1.08%	1.55%
N	323	147	83	52

iii) $\gamma_1 r + \gamma_2 r^2$	1-month	2-month	3-month	6-month
mean	0.36%	3.38%	1.37%	3.02%
st. deviation	0.28%	29.63%	1.29%	2.78%
N	323	147	83	52

iv) $\gamma_1 nvix^{\gamma_3} r + \gamma_2 nvix^{\gamma_3} r^2$	1-month	2-month	3-month	6-month
mean	0.44%	0.96%	1.15%	1.41%
st. deviation	0.95%	2.67%	1.78%	1.81%
N	323	147	83	52

v) risk-neutral	1-month	2-month	3-month	6-month
mean	0.64%	1.51%	1.79%	3.96%
st. deviation	0.94%	2.67%	1.74%	3.16%
N	323	147	83	52

vi) realized variance	1-month	2-month	3-month	6-month
	0.25%	0.56%	0.58%	1.19%

Panel C: Option-based physical skewness of log-returns across pricing kernels

i) $\gamma_1 r$	1-month	2-month	3-month	6-month
mean	-1.90	-2.06	-2.07	-1.64
st. deviation	0.96	1.03	1.02	0.54
N	323	147	83	52

ii) $\gamma_1 nvix^{\gamma_3} r$	1-month	2-month	3-month	6-month
mean	-1.90	-2.05	-2.05	-1.59
st. deviation	0.96	1.02	0.99	0.48
N	323	147	83	52

iii) $\gamma_1 r + \gamma_2 r^2$	1-month	2-month	3-month	6-month
mean	-1.54	-2.13	-2.32	-2.18
st. deviation	0.71	1.13	1.36	1.22
N	323	147	83	52

iv) $\gamma_1 nvix^{\gamma_3} r + \gamma_2 nvix^{\gamma_3} r^2$	1-month	2-month	3-month	6-month
mean	-0.86	-0.87	-1.02	-0.54
st. deviation	0.70	0.69	0.93	0.37
N	323	147	83	52

v) risk-neutral	1-month	2-month	3-month	6-month
mean	-1.96	-2.17	-2.21	-2.02
st. deviation	0.93	1.09	1.15	0.92
N	323	147	83	52

vi) realized skewness	1-month	2-month	3-month	6-month
	-1.78	-2.39	-1.44	-1.37

Panel D: Option-based physical kurtosis of log-returns across pricing kernels

i) $\gamma_1 r$	1-month	2-month	3-month	6-month
mean	10.96	12.71	12.97	9.85
st. deviation	7.33	9.34	9.53	4.97
N	323	147	83	52

ii) $\gamma_1 nvix^{\gamma_3} r$	1-month	2-month	3-month	6-month
mean	10.48	12.84	13.04	9.59
st. deviation	6.69	9.44	9.48	4.60
N	323	147	83	52

iii) $\gamma_1 r + \gamma_2 r^2$	1-month	2-month	3-month	6-month
mean	8.81	13.36	14.85	13.86
st. deviation	4.80	10.88	12.85	11.53
N	323	147	83	52

iv) $\gamma_1 nvix^{\gamma_3} r + \gamma_2 nvix^{\gamma_3} r^2$	1-month	2-month	3-month	6-month
mean	5.54	5.56	6.41	3.97
st. deviation	3.35	3.59	5.57	1.18
N	323	147	83	52

v) risk-neutral	1-month	2-month	3-month	6-month
mean	10.17	11.73	11.99	10.49
st. deviation	6.01	7.96	8.41	6.63
N	323	147	83	52

vi) realized kurtosis	1-month	2-month	3-month	6-month
	11.72	13.89	5.76	6.26

Table OA.4 Coefficient of Determination for Log-Return Moments under the Physical Measure across Pricing Kernels

This table reports coefficients of determination (R^2) from regressions of option-based moments of log-returns across the pricing kernels in equations (1), (2), (4), and (6). Panel A presents results for the 1-month expiration, Panel B for the 2-month expiration, Panel C for the 3-month expiration, and Panel D for the 6-month expiration. Option-based physical moments are derived from equation (15). The kernels are labeled by the exponents of their discount factors: $\gamma_1 r$ (equation (1)), $\gamma_1 nvix^{\gamma_3} r$ (equation (2)), $\gamma_1 r + \gamma_2 r^2$ (equation (4)), and $\gamma_1 nvix^{\gamma_3} r + \gamma_2 nvix^{\gamma_3} r^2$ (equation (6)), where r denotes log-returns and $nvix$ is the normalized VIX (the VIX divided by its 1986–1995 average and scaled to each maturity). Estimation of the pricing kernels is based on the GMM system in equation (14), with results reported in Table 1. *risk-neutral* refers to the moments of the risk-neutral density, and N is the number of observations. The sample spans January 1996–December 2022 (1-month), May 1998–November 2022 (2-month), January 2002–October 2022 (3-month), and June 1996–June 2022 (6-month).

Panel A: Coefficients of determination for 1-month expiration

R^2's of option-based expected log-returns regressions (average R^2 = 43.80%; excl. risk-neutral: 57.19%)

	$\gamma_1 r$	$\gamma_1 nvix^{\gamma_3} r$	$\gamma_1 r + \gamma_2 r^2$	$\gamma_1 nvix^{\gamma_3} r + \gamma_2 nvix^{\gamma_3} r^2$
$\gamma_1 nvix^{\gamma_3} r$	62.28%			
$\gamma_1 r + \gamma_2 r^2$	91.20%	59.22%		
$\gamma_1 nvix^{\gamma_3} r + \gamma_2 nvix^{\gamma_3} r^2$	31.42%	53.89%	45.17%	
risk-neutral	0.47%	26.34%	6.63%	61.46%

R^2's of option-based log-return variances regressions (average R^2 = 83.53%; excl. risk-neutral: 82.55%)

	$\gamma_1 r$	$\gamma_1 nvix^{\gamma_3} r$	$\gamma_1 r + \gamma_2 r^2$	$\gamma_1 nvix^{\gamma_3} r + \gamma_2 nvix^{\gamma_3} r^2$
$\gamma_1 nvix^{\gamma_3} r$	79.10%			
$\gamma_1 r + \gamma_2 r^2$	94.38%	82.69%		
$\gamma_1 nvix^{\gamma_3} r + \gamma_2 nvix^{\gamma_3} r^2$	94.05%	59.08%	86.04%	
risk-neutral	95.10%	65.74%	82.55%	96.60%

R^2's of option-based log-return skewness regressions (average R^2 = 53.54%; excl. risk-neutral: 43.85%)

	$\gamma_1 r$	$\gamma_1 nvix^{\gamma_3} r$	$\gamma_1 r + \gamma_2 r^2$	$\gamma_1 nvix^{\gamma_3} r + \gamma_2 nvix^{\gamma_3} r^2$
$\gamma_1 nvix^{\gamma_3} r$	97.35%			
$\gamma_1 r + \gamma_2 r^2$	75.55%	77.83%		
$\gamma_1 nvix^{\gamma_3} r + \gamma_2 nvix^{\gamma_3} r^2$	5.34%	3.27%	3.77%	
risk-neutral	99.02%	95.08%	69.86%	8.41%

R^2's of option-based log-return kurtosis regressions (average R^2 = 55.35%; excl. risk-neutral: 44.85%)

	$\gamma_1 r$	$\gamma_1 nvix^{\gamma_3} r$	$\gamma_1 r + \gamma_2 r^2$	$\gamma_1 nvix^{\gamma_3} r + \gamma_2 nvix^{\gamma_3} r^2$
$\gamma_1 nvix^{\gamma_3} r$	98.72%			
$\gamma_1 r + \gamma_2 r^2$	72.28%	70.96%		
$\gamma_1 nvix^{\gamma_3} r + \gamma_2 nvix^{\gamma_3} r^2$	12.69%	13.63%	0.87%	
risk-neutral	99.13%	98.08%	73.78%	13.41%

Panel B: Coefficients of determination for 2-month expiration

R^2's of option-based expected log-returns regressions (average R^2 = 27.22%; excl. risk-neutral: 22.28%)

	$\gamma_1 r$	$\gamma_1 nvix^{\gamma_3} r$	$\gamma_1 r + \gamma_2 r^2$	$\gamma_1 nvix^{\gamma_3} r + \gamma_2 nvix^{\gamma_3} r^2$
$\gamma_1 nvix^{\gamma_3} r$	65.82%			
$\gamma_1 r + \gamma_2 r^2$	4.27%	5.69%		
$\gamma_1 nvix^{\gamma_3} r + \gamma_2 nvix^{\gamma_3} r^2$	22.76%	0.58%	34.53%	
risk-neutral	0.14%	26.95%	41.93%	69.55%

R^2's of option-based log-return variances regressions (average R^2 = 79.83%; excl. risk-neutral: 74.92%)

	$\gamma_1 r$	$\gamma_1 nvix^{\gamma_3} r$	$\gamma_1 r + \gamma_2 r^2$	$\gamma_1 nvix^{\gamma_3} r + \gamma_2 nvix^{\gamma_3} r^2$
$\gamma_1 nvix^{\gamma_3} r$	97.23%			
$\gamma_1 r + \gamma_2 r^2$	41.64%	55.75%		
$\gamma_1 nvix^{\gamma_3} r + \gamma_2 nvix^{\gamma_3} r^2$	85.57%	94.90%	74.44%	
risk-neutral	87.12%	94.35%	71.90%	95.39%

R^2's of option-based log-return skewness regressions (average R^2 = 61.95%; excl. risk-neutral: 52.58%)

	$\gamma_1 r$	$\gamma_1 nvix^{\gamma_3} r$	$\gamma_1 r + \gamma_2 r^2$	$\gamma_1 nvix^{\gamma_3} r + \gamma_2 nvix^{\gamma_3} r^2$
$\gamma_1 nvix^{\gamma_3} r$	99.52%			
$\gamma_1 r + \gamma_2 r^2$	97.99%	98.82%		
$\gamma_1 nvix^{\gamma_3} r + \gamma_2 nvix^{\gamma_3} r^2$	4.34%	6.58%	8.25%	
risk-neutral	96.74%	98.16%	99.11%	10.02%

R^2's of option-based log-return kurtosis regressions (average R^2 = 65.54%; excl. risk-neutral: 57.12%)

	$\gamma_1 r$	$\gamma_1 nvix^{\gamma_3} r$	$\gamma_1 r + \gamma_2 r^2$	$\gamma_1 nvix^{\gamma_3} r + \gamma_2 nvix^{\gamma_3} r^2$
$\gamma_1 nvix^{\gamma_3} r$	99.71%			
$\gamma_1 r + \gamma_2 r^2$	97.55%	96.93%		
$\gamma_1 nvix^{\gamma_3} r + \gamma_2 nvix^{\gamma_3} r^2$	14.88%	16.20%	17.46%	
risk-neutral	97.01%	98.00%	96.04%	21.65%

Panel C: Coefficients of determination for 3-month expiration

R^2's of option-based expected log-returns regressions (average R^2 = 37.35%; excl. risk-neutral: 41.17%)

	$\gamma_1 r$	$\gamma_1 nvix^{\gamma_3} r$	$\gamma_1 r + \gamma_2 r^2$	$\gamma_1 nvix^{\gamma_3} r + \gamma_2 nvix^{\gamma_3} r^2$
$\gamma_1 nvix^{\gamma_3} r$	60.65%			
$\gamma_1 r + \gamma_2 r^2$	92.07%	72.60%		
$\gamma_1 nvix^{\gamma_3} r + \gamma_2 nvix^{\gamma_3} r^2$	14.08%	3.10%	4.50%	
risk-neutral	6.61%	56.39%	20.92%	42.56%

R^2's of option-based log-return variances regressions (average R^2 = 92.45%; excl. risk-neutral: 92.82%)

	$\gamma_1 r$	$\gamma_1 nvix^{\gamma_3} r$	$\gamma_1 r + \gamma_2 r^2$	$\gamma_1 nvix^{\gamma_3} r + \gamma_2 nvix^{\gamma_3} r^2$
$\gamma_1 nvix^{\gamma_3} r$	98.33%			
$\gamma_1 r + \gamma_2 r^2$	89.79%	90.22%		
$\gamma_1 nvix^{\gamma_3} r + \gamma_2 nvix^{\gamma_3} r^2$	92.52%	96.35%	89.70%	
risk-neutral	90.75%	90.35%	98.66%	87.78%

R^2's of option-based log-return skewness regressions (average R^2 = 63.85%; excl. risk-neutral: 54.82%)

	$\gamma_1 r$	$\gamma_1 nvix^{\gamma_3} r$	$\gamma_1 r + \gamma_2 r^2$	$\gamma_1 nvix^{\gamma_3} r + \gamma_2 nvix^{\gamma_3} r^2$
$\gamma_1 nvix^{\gamma_3} r$	98.66%			
$\gamma_1 r + \gamma_2 r^2$	91.91%	95.01%		
$\gamma_1 nvix^{\gamma_3} r + \gamma_2 nvix^{\gamma_3} r^2$	7.97%	14.11%	21.28%	
risk-neutral	96.96%	98.69%	97.42%	16.55%

R^2's of option-based log-return kurtosis regressions (average R^2 = 69.04%; excl. risk-neutral: 61.19%)

	$\gamma_1 r$	$\gamma_1 nvix^{\gamma_3} r$	$\gamma_1 r + \gamma_2 r^2$	$\gamma_1 nvix^{\gamma_3} r + \gamma_2 nvix^{\gamma_3} r^2$
$\gamma_1 nvix^{\gamma_3} r$	99.55%			
$\gamma_1 r + \gamma_2 r^2$	95.00%	95.73%		
$\gamma_1 nvix^{\gamma_3} r + \gamma_2 nvix^{\gamma_3} r^2$	19.85%	23.52%	33.49%	
risk-neutral	98.47%	99.08%	97.46%	28.20%

Panel D: Coefficients of determination for 6-month expiration

R^2's of option-based expected log-returns regressions (average R^2 = 33.82%; excl. risk-neutral: 38.92%)

	$\gamma_1 r$	$\gamma_1 nvix^{\gamma_3} r$	$\gamma_1 r + \gamma_2 r^2$	$\gamma_1 nvix^{\gamma_3} r + \gamma_2 nvix^{\gamma_3} r^2$
$\gamma_1 nvix^{\gamma_3} r$	52.72%			
$\gamma_1 r + \gamma_2 r^2$	79.44%	74.41%		
$\gamma_1 nvix^{\gamma_3} r + \gamma_2 nvix^{\gamma_3} r^2$	8.19%	18.77%	0.00%	
risk-neutral	0.02%	35.25%	15.09%	54.36%

R^2's of option-based log-return variances regressions (average R^2 = 85.53%; excl. risk-neutral: 84.31%)

	$\gamma_1 r$	$\gamma_1 nvix^{\gamma_3} r$	$\gamma_1 r + \gamma_2 r^2$	$\gamma_1 nvix^{\gamma_3} r + \gamma_2 nvix^{\gamma_3} r^2$
$\gamma_1 nvix^{\gamma_3} r$	97.42%			
$\gamma_1 r + \gamma_2 r^2$	76.73%	79.97%		
$\gamma_1 nvix^{\gamma_3} r + \gamma_2 nvix^{\gamma_3} r^2$	85.95%	94.40%	71.38%	
risk-neutral	87.88%	89.60%	92.92%	79.05%

R^2's of option-based log-return skewness regressions (average R^2 = 50.41%; excl. risk-neutral: 39.64%)

	$\gamma_1 r$	$\gamma_1 nvix^{\gamma_3} r$	$\gamma_1 r + \gamma_2 r^2$	$\gamma_1 nvix^{\gamma_3} r + \gamma_2 nvix^{\gamma_3} r^2$
$\gamma_1 nvix^{\gamma_3} r$	81.72%			
$\gamma_1 r + \gamma_2 r^2$	65.41%	82.65%		
$\gamma_1 nvix^{\gamma_3} r + \gamma_2 nvix^{\gamma_3} r^2$	2.22%	3.54%	2.29%	
risk-neutral	86.11%	88.81%	91.31%	0.02%

R^2's of option-based log-return kurtosis regressions (average R^2 = 54.78%; excl. risk-neutral: 44.16%)

	$\gamma_1 r$	$\gamma_1 nvix^{\gamma_3} r$	$\gamma_1 r + \gamma_2 r^2$	$\gamma_1 nvix^{\gamma_3} r + \gamma_2 nvix^{\gamma_3} r^2$
$\gamma_1 nvix^{\gamma_3} r$	91.73%			
$\gamma_1 r + \gamma_2 r^2$	76.42%	88.34%		
$\gamma_1 nvix^{\gamma_3} r + \gamma_2 nvix^{\gamma_3} r^2$	0.05%	4.22%	4.21%	
risk-neutral	91.12%	95.57%	94.060%	1.53%

Table OA.5 Coefficient of Determination for Third and Fourth Log-Return Moments under the Physical Measure across Pricing Kernels

This table reports coefficients of determination (R^2) from regressions of option-based third and fourth central moments of log-returns across the pricing kernels in equations (1), (2), (4), and (6). Panel A presents R^2 values for the 1-month expiration, Panel B for the 2-month expiration, Panel C for the 3-month expiration, and Panel D for the 6-month expiration. Option-based physical moments are derived from equation (15). The pricing kernels are labeled by the exponents of their discount factors: $\gamma_1 r$ (equation (1)), $\gamma_1 nvix^{\gamma_3} r$ (equation (2)), $\gamma_1 r + \gamma_2 r^2$ (equation (4)), and $\gamma_1 nvix^{\gamma_3} r + \gamma_2 nvix^{\gamma_3} r^2$ (equation (6)), where r denotes log-returns and $nvix$ is the normalized VIX (the VIX divided by its 1986–1995 average and scaled to each maturity to avoid look-ahead bias). Pricing kernel estimation is based on the GMM system in equation (14), with results reported in Table 1. *risk-neutral* refers to the moments of the risk-neutral density, and N is the number of observations. The sample spans January 1996–December 2022 (1-month), May 1998–November 2022 (2-month), January 2002–October 2022 (3-month), and June 1996–June 2022 (6-month).

Panel A: Coefficients of determination for 1-month expiration

R^2's of option-based third central moment regressions (average R^2 = 53.65%; excl. risk-neutral: 46.38%)

	$\gamma_1 r$	$\gamma_1 nvix^{\gamma_3} r$	$\gamma_1 r + \gamma_2 r^2$	$\gamma_1 nvix^{\gamma_3} r + \gamma_2 nvix^{\gamma_3} r^2$
$\gamma_1 nvix^{\gamma_3} r$	24.80%			
$\gamma_1 r + \gamma_2 r^2$	73.90%	37.73%		
$\gamma_1 nvix^{\gamma_3} r + \gamma_2 nvix^{\gamma_3} r^2$	86.24%	3.31%	52.28%	
risk-neutral	92.81%	11.50%	57.36%	96.60%

R^2's of option-based fourth central moment regressions (average R^2 =54.22%; excl. risk-neutral: 46.67%)

	$\gamma_1 r$	$\gamma_1 nvix^{\gamma_3} r$	$\gamma_1 r + \gamma_2 r^2$	$\gamma_1 nvix^{\gamma_3} r + \gamma_2 nvix^{\gamma_3} r^2$
$\gamma_1 nvix^{\gamma_3} r$	18.95%			
$\gamma_1 r + \gamma_2 r^2$	82.17%	24.31%		
$\gamma_1 nvix^{\gamma_3} r + \gamma_2 nvix^{\gamma_3} r^2$	89.44%	4.48%	60.70%	
risk-neutral	92.01%	9.05%	62.12%	98.95%

Panel B: Coefficients of determination for 2-month expiration

R^2's of option-based third central moment regressions (average R^2 = 85.06%; excl. risk-neutral: 81.08%)

	$\gamma_1 r$	$\gamma_1 nvix^{\gamma_3} r$	$\gamma_1 r + \gamma_2 r^2$	$\gamma_1 nvix^{\gamma_3} r + \gamma_2 nvix^{\gamma_3} r^2$
$\gamma_1 nvix^{\gamma_3} r$	92.10%			
$\gamma_1 r + \gamma_2 r^2$	55.48%	78.65%		
$\gamma_1 nvix^{\gamma_3} r + \gamma_2 nvix^{\gamma_3} r^2$	72.64%	92.63%	94.97%	
risk-neutral	79.53%	94.46%	92.64%	97.53%

R^2's of option-based fourth central moment regressions (average R^2 = 88.88%; excl. risk-neutral: 86.23%)

	$\gamma_1 r$	$\gamma_1 nvix^{\gamma_3} r$	$\gamma_1 r + \gamma_2 r^2$	$\gamma_1 nvix^{\gamma_3} r + \gamma_2 nvix^{\gamma_3} r^2$
$\gamma_1 nvix^{\gamma_3} r$	90.72%			
$\gamma_1 r + \gamma_2 r^2$	67.13%	90.24%		
$\gamma_1 nvix^{\gamma_3} r + \gamma_2 nvix^{\gamma_3} r^2$	75.11%	95.23%	98.94%	
risk-neutral	77.68%	95.77%	98.48%	99.51%

Panel C: Coefficients of determination for 3-month expiration

R^2's of option-based third central moment regressions (average R^2 = 83.46%; excl. risk-neutral: 81.73%)

	$\gamma_1 r$	$\gamma_1 nvix^{\gamma_3} r$	$\gamma_1 r + \gamma_2 r^2$	$\gamma_1 nvix^{\gamma_3} r + \gamma_2 nvix^{\gamma_3} r^2$
$\gamma_1 nvix^{\gamma_3} r$	92.78%			
$\gamma_1 r + \gamma_2 r^2$	77.78%	76.04%		
$\gamma_1 nvix^{\gamma_3} r + \gamma_2 nvix^{\gamma_3} r^2$	77.02%	91.76%	75.02%	
risk-neutral	89.35%	83.32%	95.84%	75.67%

R^2's of option-based fourth central moment regressions (average R^2 = 81.30%; excl. risk-neutral: 79.01%)

	$\gamma_1 r$	$\gamma_1 nvix^{\gamma_3} r$	$\gamma_1 r + \gamma_2 r^2$	$\gamma_1 nvix^{\gamma_3} r + \gamma_2 nvix^{\gamma_3} r^2$
$\gamma_1 nvix^{\gamma_3} r$	92.11%			
$\gamma_1 r + \gamma_2 r^2$	72.73%	70.92%		
$\gamma_1 nvix^{\gamma_3} r + \gamma_2 nvix^{\gamma_3} r^2$	75.05%	90.59%	72.69%	
risk-neutral	87.76%	81.35%	94.94%	74.90%

Panel D: Coefficients of determination for 6-month expiration

R^2's of option-based third central moment regressions (average R^2 = 72.35%; excl. risk-neutral: 68.86%)

	$\gamma_1 r$	$\gamma_1 nvix^{\gamma_3} r$	$\gamma_1 r + \gamma_2 r^2$	$\gamma_1 nvix^{\gamma_3} r + \gamma_2 nvix^{\gamma_3} r^2$
$\gamma_1 nvix^{\gamma_3} r$	92.48%			
$\gamma_1 r + \gamma_2 r^2$	61.48%	63.17%		
$\gamma_1 nvix^{\gamma_3} r + \gamma_2 nvix^{\gamma_3} r^2$	68.00%	87.65%	40.38%	
risk-neutral	85.48%	81.78%	87.29%	55.81%

R^2's of option-based fourth central moment regressions (average R^2 = 70.71%; excl. risk-neutral: 66.85%)

	$\gamma_1 r$	$\gamma_1 nvix^{\gamma_3} r$	$\gamma_1 r + \gamma_2 r^2$	$\gamma_1 nvix^{\gamma_3} r + \gamma_2 nvix^{\gamma_3} r^2$
$\gamma_1 nvix^{\gamma_3} r$	93.41%			
$\gamma_1 r + \gamma_2 r^2$	59.37%	56.43%		
$\gamma_1 nvix^{\gamma_3} r + \gamma_2 nvix^{\gamma_3} r^2$	71.79%	89.14%	30.93%	
risk-neutral	86.76%	80.33%	85.47%	53.51%

Online Appendix C Details of the GMM Estimation of Pricing Kernels

The parameters in the pricing kernels of equations (2), (4), and (6) are estimated using an exactly identified single-stage GMM. If the number of parameters in the discount factor is m, the GMM system in equation (14) consists of $m-1$ uniform moments conditions (equation (10)) together with the rational expectations condition (equation (11)). In the special case where $m = 1$ in equation (14), namely, the simple power utility model of equation (1), GMM estimation is over-identified in a 2×2 system with one degree of freedom. This over-identification arises because the one-parameter discount factor must satisfy both the uniform moments condition (equation (10)) and the rational expectations condition (equation (11)).

For all pricing kernels, I use an $m \times m$ diagonal weighting matrix with diagonal elements $1, 1, \ldots, 100$. Uniform moments conditions (equation (10)) are assigned a weight of one, while the rational expectations condition (equation (11)) is assigned a weight of 100, reflecting its smaller scale relative to the uniform moments. For the exactly identified GMM system corresponding to the discount factors in equations (1), (4), and (6), the choice of weighting matrix is immaterial. The weighting scheme primarily affects estimation of the monotonic fixed-parameter model (equation (1)), whose GMM system is over-identified. In all cases, the gradient of the GMM objective is computed numerically by differentiating equation (14) with respect to model parameters.

Standard errors are computed following Cochrane (2005) and are corrected for autocorrelation and heteroscedasticity using the Newey and West (1987) methodology with 12, 6, 4, and 2 lags for the 1-, 2-, 3-, and 6-month expirations, respectively. For the over-identified GMM system corresponding to the standard power utility model in equation (1), the χ^2 test for GMM errors has one degree of freedom. By contrast, for the exactly identified GMM systems of the discount factors in equations (2), (4), and (6), the χ^2 test has zero degrees of freedom.

Online Appendix D Derivation of the Risk-neutral Density

The derivation of the risk-neutral density (RND) follows the methodology in Figlewski (2010), Birru and Figlewski (2012), Linn et al. (2018), and Alexiou et al. (2025). The first step is to construct the implied volatility (IV) curve across strike prices. For strike prices (K) outside the $\pm 2\%$ range of the underlying spot price (S_t), I use IV's provided by OptionMetrics. For strike prices inside the

$\pm 2\%$ range of the underlying spot price, I combine the IV's of OptionMetrics for puts (IV_p) and calls (IV_c) with the same strike price into a single point

$$IV\big(K \in (1 \pm 2\%)S_t\big) = \omega IV_p\big(K \in (1 \pm 2\%)S_t\big) + (1-\omega)IV_c\big(K \in (1 \pm 2\%)S_t\big),$$

where $\omega = (K_{max} - K)/(K_{max} - K_{min})$, and K_{max} and K_{min} are, respectively, the maximum and minimum strike prices in the $\pm 2\%$ moneyness range. As in Alexiou et al. (2025), this is done to avoid an artificial jump at the ATM region, which could arise from ATM puts trading at higher IV relative to ATM calls.

The IV curve is constructed by fitting a quintic spline with 1,000 moneyness nodes to the derived IV estimates. Using the Black and Scholes (1973) formula, the IV curve is then converted into a curve of call option prices, $C_{t,t+T}(S_t R_{i,t}, S_t, \widetilde{r}_{f,t,t+T}, IV_{t,t+T}(K), div_{t,t+T})$, where $R_{i,t} = K_{i,t}/S_t$ is the moneyness (or gross return) for every strike price, $\widetilde{r}_{f,t,t+T}$ is the continuously-compounded risk-free rate (Federal funds rate), and $div_{t,t+T}$ is the continuously-compounded dividend yield from OptionMetrics. The risk-neutral density, $\widetilde{q}_{t,t+T}(SR) = d\widetilde{Q}_{t,t+T}(SR)/d(SR)$, is derived using the result in Breeden and Litzenberger (1978):

$$\widetilde{q}_{t,t+T}(S_t R_{t,t+T}) = e^{T\ \widetilde{r}_{f,t,t+T}} \frac{\partial^2 C_{t,t+T}(S_t R_{t,t+T}, S_t, \widetilde{r}_{f,t,t+T}, IV_{t,t+T}(K), div_{t,+T})}{\partial (S_t R_{t,t+T})^2}.$$

The chain rule implies that the risk-neutral density expressed in terms of gross returns is

$$\widetilde{q}_{t,t+T}(R_{t,t+T}) = S_t e^{T\ \widetilde{r}_{f,t,t+T}} \frac{\partial^2 C_{t,t+T}(S_t R_{t,t+T}, S_t, \widetilde{r}_{f,t,t+T}, IV_{t,t+T}(K), div_{t,+T})}{\partial (S_t R_{t,t+T})^2}.$$

The second derivative above is calculated using a second-order centered difference approximation. Further, I can rescale the RND with the factor

$$\widehat{q}_{t,t+T}(R_{i,t}) = \frac{\widetilde{q}_{t,t+T}(R_{i,t})}{\sum_{i=1}^{1,000} \widetilde{q}_{t,t+T}(R_{i,t})(R_{i+1,t} - R_{i,t})}.$$

In this case, $\widehat{q}_{t,t+T}(R_{i,t})$ is a well-defined density function for gross returns (moneyness) since

$$\sum_{i=1}^{1,000} \widehat{q}_{t,t+T}(R_{i,t})(R_{i+1,t} - R_{i,t}) = \sum_{i=1}^{1,000} \frac{\widetilde{q}_{t,t+T}(R_{i,t})(R_{i+1,t} - R_{i,t})}{\sum_{i=1}^{1,000} \widetilde{q}_{t,t+T}(R_i)(R_{i+1,t} - R_{i,t})} = 1.$$

The derived density is truncated at its tails because options for extreme values of the stock market index are dropped from the sample ($< \$3/8$) or the corresponding prices are zero. Hence, as in Figlewski (2010) and Linn et al. (2018), the final step in deriving the RND is to adjust its tails by appending heavy-tailed distributions. To this end, I assume that the left (l) and right (r) tails of the RND are given by two-parameter Pareto density functions, $f_l(R)$ and $f_r(R)$:

$$f_l(R) = \frac{\alpha_l(\lambda_l - R)^{-\alpha_l - 1}}{\lambda_l^{-\alpha_l}}, R \leq \lambda_l, \quad f_r(R) = \frac{\alpha_r R^{-\alpha_r - 1}}{\lambda_r^{-\alpha_r}}, R \geq \lambda_r. \tag{OA.1}$$

The two parameters, α_l and λ_l (α_r and λ_r) are identified by solving a 2×2 system of non-linear equations where I set the left (right) Pareto density above equal to the values of the derived RND at the 2% and 5% (95% and 98%) percentiles. Finally, using the solutions for the parameters in the tail distributions, I extend the domain of moneyness by approximately 60% (30% in the left tail and 30% in the right tail) from 1,000 to 1,600 nodes, and re-normalize the RND to obtain a well-defined density that integrates to one:

$$q_{t,t+T}(R_i) = \frac{\widehat{q}_{t,t+T}(R_i)}{\sum_{i=1}^{1,400} \widehat{q}_{t,t+T}(R_i)(R_{i+1} - R_i)}.$$

Overall, I obtain 323 RND's for the 1-month expiration, 147 for the 2-month, 83 for the 3-month, and 52 RND's for the 6-month expiration. Figure OA.1 in the Online Appendix shows the average RND, with and without tail adjustments, obtained from option prices across expirations. These graphs are similar to those in Linn et al. (2018).

Online Appendix E Proofs

E.1 Pricing Kernels and Log-normal Densities

This section derives the resulting probability densities from combining linear or quadratic pricing kernels with log-normal or skew log-normal distributions. The log-normal probability density function is proportional to

$$\frac{1}{y} Exp\Big[\frac{(lny + \omega)^2}{2\sigma^2}\Big].$$

The constants ω and σ^2 are the location and scale parameters of the distribution. The skew log-normal probability density function is proportional to

$$\frac{1}{y}Exp\Big[\frac{(lny+\omega)^2}{2\sigma^2}\Big]\Phi\Big(\lambda\frac{lny-\omega}{\sigma}+\xi\Big),$$

where $\Phi()$ is the standard normal cumulative distribution function. The constants ω and σ^2 are the location and scale parameters. The parameters λ and ξ are the skewness and kurtosis parameters for $R > 0$. Based on the probability density functions above for the log-normal and the skew log-normal distributions, the distributions resulting from the linear and quadratic pricing kernels can be easily calculated.

Linear Pricing Kernel and Log-normal Distribution

$$\frac{1}{y}Exp\Big[\gamma_1 lny-\frac{(lny-\omega)^2}{2\sigma^2}\Big]\propto\frac{1}{y}Exp\Big[-\frac{\big(lny-(\omega+\gamma_1\sigma^2)\big)^2}{2\sigma^2}\Big].$$

Quadratic Pricing Kernel and Log-normal Distribution

$$\frac{1}{y}Exp\Big[\gamma_1 lny+\gamma_2 ln^2y-\frac{(lny-\omega)^2}{2\sigma^2}\Big]\propto\frac{1}{y}Exp\Big[-\frac{\big(lny-\frac{\omega+\gamma_1\sigma^2}{1-2\gamma_2\sigma^2}\big)^2}{2\frac{\sigma^2}{1-2\gamma_2\sigma^2}}\Big].$$

Linear Pricing Kernel and Skew Log-normal Distribution

$$\frac{1}{y}Exp\Big[\gamma_1 lny-\frac{(lny-\omega)^2}{2\sigma^2}\Big]\Phi\Big(\lambda\frac{lny-\omega}{\sigma}+\xi\Big)\propto$$
$$\frac{1}{y}Exp\Big[-\frac{\big(lny-(\omega+\gamma_1\sigma^2)\big)^2}{2\sigma^2}\Big]\Phi\Big(\lambda\frac{lny-(\omega+\gamma_1\sigma^2)}{\sigma}+\xi+\lambda\gamma_1\sigma\Big).$$

Quadratic Pricing Kernel and Skew Log-normal Distribution

$$\frac{1}{y}Exp\Big[\gamma_1 lny+\gamma_2 ln^2y-\frac{(lny-\omega)^2}{2\sigma^2}\Big]\Phi\Big(\lambda\frac{lny-\omega}{\sigma}+\xi\Big)\propto$$

$$\frac{1}{y}Exp\Big[-\frac{\big(lny-\frac{\omega+\gamma_1\sigma^2}{1-2\gamma_2\sigma^2}\big)^2}{2\frac{\sigma^2}{1-2\gamma_2\sigma^2}}\Big]\Phi\Big(\frac{\lambda}{\sqrt{1-2\gamma_2\sigma^2}}\frac{lny-\frac{\omega+\gamma_1\sigma^2}{1-2\gamma_2\sigma^2}}{\frac{\sigma}{\sqrt{1-2\gamma_2\sigma^2}}}+\xi+\lambda\frac{\gamma_1+2\omega\gamma_2}{1-2\gamma_2\sigma^2}\sigma\Big).$$

E.2 Location-Scale Moments

Let Y be a location-scale transformation of a standardized random variable Z:

$$Y=\omega+Z\sigma,$$

where ω and σ are the location and scale parameters. Then, it follows that

$$\begin{aligned}
E[Y] &= \omega+E[Z]\sigma \\
E[(Y-E[Y])^2] &= E[(Z-E[Z])^2]\sigma^2 \\
E[(Y-E[Y])^3] &= E[(Z-E[Z])^3]\sigma^3 \\
E[(Y-E[Y])^4] &= E[(Z-E[Z])^4]\sigma^4.
\end{aligned}$$

E.3 Truncated Normal Moments

This section derives the moments of a standard normal variable, T, truncated below $-\frac{\xi}{\sqrt{1+\lambda^2}}$:

$$T\sim\frac{N(0,1)}{1-\Phi\big(-\frac{\xi}{\sqrt{1+\lambda^2}}\big)},\ T>-\frac{\xi}{\sqrt{1+\lambda^2}}.$$

The first moment is

$$E[T]=\frac{\phi\big(-\frac{\xi}{\sqrt{1+\lambda^2}}\big)}{1-\Phi\big(-\frac{\xi}{\sqrt{1+\lambda^2}}\big)}.$$

The second and third moments are, respectively,

$$E[T^2]=1-\frac{\xi}{\sqrt{1+\lambda^2}}\frac{\phi\big(-\frac{\xi}{\sqrt{1+\lambda^2}}\big)}{1-\Phi\big(-\frac{\xi}{\sqrt{1+\lambda^2}}\big)}$$

$$E[T^3] = \frac{\left(2 + \left(\frac{\xi}{\sqrt{1+\lambda^2}}\right)^2\right)\phi\left(-\frac{\xi}{\sqrt{1+\lambda^2}}\right)}{1-\Phi\left(-\frac{\xi}{\sqrt{1+\lambda^2}}\right)}.$$

Hence, the second and third central moments are, respectively,

$$E[(T-E[T])^2] = 1 - \frac{\xi}{\sqrt{1+\lambda^2}}\frac{\phi\left(-\frac{\xi}{\sqrt{1+\lambda^2}}\right)}{1-\Phi\left(-\frac{\xi}{\sqrt{1+\lambda^2}}\right)} - \frac{\phi\left(-\frac{\xi}{\sqrt{1+\lambda^2}}\right)^2}{\left(1-\Phi\left(-\frac{\xi}{\sqrt{1+\lambda^2}}\right)\right)^2}$$

$$E[(T-E[T])^3] = \frac{\left(2 + \left(\frac{\xi}{\sqrt{1+\lambda^2}}\right)^2\right)\phi\left(-\frac{\xi}{\sqrt{1+\lambda^2}}\right)}{1-\Phi\left(-\frac{\xi}{\sqrt{1+\lambda^2}}\right)}$$

$$-3\frac{\phi\left(-\frac{\xi}{\sqrt{1+\lambda^2}}\right)}{1-\Phi\left(-\frac{\xi}{\sqrt{1+\lambda^2}}\right)}\left(1 - \frac{\xi}{\sqrt{1+\lambda^2}}\frac{\phi\left(-\frac{\xi}{\sqrt{1+\lambda^2}}\right)}{1-\Phi\left(-\frac{\xi}{\sqrt{1+\lambda^2}}\right)}\right) + 2\frac{\phi\left(-\frac{\xi}{\sqrt{1+\lambda^2}}\right)^3}{\left(1-\Phi\left(-\frac{\xi}{\sqrt{1+\lambda^2}}\right)\right)^3}$$

$$\frac{\left(\left(\frac{\xi}{\sqrt{1+\lambda^2}}\right)^2 - 1\right)\phi\left(-\frac{\xi}{\sqrt{1+\lambda^2}}\right)}{1-\Phi\left(-\frac{\xi}{\sqrt{1+\lambda^2}}\right)} + 3\frac{\xi}{\sqrt{1+\lambda^2}}\frac{\phi\left(-\frac{\xi}{\sqrt{1+\lambda^2}}\right)^2}{\left(1-\Phi\left(-\frac{\xi}{\sqrt{1+\lambda^2}}\right)\right)^2} + 2\frac{\phi\left(-\frac{\xi}{\sqrt{1+\lambda^2}}\right)^3}{\left(1-\Phi\left(-\frac{\xi}{\sqrt{1+\lambda^2}}\right)\right)^3}.$$

.

E.4 Standard Skew-Normal Moments

The standard skew-normal random variable, Z, can be derived as a linear combination of a truncated standard normal variable, T, truncated above $-\frac{\xi}{\sqrt{1+\lambda^2}}$, and a standard normal variable, V:

$$Z = \frac{\lambda}{\sqrt{1+\lambda^2}}T + \frac{1}{\sqrt{1+\lambda^2}}V,\ T \sim \frac{N(0,1)}{1-\Phi\left(-\frac{\xi}{\sqrt{1+\lambda^2}}\right)},\ T > -\frac{\xi}{\sqrt{1+\lambda^2}},\ V \sim N(0,1).$$

Using the binomial expansion, the general formula for the moments of Z as a function of the moments of T and V is given by

$$E[Z^n] = \sum_{i=0}^{n}\binom{n}{i}\left(\frac{\lambda}{\sqrt{1+\lambda^2}}\right)^i\left(\frac{1}{\sqrt{1+\lambda^2}}\right)^{n-i}E[T^i]E[V^{n-i}].$$

Hence, the first moment of Z is

$$E[Z^1] = \frac{\lambda}{\sqrt{1+\lambda^2}}E[T^1] = \frac{\lambda}{\sqrt{1+\lambda^2}}\frac{\phi\left(-\frac{\xi}{\sqrt{1+\lambda^2}}\right)}{1-\Phi\left(-\frac{\xi}{\sqrt{1+\lambda^2}}\right)},$$

where $\phi()$ is the standard normal density function. The second moment of Z is given by

$$E[Z^2] = \frac{1}{1+\lambda^2} + \frac{\lambda^2}{1+\lambda^2}\Big(1 - \frac{\xi}{\sqrt{1+\lambda^2}}\frac{\phi\big(-\frac{\xi}{\sqrt{1+\lambda^2}}\big)}{1-\Phi\big(-\frac{\xi}{\sqrt{1+\lambda^2}}\big)}\Big),$$

and its variance is equal to

$$var(Z) = 1 - \frac{\lambda^2}{1+\lambda^2}\frac{\xi}{\sqrt{1+\lambda^2}}\frac{\phi\big(-\frac{\xi}{\sqrt{1+\lambda^2}}\big)}{1-\Phi\big(-\frac{\xi}{\sqrt{1+\lambda^2}}\big)} - \frac{\lambda^2}{1+\lambda^2}\frac{\phi\big(-\frac{\xi}{\sqrt{1+\lambda^2}}\big)^2}{\Big(1-\Phi\big(-\frac{\xi}{\sqrt{1+\lambda^2}}\big)\Big)^2}.$$

Similarly, the third central moment of Z is

$$E[(Z-E[Z])^3] = \\ \frac{\lambda^3}{(1+\lambda^2)^{3/2}}\Big[\frac{\Big(\Big(\frac{\xi}{\sqrt{1+\lambda^2}}\Big)^2 - 1\Big)\phi\big(-\frac{\xi}{\sqrt{1+\lambda^2}}\big)}{1-\Phi\big(-\frac{\xi}{\sqrt{1+\lambda^2}}\big)} + 3\frac{\xi}{\sqrt{1+\lambda^2}}\frac{\phi\big(-\frac{\xi}{\sqrt{1+\lambda^2}}\big)^2}{\big(1-\Phi\big(-\frac{\xi}{\sqrt{1+\lambda^2}}\big)\big)^2} + 2\frac{\phi\big(-\frac{\xi}{\sqrt{1+\lambda^2}}\big)^3}{\big(1-\Phi\big(-\frac{\xi}{\sqrt{1+\lambda^2}}\big)\big)^3}\Big].$$

E.5 Derivative of the Inverse Mills Ratio

The inverse Mills ratio for a standard normal variable is

$$\frac{\phi(x)}{1-\Phi(x)}.$$

Its derivative is

$$\frac{\phi(x)}{1-\Phi(x)}\Big(-x + \frac{\phi(x)}{1-\Phi(x)}\Big).$$

From Section E.3 above, if $\widetilde{T}$ is a standard normal variable truncated below x, then

$$E[\widetilde{T}|\widetilde{T} \geq x] = \frac{\phi(x)}{1-\Phi(x)}.$$

Thus, for a standard normal variable truncated below x, the following holds

$$E[\widetilde{T}|\widetilde{T} \geq x] = \frac{\phi(x)}{1-\Phi(x)} > x,$$

and the inverse Mills ratio for a standard normal variable is strictly increasing.

E.6 Moments of Location-Scale Skew-Normal Distribution

Based on the results from the Online Appendices D.2 and D.3, for a skew log-normal random variable Y with location, scale, and shape parameters ω, σ, λ, and ξ the density function, mean and variance are, respectively, given by

$$dQ_Y(y) \propto \frac{1}{y} Exp\Big[- \frac{\big(lny - \omega\big)^2}{2\sigma^2} \Big] \Phi\Big(\lambda \frac{lny - \omega}{\sigma} + \xi\Big)$$

$$E[lnY]^{RND} = \omega + \frac{\lambda}{\sqrt{1+\lambda^2}} \frac{\phi\big(-\frac{\xi}{\sqrt{1+\lambda^2}}\big)}{1 - \Phi\big(-\frac{\xi}{\sqrt{1+\lambda^2}}\big)} \sigma$$

$$var\big(lnY\big)^{RND} = \Big[1 - \frac{\lambda^2}{1+\lambda^2} \frac{\xi}{\sqrt{1+\lambda^2}} \frac{\phi\big(-\frac{\xi}{\sqrt{1+\lambda^2}}\big)}{1 - \Phi\big(-\frac{\xi}{\sqrt{1+\lambda^2}}\big)} - \frac{\lambda^2}{1+\lambda^2} \frac{\phi\big(-\frac{\xi}{\sqrt{1+\lambda^2}}\big)^2}{\Big(1 - \Phi\big(-\frac{\xi}{\sqrt{1+\lambda^2}}\big)\Big)^2} \Big] \sigma^2.$$

Linear Pricing Kernel

According to Section E.1 in the Online Appendix, after applying the linear pricing kernel to the skew-normal RND, the density function, mean, and variance, respectively, become

$$dP_Y(y) \propto \frac{1}{y} Exp\Big[- \frac{\big(lny - (\omega + \gamma_1\sigma^2)\big)^2}{2\sigma^2} \Big] \Phi\Big(\lambda \frac{lny - (\omega + \gamma_1\sigma^2)}{\sigma} + \xi + \lambda\gamma_1\sigma\Big) \tag{OA.2}$$

$$E[lnY] = \omega + \gamma_1\sigma^2 + \frac{\lambda}{\sqrt{1+\lambda^2}} \frac{\phi\big(-\frac{\xi+\lambda\gamma_1\sigma}{\sqrt{1+\lambda^2}}\big)}{1 - \Phi\big(-\frac{\xi+\lambda\gamma_1\sigma}{\sqrt{1+\lambda^2}}\big)} \sigma \tag{OA.3}$$

$$var(lnY) = \Big[1 - \frac{\lambda^2}{1+\lambda^2} \frac{\xi + \lambda\gamma_1\sigma}{\sqrt{1+\lambda^2}} \frac{\phi\big(-\frac{\xi+\lambda\gamma_1\sigma}{\sqrt{1+\lambda^2}}\big)}{1 - \Phi\big(-\frac{\xi+\lambda\gamma_1\sigma}{\sqrt{1+\lambda^2}}\big)} - \frac{\lambda^2}{1+\lambda^2} \frac{\phi\big(-\frac{\xi+\lambda\gamma_1\sigma}{\sqrt{1+\lambda^2}}\big)^2}{\Big(1 - \Phi\big(-\frac{\xi+\lambda\gamma_1\sigma}{\sqrt{1+\lambda^2}}\big)\Big)^2} \Big] \sigma^2. \tag{OA.4}$$

According to the last equation above, when the risk-neutral density departs from normality, the linear pricing kernel alters both the expected return and the variance of the risk-neutral density by shifting the shape parameter in the inverse Mills ratio from ξ to $\xi + \lambda\gamma_1\sigma$. Thus, a linear pricing kernel with a positive risk-aversion parameter γ_1 raises the mean of the risk-neutral distribution by $\gamma_1\sigma^2$, as in the normal RND case (Online Appendix, Section E.1), while simultaneously reducing,

in absolute value, the negative skewness adjustment term.

$$\frac{\lambda}{\sqrt{1+\lambda^2}}\frac{\phi\big(-\frac{\xi+\lambda\gamma_1\sigma}{\sqrt{1+\lambda^2}}\big)}{1-\Phi\big(-\frac{\xi+\lambda\gamma_1\sigma}{\sqrt{1+\lambda^2}}\big)}\sigma.$$

Since λ is negative for a negatively skewed RND and the inverse Mills ratio, $\frac{\phi(x)}{1-\Phi(x)}$, is strictly increasing (Online Appendix D.5), increasing ξ to $\xi+\lambda\gamma_1\sigma$, decreases the absolute magnitude of the negative term

$$\text{from}\quad \frac{\lambda}{\sqrt{1+\lambda^2}}\frac{\phi\big(-\frac{\xi}{\sqrt{1+\lambda^2}}\big)}{1-\Phi\big(-\frac{\xi}{\sqrt{1+\lambda^2}}\big)}\sigma\quad\text{to}\quad \frac{\lambda}{\sqrt{1+\lambda^2}}\frac{\phi\big(-\frac{\xi+\lambda\gamma_1\sigma}{\sqrt{1+\lambda^2}}\big)}{1-\Phi\big(-\frac{\xi+\lambda\gamma_1\sigma}{\sqrt{1+\lambda^2}}\big)}\sigma. \tag{OA.5}$$

Quadratic Pricing Kernel

According to Section E.1 of the Online Appendix, after applying the quadratic pricing kernel to the skew-normal RND, the density function, mean, and variance, respectively, become

$$dP_Y(y)\propto\frac{1}{R}Exp\Big[-\frac{\big(lny-\frac{\omega+\gamma_1\sigma^2}{1-2\gamma_2\sigma^2}\big)^2}{2\frac{\sigma^2}{1-2\gamma_2\sigma^2}}\Big] \tag{OA.6}$$

$$\times\Phi\Big(\frac{\lambda}{\sqrt{1-2\gamma_2\sigma^2}}\frac{lny-\frac{\omega+\gamma_1\sigma^2}{1-2\gamma_2\sigma^2}}{\frac{\sigma}{\sqrt{1-2\gamma_2\sigma^2}}}+\xi+\frac{\lambda}{\sigma}\frac{2\omega\gamma_2\sigma^2+\gamma_1\sigma^2}{1-2\gamma_2\sigma^2}\Big)$$

$$E[lnY]=\frac{\omega+\gamma_1\sigma^2}{1-2\gamma_2\sigma^2}+\frac{\frac{\lambda}{\sqrt{1-2\gamma_2\sigma^2}}}{\sqrt{1+\frac{\lambda^2}{1-2\gamma_2\sigma^2}}}\frac{\phi\Big(-\frac{\xi+\frac{\lambda}{\sigma}\frac{2\omega\gamma_2\sigma^2+\gamma_1\sigma^2}{1-2\gamma_2\sigma^2}}{\sqrt{1+\frac{\lambda^2}{1-2\gamma_2\sigma^2}}}\Big)}{1-\Phi\Big(-\frac{\xi+\frac{\lambda}{\sigma}\frac{2\omega\gamma_2\sigma^2+\gamma_1\sigma^2}{1-2\gamma_2\sigma^2}}{\sqrt{1+\frac{\lambda^2}{1-2\gamma_2\sigma^2}}}\Big)}\sigma$$

$$var(lnY)=\Big[1-\frac{\frac{\lambda^2}{1-2\gamma_2\sigma^2}}{1+\frac{\lambda^2}{1-2\gamma_2\sigma^2}}\frac{\xi+\frac{\lambda}{\sigma}\frac{2\omega\gamma_2\sigma^2+\gamma_1\sigma^2}{1-2\gamma_2\sigma^2}}{\sqrt{1+\frac{\lambda^2}{1-2\gamma_2\sigma^2}}}\frac{\phi\Big(-\frac{\xi+\frac{\lambda}{\sigma}\frac{2\omega\gamma_2\sigma^2+\gamma_1\sigma^2}{1-2\gamma_2\sigma^2}}{\sqrt{1+\frac{\lambda^2}{1-2\gamma_2\sigma^2}}}\Big)}{1-\Phi\Big(-\frac{\xi+\frac{\lambda}{\sigma}\frac{2\omega\gamma_2\sigma^2+\gamma_1\sigma^2}{1-2\gamma_2\sigma^2}}{\sqrt{1+\frac{\lambda^2}{1-2\gamma_2\sigma^2}}}\Big)}$$

$$-\frac{\frac{\lambda^2}{1-2\gamma_2\sigma^2}}{1+\frac{\lambda^2}{1-2\gamma_2\sigma^2}}\frac{\phi\Big(-\frac{\xi+\frac{\lambda}{\sigma}\frac{2\omega\gamma_2\sigma^2+\gamma_1\sigma^2}{1-2\gamma_2\sigma^2}}{\sqrt{1+\frac{\lambda^2}{1-2\gamma_2\sigma^2}}}\Big)^2}{\Big(1-\Phi\Big(-\frac{\xi+\frac{\lambda}{\sigma}\frac{2\omega\gamma_2\sigma^2+\gamma_1\sigma^2}{1-2\gamma_2\sigma^2}}{\sqrt{1+\frac{\lambda^2}{1-2\gamma_2\sigma^2}}}\Big)\Big)^2}\Big]\frac{\sigma^2}{1-2\gamma_2\sigma^2}.$$

For negative (positive) quadratic parameter γ_2, the scale parameter decreases (increases) from

σ to $\sigma/\sqrt{1-2\gamma_2\sigma^2}$. Further, for positive linear parameter γ_1, the location parameter increases by the term $\frac{\gamma_1\sigma^2}{1-2\gamma_2\sigma^2}$ and by decreasing the absolute value of the negative skewness adjustment term

$$\frac{\frac{\lambda}{\sqrt{1-2\gamma_2\sigma^2}}}{\sqrt{1+\frac{\lambda^2}{1-2\gamma_2\sigma^2}}}\frac{\phi\Big(-\frac{\xi+\frac{\lambda}{\sigma}\frac{2\omega\gamma_2\sigma^2+\gamma_1\sigma^2}{1-2\gamma_2\sigma^2}}{\sqrt{1+\frac{\lambda^2}{1-2\gamma_2\sigma^2}}}\Big)}{1-\Phi\Big(-\frac{\xi+\frac{\lambda}{\sigma}\frac{2\omega\gamma_2\sigma^2+\gamma_1\sigma^2}{1-2\gamma_2\sigma^2}}{\sqrt{1+\frac{\lambda^2}{1-2\gamma_2\sigma^2}}}\Big)}\sigma. \tag{OA.7}$$

Interestingly, even if γ_1 is zero or negative, so that the direct effect of $\gamma_1\sigma^2$ is zero or leads to a decreases in the risk-neutral mean, the mean of the physical density may still exceed that of the RND. This occurs when the quadratic parameter γ_2 is negative. In that case, the quadratic adjustment decreases the absolute magnitude of the negative term in equation (OA.7), effectively offsetting or dominating the impact of γ_1.